nagra
National Cooperative for the
Disposal of Radioactive Waste

TECHNICAL REPORT 04-02

Experimental and Modelling Investigations on Na-Illite:

Acid-Base Behaviour and the Sorption of Strontium, Nickel, Europium and Uranyl

June 2005

M.H. Bradbury and B. Baeyens

Paul Scherrer Institut, Villigen PSI

Hardstrasse 73, CH-5430 Wettingen/Switzerland, Telephone +41-56-437 11 11

nagra National Cooperative for the Disposal of Radioactive Waste

TECHNICAL REPORT 04-02

Experimental and Modelling Investigations on Na-Illite:

Acid-Base Behaviour and the Sorption of Strontium, Nickel, Europium and Uranyl

June 2005

M.H. Bradbury and B. Baeyens

Paul Scherrer Institut, Villigen PSI

Hardstrasse 73, CH-5430 Wettingen/Switzerland, Telephone +41-56-437 11 11

This report was prepared on behalf of Nagra. The viewpoints presented and conclusions reached are those of the author(s) and do not necessarily represent those of Nagra.

PREFACE

The Laboratory for Waste Management of the Nuclear Energy and Safety Research Department at the Paul Scherrer Institut is performing work to develop and test models as well as to acquire specific data relevant to performance assessments of planned Swiss nuclear waste repositories. These investigations are undertaken in close co-operation with, and with the financial support of, the National Cooperative for the Disposal of Radioactive Waste (Nagra). The present report is issued simultaneously as a PSI-Bericht and a Nagra Technical Report.

ISSN 1015-2636

Abstract

In an extensive study the physico-chemical, protolysis and sorption characteristics of Sr(II), Ni(II), Eu(III) and U(VI) have been measured on illite and modelled over a wide range of pH, sorbate and $NaClO_4$ concentrations.

Samples of Illite du Puy, collected in the region of Le Puy-en-Velay, France, were carefully conditioned to the Na-form and physico-chemically characterised. Potentiometric titrations on suspensions of the Na-illite were carried out using a batch back titration technique in 0.01, 0.1 and 0.5 M $NaClO_4$ background electrolytes from pH~2 to ~12 in an inert atmosphere glove box. The supernatant solutions from each titration experiment in each series were analysed for K, Mg, Ca, Sr, Si, Al, Fe and Mn.

Sorption edges (solid/liquid distribution ratios versus pH at trace sorbate concentrations and constant ionic strength) were determined for Sr, Ni, Eu and U on Na-illite as a function of $NaClO_4$ concentration under anoxic conditions ($CO_2 \leq 2$ ppm, $O_2 \leq 2$ ppm.). Sorption isotherms for the same set of radionuclides under similar conditions were measured for Na-illite suspensions in 0.1 M $NaClO_4$ at fixed pH values.

The titration data were modelled in terms of the protolysis of two amphoteric edge sites ($\equiv S^{W1}OH$ and $\equiv S^{W2}OH$) without an electrostatic term. The protonation/deprotonation constants and site capacities obtained from the titration measurements were then fixed. The sorption edge and isotherm data were modelled with strong ($\equiv S^{S}OH$) and weak ($\equiv S^{W1}OH$) surface complexation sites, assumed to have the same protolysis constants, again without electrostatic terms. Uptake by cation exchange was included in all of the calculations. This sorption model, the 2 site protolysis non electrostatic surface complexation and cation exchange model, had been developed previously for montmorillonite and was successful in describing the sorption characteristics of Sr, Ni, Eu and U on Na-illite over a wide range of conditions.

Cation exchange capacity, strong and weak site capacities and protolysis constants for Na-illite are given, together with surface complexation constants and selectivity coefficients for Sr, Ni, Eu and U.

At 0.01 M $NaClO_4$ and pH < 8 the sorption of Sr, Ni, Eu and U was dominated by a cation exchange mechanism. The strong dependency of sorption on pH observed under these conditions arose from the competitive effects of Ca and Al on the uptake of the sorbate. Selectivity coefficients for Ca and Al with respect to Na were deduced from these measurements.

Zusammenfassung

Im Rahmen einer ausführlichen Studie wurden die physikalisch-chemischen sowie die Protolyse- und Sorptionseigenschaften von Sr(II), Ni(II), Eu(III) und U(VI) an Illit gemessen und für ein breites Spektrum von pH-Werten, Sorbat- und $NaClO_4$-Konzentrationen modelliert.

Dafür wurden Proben von 'Illite du Puy' aus der Region von Le Puy-en-Velay in Frankreich sorgfältig zu der reinen Na-Form konditioniert und physikalisch-chemisch charakterisiert. An Na-Illit-Suspensionen erfolgten potentiometrische Titrationen durch Anwendung eines Batchverfahrens mit Rücktitration in 0.01, 0.1 und 0.5 molaren $NaClO_4$ Elektrolytlösungen im Bereich von pH ~2 bis ~12. Solche Experimente wurden in einer Handschuhbox unter Bedingungen einer inerten Atmosphäre durchgeführt. An den überstehenden Lösungen aus den einzelnen Titrationsexperimenten jeder Experimentserie wurden K, Mg, Ca, Sr, Si, Al, Fe und Mn bestimmt.

Zur Bestimmung der pH-abhängigen Sorption wurden Verteilungsverhältnisse (fest/flüssig, aufgetragen gegen den pH-Wert für Sorbatkonzentrationen im Spurenbereich und bei konstanter Ionenstärke, sogenannte "Sorption Edges") für Sr, Ni, Eu und U auf Na-Illit als Funktion der $NaClO_4$-Konzentration unter anoxischen Bedingungen ($CO_2 \leq 2$ ppm, $O_2 \leq 2$ ppm) gemessen. Unter ähnlichen Bedingungen wurden für dieselben Radionuklide Sorptionsisotherme für Na-Illit-Suspensionen in einer 0.1 molaren $NaClO_4$-Lösung bei fixierten pH-Werten bestimmt.

Die Titrationsdaten wurden hinsichtlich der Protolyse zweier amphoterischer Gruppen ($\equiv S^{W1}OH$ and $\equiv S^{W2}OH$) ohne elektrostatischen Term modelliert. Die aus den Titrationsbestimmungen erhaltenen Protonierungs-/Deprotonierungskonstanten und Gesamtkonzentrationen wurden dann festgelegt. Die pH-abhängigen Sorptions- und die Isothermendaten wurden mit starken ($\equiv S^{S}OH$) und schwachen ($\equiv S^{W1}OH$) Oberflächenkomplexierungsgruppen unter Annahme gleicher Protolysekonstanten ohne elektrostatischen Term modelliert. Bei sämtlichen Berechnungen wurde eine Aufnahme durch Kationenaustausch berücksichtigt. Dieses Sorptionsmodell, d.h. die Protolyse zweier Gruppen mit nicht-elektrostatischer Oberflächenkomplexierung und Kationenaustausch wurde zuvor für Montmorillonit entwickelt und beschreibt erfolgreich die Sorptionseigenschaften von Sr, Ni, Eu und U auf Na-Illit für ein grosses Spektrum an chemischen Bedingungen.

Kationenaustauschkapazität, starke und schwache Oberflächenkomplexierungskapazität und Protolysekonstanten werden für Na-Illit zusammen mit Oberflächenkomplexierungskonstanten und Selektivitätskoeffizienten für Sr, Ni, Eu und U angegeben.

Die Sorption von Sr, Ni, Eu und U wurde bei einer 0.01 molaren $NaClO_4$-Lösung und einem pH-Wert < 8 von Kationenaustauschmechanismen dominiert. Die unter diesen Bedingungen beobachtete starke pH-Abhängigkeit wurde durch die Konkurrenzierung von Ca und Al bei der Aufnahme von Sorbat hervorgerufen. Aus diesen Messungen konnten Selektivitätskoeffizienten für Ca und Al bezüglich Na abgeleitet werden.

Résumé

Cette étude systématique a permis de déterminer les caractéristiques physico-chimiques, les paramètres de réaction acido-basique et de sorption du Sr(II), du Ni(II), de l' Eu(III) et de l'U(VI) sur une illite. Ces réactions ont été modélisées sur une large échelle de pH, de concentrations d'élément sorbable et de $NaClO_4$.

Les échantillons d'illite du Puy, prélevés dans la région du Puy-en-Velay en France, ont d'abord été conditionnés en échangeant les cations compensateurs avec du Na avant d'être caractérisés physico-chimiquement. Les titrations potentiométriques des suspensions d'illite sodique ont été effectuées en batch par titration réversible sous atmosphère inerte d'une boîte à gants en solution électrolytique de 0.01, 0.1 et 0.5 M $NaClO_4$ et de pH ~2 à ~12. Les teneurs en K, Mg, Ca, Sr, Si, Al, Fe and Mn de la solution aqueuse ont ensuite été analysés après chaque titration.

On a également déterminé la variation du coefficient de distribution, $R_{d,}$, du Sr, du Ni, de l'Eu et de l'U sur une illite sodique, en fonction du pH à force ionique fixe pour différentes concentrations de $NaClO_4$ en conditions anoxiques ($CO_2 \leq 2$ ppm, $O_2 \leq 2$ ppm.). De plus, on a mesuré dans des conditions similaires les isothermes d'adsorption du même groupe de radionucléides sur une illite sodique dans des suspensions de 0.1 M $NaClO_4$ et à pH fixe.

Par la suite, les données de titration ont été simulées par un modèle de complexation de surface sans terme électrostatique comprenant deux sites acido-basiques amphotères ($\equiv S^{W1}OH$ et $\equiv S^{W2}OH$). A l'aide de ce modèle et des données de titration on a déterminé les constantes de dissociation et les capacités d'adsorption de l'illite sodique. Les résultats des expériences de sorption ont ensuite été modélisés à l'aide de deux sites d'adsorption, un site fort ($\equiv S^{S}OH$) et un site faible ($\equiv S^{W1}OH$), tous deux ayant les mêmes constantes de dissociation. L'adsorption par échange cationique était également prise en compte dans chaque simulation. Un modèle analogue de sorption qui comprend l'adsorption, la réaction acido-basique sur deux sites de surface sans terme électrostatique ainsi que l'échange cationique avait été développé auparavant pour la montmorillonite. Il a permis de décrire ici avec succès les caractéristiques de sorption du Sr, du Ni, de l'Eu et de l'U sur une illite sodique dans une large échelle de conditions.

La capacité d'échange cationique, les capacités d'adsorption des sites forts et faibles et les constantes de dissociation sont indiquées de même que les constantes d'adsorption et les cœfficients de sélectivité pour le Sr, le Ni, l'Eu et l'U sur une illite sodique.

Dans une solution de 0.01 M $NaClO_4$ et pH < 8 le mécanisme de sorption dominant dans le cas du Sr, Ni, Eu et de l'U est l'échange cationique. L'interdépendance importante entre sorption et pH qu'on observe dans ces conditions est due aux effets compétitifs du Ca et de l'Al sur la sorption. Les coefficients de sélectivité du Ca et de l'Al par rapport au Na ont été déduits sur la base de ces mesures.

Table of contents

List of Tables

List of Figures

1 Introduction

Argillaceous rocks are being viewed with continuing interest in many waste management programmes as suitable host formations for the deep geological disposal of radioactive waste: Opalinus clay, Switzerland (NAGRA, 2002); Boom and Ypresian clays, Belgium (ONDRAF, 2001); Callovo-Oxfordian and Toarcian clays, France (ANDRA, 2001, BONIN, 1998); Horonobe sediments, Japan (AOKI, 2002). Clay minerals such as illite, smectite, illite/smectite mixed layers and kaolinite are important components in such rock types and can often make up 50 or more wt.% of the total mass. One of the most important characteristics of many clay minerals, as far as repository performance assessment studies are concerned, is their generally strong radionuclide retention properties. Although sorption values may be required over a wide range of geochemical conditions, most of the available data are expressed in terms of empirical parameters/relations which are difficult to extrapolate. Consequently, a knowledge of sorption processes, and the system parameters which influences them, is becoming increasingly essential.

In recent years attempts have been made to develop models which are capable of describing and predicting the sorption of radionuclides on clay minerals over a wide range of conditions. The hypothesis behind many of these studies is that by understanding and being able to model sorption on clay minerals, sorption in natural systems containing significant levels of such minerals can be predicted because they provide the major sinks for radionuclides (the so called "bottom-up" approach).

In a series of papers BRADBURY & BAEYENS (1997a, 1999, 2002) have developed and applied a relatively simple **2 s**ite **p**rotolysis **n**on **e**lectrostatic **s**urface **c**omplexation and **c**ation **e**xchange model (2SPNE SC/CE model) to describe the uptake of dissolved metal species (Ni, Zn and Eu) on Na- and Ca- montmorillonites.

The aim in this current work was to extend these investigations to another important clay mineral system, illite, by measuring titration data and making sorption edge and isotherm measurements for Sr(II), Ni(II), Eu(III) and U(VI). Because the unit cells of montmorillonite and illite are similar, the expectation was that the 2SPNE SC/CE model could also be used to model the radionuclide uptake on illite as a function of sorbate concentrations, pH and ionic strength.

2 Preparation of materials and solutions

All the $NaClO_4$ solutions were prepared from Fluka "supra-pur" grade chemicals and ultra-pure de-ionised water (resistivity ~18 MΩ cm). The solutions were purified using the methodology given in BAEYENS & BRADBURY (1995a) which resulted in decreases in impurity levels by a factor 10 to 100 depending on the particular metal.

The source material used in these investigations was an illite du Puy (GABIS, 1958) collected from within an 80 m thick Oligocene geological formation in the region of Le Puy-en-Velay (Haute-Loire), France. Samples of illite were crushed, then powdered in a mortar and finally the < 63 μm fraction was separated by sieving. The clay mineral preparation procedures have been described in detail elsewhere (BAEYENS & BRADBURY, 1995a, 1997; POINSSOT et al., 1999) and only an outline will be given here.

A purifying procedure was applied to the "as received" powder so as to obtain, as far as possible, a single phased suspension of Na-illite in a 1:1 background electrolyte for the titration measurements and sorption investigations. One hundred gram quantities of the illite powder were contacted with approximately 2 litres of a purified 1 M $NaClO_4$ solution (see Table 2.1), shaken end-over-end for several hours and allowed to flocculate over night before decanting off the supernatant solution. This procedure was repeated three times, which was sufficient to remove any soluble salts and to convert the clay to the homo-ionic Na-form.

Separation of the < 0.5 μm Na-illite fraction was achieved by dividing the 2 litre suspension more or less equally into twelve 250 ml centrifuge bottles which were then filled with de-ionised water pre-equilibrated with a small quantity of illite. After allowing the illite to peptise for ~15 minutes and centrifuging for ~7 minutes at ~600 *g* (max.), the Na-illite fraction in the supernatant solution (< 0.5 μm) was transferred into a large polyethylene container. A fresh 1 M $NaClO_4$ solution was then immediately added in order to flocculate the fine clay particles and to prevent hydrolysis. After repeating the whole procedure approximately 20 times, a yield of ~35 wt.% of peptised illite was achieved. Soluble hydroxy-aluminium compounds were removed by an acid treatment (pH 3.5, 1 hour) followed by phase separation and neutralisation (pH 7). The resulting stock suspension (~20 g L^{-1} of Na-illite in ~0.4 M $NaClO_4$) was stored in the dark at 4 °C and kept no longer than 6 months.

Batches were prepared at various ionic strengths from the stock suspension for the sorption experiments. This was achieved by placing four 35 mm diameter dialysis bags, each containing ~75 ml of the suspension, in a 1 litre polyethylene flask filled with the desired concentration of the $NaClO_4$ solution. The flask was shaken end-over-end for ~3 hours. This procedure was repeated until the electrical conductivity of the equilibrium solution was the same as the original solution, indicating that the conditioning process was completed.

Finally, the contents of the dialysis bags from other parallel experiments were emptied into a polythene container and diluted with the last equilibrium solution to yield suspensions between 7 and 14 g L^{-1} at the desired $NaClO_4$ concentration. The clay content in the suspensions was determined by heating weighed aliquots to constant weight at 105 °C and correcting for the salt content.

Typical examples of the water chemistries of the last conditioning waters from the preparation of such illite batches are given in Table 2.1. (For comparison purposes an analysis of a 1 M $NaClO_4$ solution is given.)

Table 2.1: Chemical analyses (mol L^{-1}) of the purified 1 M $NaClO_4$ solution and the last conditioning water from the preparation of conditioned Na-illite in $NaClO_4$ at 0.1 and 0.01 M, pH ~7, POINSSOT et al. (1999). (Measurements were carried out by ICP-OES, Varian Vista AX CCD simultaneous ICP-OES.)

Element	1 M $NaClO_4$	Na-illite in 0.1 M $NaClO_4$	Na-illite in 0.01 M $NaClO_4$
Si	1.3×10^{-6}	3×10^{-5}	4×10^{-5}
Al	1.0×10^{-6}	3×10^{-6}	5×10^{-6}
Fe	$< (2 \times 10^{-7})$	3×10^{-7}	$< (2 \times 10^{-7})$
Mg	1.0×10^{-6}	3×10^{-6}	2×10^{-6}
Mn	1.0×10^{-6}	7×10^{-8}	8×10^{-8}
K	1.1×10^{-4}	1.5×10^{-5}	5×10^{-6}
Ca	2.0×10^{-6}	10^{-5}	7×10^{-6}
Ba	2.0×10^{-7}	2×10^{-7}	$< (9 \times 10^{-9})$
Zn	$< (4 \times 10^{-7})$	4×10^{-7}	5×10^{-7}
Ni	$< (5 \times 10^{-7})$	$< (5 \times 10^{-7})$	$< (5 \times 10^{-7})$
Sr	3.3×10^{-7}	5×10^{-8}	$\sim 10^{-8}$
P	$< (10^{-6})$	10^{-5}	10^{-5}
S	$< (2 \times 10^{-6})$	$< (2 \times 10^{-6})$	$< (2 \times 10^{-6})$

The numbers given in the parentheses are “reliable detection limits” which are taken to be 10 times higher than the ICP-OES detection limits. The elements Pb, Co, Cd, Cu, Rb, Cs, Hg could not be detected and were therefore below the ICP-OES detection limits ($< 10^{-8}$ M).

3 Physico-chemical characterisation of the conditioned Na-illite

3.1 Mineralogical composition, structural formula and surface areas of Na conditioned illite du Puy

Illite du Puy (IdP), obtained from two different sampling campaigns (IdP-1 and IdP-2), was used in the investigations reported in this work. Both were conditioned and purified according to the procedures given in the previous chapter.

IdP-1 was used in Sr, Ni and Eu sorption experiments (POINSSOT et al., 1999) and in the titration measurements, Chapter 4. X-ray diffraction (XRD) data and bulk chemical analyses of the Na conditioned IdP-1 revealed a composition of ~93 wt.% illite and ~7 wt.% kaolinite.

The composition of IdP-2, conditioned to the Na form, was determined from XRD data to be ~88 wt.% illite and ~12 wt.% sanidine (KAHR, pers. comm.), a K-feldspar. Sorption experiments with Eu and U were performed with this material. Comparative sorption experiments on IdP-1 and IdP-2 using Ni (see Fig. 10.2) and Eu (see Figs. 10.7 and 10.11) indicated that within experimental error both materials behaved the same.

The mean structural formula of the conditioned Na-illite (IdP-1) deduced from energy dispersive spectroscopy and bulk analyses results is given in POINSSOT et al. (1999) as:

$$[(Si_{3.52}Al_{0.48})O_{10}(OH)_2](Al_{1.17}Fe_{0.49}Mg_{0.33})(Ca_{0.04}Na_{0.12}K_{0.64})$$

Note that iron is present as Fe(III) in the illite lattice.

Surface area measurement data carried out by the French National Institute for Agronomy Research (INRA), Laboratory for Soil Science (Versailles, France) are summarised in Table 3.1.

Table 3.1: N_2-BET and ethylene-glycol-monoethyl-ether (EGME) surface area measurements for the as received and Na-conditioned illite du Puy (IdP-1) (POINSSOT et al., 1999).

Sample	N_2-BET ($m^2\ g^{-1}$)	EGME ($m^2\ g^{-1}$)
"as received" illite	97	95
conditioned Na-illite	-	129

3.2 Cation exchange capacity of Na-illite

The isotope dilution technique was used to measure the cation exchange capacity (CEC) of purified illite du Puy. In contrast to previous studies (POINSSOT et al., 1999), Cs was preferred to Na as the index cation because at the low $NaClO_4$ concentrations (~10^{-3} M) used in the previous CEC determinations, the Ca and Mg in the system were competing with Na resulting in CEC measurements which were too low (BAEYENS & BRADBURY, 2004).

Na-illite suspensions were converted into the homo-ionic Cs form by placing 35 mm diameter dialysis bags, each containing ~75 ml of the Na-illite stock suspension, in a 1 litre polyethylene

flask filled with 0.1 M $CsNO_3$. The flask was shaken end-over-end for ~3 hours. This procedure was repeated until the electrical conductivity of the equilibrium solution was the same as the original solution, indicating that the conditioning process was completed. (Generally 5 exchange cycles were necessary). Using a similar procedure, the Cs-illite was further conditioned to a solution concentration of 5 x 10^{-3} M $CsNO_3$. The Cs concentration in the final conditioning solution was analysed by plasma-emission spectroscopy (Varian Vista AX CCD simultaneous ICP-OES).

In order to obtain reproducible CEC results, the experimental set up had to be arranged such that the "moles" of Cs in solution were approximately twice the "moles" of Cs on the illite. Aliquots of Cs-illite suspensions were equilibrated with final conditioning solutions labelled with ^{134}Cs for at least 3 days. At the end of this time the samples were centrifuged (96000 *g* (max.) for 1 hour), the pH determined in the supernatant solutions (~7) and the activities measured by gamma counting. The Cs-CEC values were calculated from the initial and final activities in solution.

A series of CEC determinations on four different clay batches carried out at neutral pH in 5 x 10^{-3} M $CsNO_3$ at S:L ratios of ~12 g L^{-1} yielded an average Cs-CEC value of 225 ±10 meq kg^{-1}. This value is considerably higher than the Na-CEC of ~130 meq kg^{-1} reported in POINSSOT et al. (1999). As mentioned previously, the discrepancy is interpreted as being due to competition from Ca/Mg in the Na-CEC determinations (see BAEYENS & BRADBURY, 2004**).** Gorgeon (1994) has reported similar CEC values for Illite du Puy samples to those given here measured at neutral pH using Co-hexamine as the index cation. She also reports Cs-CEC values as a function of pH but these only reach comparable values at pH > 10.

4 Titration measurements

4.1 Background

Potentiometric titrations of single mineral suspensions in a simple background electrolyte have been used extensively in many systems to gain information on site capacities and protolysis behaviour of ≡SOH type surface sites (DAVIS et al., 1978; JAMES & PARKS, 1982; SCHINDLER & STUMM, 1987; HIEMSTRA et al., 1987; LÖVGREN et al., 1990; HAYES et al., 1991; BEENE et al., 1991; WANNER et al., 1994; BAEYENS & BRADBURY, 1995a, 1997; KRAEPIEL et al., 1998, SINITSYN et al., 2000; KULIK et al., 2000).

In practice the interpretation of such titration curves can be quite difficult. The amphoteric behaviour of the ≡SOH type surface sites may not be the only significant proton consuming/ releasing mechanism responsible for the form of the titration curve. All minerals are soluble to some extent, particularly at extreme pH values, and in order to obtain a net titration curve the solubilisation of the solid phases as a function of pH has to be taken into account. This is particularly so in clay mineral systems where dissolution processes can become significant at pH values less than 4 and greater than 10, see for example BAEYENS & BRADBURY (1995a, 1997).

This has been realised for some time, and SCHULTHESS & SPARKS (1986, 1987, 1988) have described a back titration method as a potential means of overcoming this problem. The supernatant solution from each batch titration is back titrated to a common end point. The quantities of acid (or base) required in the back titration of the supernatant solutions are subtracted from the original quantities of base (or acid) added in the forward titration, to yield, in the ideal case, the net quantity consumed by the surface.

However, the back titration procedure is by no means a definitive solution to the problem in the case of clay minerals. Inherent in the method are a number of unknowns and uncertainties which are difficult to quantify e.g. the potential influences of differences in dissolution/ precipitation reactions and kinetics in the forward and back titrations; the effect of incongruent dissolution on the distribution of ≡SOH sites and their protolysis behaviour; proton exchange and/or cation exchange coupled with solid phase dissolution. The main uncertainties are associated with the incongruent dissolution of the clay mineral. As will be shown later, even in cases where a much better quantitative understanding of certain processes has been achieved (e.g. the influence of Al and Ca exchange reactions at low pH), such corrections only have a marginal effect on the results.

4.2 Experimental

Suspensions of Na-illite at solid to liquid ratios between 8 and 13 g L^{-1} in 0.01, 0.1 and 0.5 M $NaClO_4$ background electrolyte were prepared. The titrations were carried out in a batch-wise manner in an inert atmosphere glove box where the partial pressure of CO_2 was < $10^{-5.5}$ bar.

Standard acid and base solutions at concentrations of 0.2 or 0.02 M were made up from Merck Titrisol analytical grade starting solutions in the three $NaClO_4$ concentrations. Aliquots of acid or base were taken from the standard solutions and added to the suspensions in the 40 ml centrifuge tubes to give a series of initial pH values between 2.5 and 11.5. (Preliminary tests had indicated the approximate quantities of acid or base required.) To some samples no acid or base was added and these provided the reference pH values. All centrifuge tubes were tightly capped and shaken end-over-end for 24 hours.

After this shaking time, the closed tubes were transferred out of the glove box, centrifuged for 1 hour at 96000 *g* (max.) and then returned to the glove box for sampling. Two aliquots of the supernatant solutions were taken; one of 10 ml, for cation analysis (Varian Vista AX CCD simultaneous ICP-OES), and the other of 25 ml for final pH measurement and subsequent back titration. The back titrations were carried out in the glove box with an autotitrating system (Metrohm Titroprocessor 660) set up in the monotonic titration mode i.e. aliquots of acid or base in 0.01 (0.1, 0.5) M $NaClO_4$, were added at ~5 minutes intervals until the pH was at least one unit greater or smaller than the pH of the reference samples to which no acid/base had been added. The experiments were arranged such that there were no significant delays in sampling, measuring the final pH and starting the back titrations.

4.3 Titration results

The results from forward and back titration experiments, grouped according to ionic strength (I.S.), are presented in Tables A-2, A-6, A-7 and A-12 in Appendix A. The "Total H^+ (OH^-) consumed" columns represents the quantities of H^+ (OH^-) consumed by all processes not accounted for in the back titration measurements. Corresponding analysis data for K, Mg, Ca, Sr, Si, Al, Fe and Mn for each supernatant solution in each titration series are also presented in Appendix A in the form of tables and figures. For the data measured in 0.5 M $NaClO_4$ the K and Si concentrations for IdP-1, Table A3, are slightly higher than those for IdP-2, Table A4, which could indicate that the two illite samples might have different titration behaviour. Unfortunately a direct comparison is not possible because titration data for IdP-2 are not available. However, at 0.1 M $NaClO_4$ the titration measurements for IdP-1 and IdP-2 are consistent and the K and Si concentrations measured in 0.1 and 0.01M $NaClO_4$ respectively are similar.

A summary of the titration data at each of the three $NaClO_4$ concentrations, plotted as the quantities of total H^+ (OH^-) consumed as a function of pH, is given in Fig. 4.1.

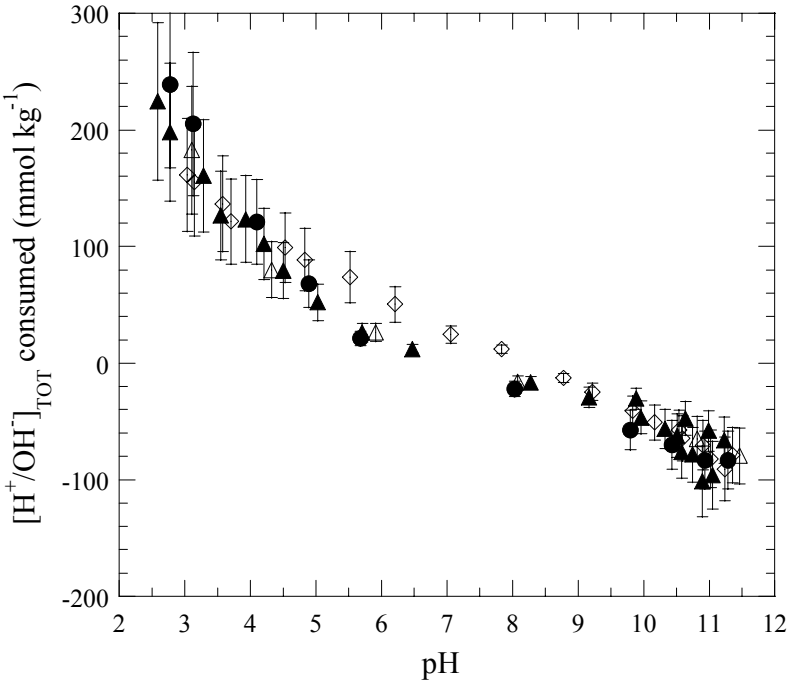

Fig. 4.1: Total acid/base consumption by all processes not accounted for in the back titration measurements for the titration of conditioned Na-illite in 0.01 M $NaClO_4$ (●, IdP-1), 0.1 M $NaClO_4$ (▲, IdP-1, △, IdP-2) and 0.5 M $NaClO_4$ (◇, IdP-1).

If only protolysis reactions contribute to the titration then it would be expected that the plots would plateau at low and high pH values because the site capacity of the edge sites is finite and eventually all sites must be protonated or deprotonated and no further consumption/release of protons occurs. The form of the curve may or may not be symmetrical.

At high pH all of the points measured at the different ionic strengths are similar, and there appears to be a tendency to form a plateau. At low pH (particularly for pH values < 4) the proton consumption tends to increase rapidly. Within the $NaClO_4$ concentration range studied (0.01 to 0.5 M) little or no dependency can be seen i.e. there are no significant ionic strength effects within the uncertainties associated with the data, see section 4.4 and 4.5.

4.4 Errors

Despite all the precautions taken with the measurements described in the previous sections, the uncertainties in titration data can be potentially quite large, particularly at high and low pH values. The experimental errors associated with acid/base additions and back titration measurements were estimated to be ~15 %. For most of the data measured between pH 3.5 and 10, the errors in the quantities of H^+ (OH^-) consumed originate from these two sources. For the pH regions < 3.5 and > 10, the errors in the calculated values for H^+ (OH^-) consumed are larger and estimated to be ~30 % because the amounts of acid (base) required in the back titrations are larger and close to the quantities of base (acid) added in the forward titrations (BAEYENS & BRADBURY, 1995a).

For acid or base additions resulting in pH values in the range 6-8, some kinetic effects were observed i.e. the system tended to buffer itself back as a function of time to the starting pH of ~7. This led to some uncertainty in the value of the pH in the forward titrations.

The titration data plotted in Fig. 4.1 are taken from titration measurements made on different batches of Na-illite (IdP-1 and IdP-2), carried out on different occasions and under different conditions. Differences in comparable data points measured at different ionic strengths are considered to reflect the uncertainties associated with such measurements rather than any mechanistic related effects i.e. the overall conclusion is that no significant ionic strength effect is evident in the titration data for conditioned Na-Illite du Puy.

4.5 Process understanding

Two previously published reports can be used to help in understanding the behaviour of illite suspensions as a function of pH. The first is a study on the titration characteristics of Na-montmorillonite by BAEYENS & BRADBURY (1995a) and the second deals with some investigations carried out by POINSSOT et al. (1999) in connection with the pH dependency of sorption on Na-illite du Puy. In particular, the conclusions drawn from measurements on the water chemistry of illite suspensions below pH ~4 are relevant to the understanding of the processes influencing the form of the titration curve. The main conclusions will be briefly summarised here.

At low pH the structural elements of illite, Si, Mg and K, exhibit the same trend and show a regular increase in concentration as a function of time which is dependent on the solid to liquid ratio but independent of the $NaClO_4$ concentration. The authors were able to deduce a dissolution rate for illite at pH ~3 of ~4 x 10^{-14} mol m^{-2} s^{-1} which is similar to the values given in NAGY (1995).

The behaviour of Al, another structural element, is similar, but there is a clear influence of electrolyte concentration at pH values where the Al^{3+} cation is dominant, indicating cation exchange reactions.

Ca and Sr behave similarly, but differently from Si, Mg, K and Al. At pH 3 neither cation exhibits any release kinetics, the quantities released depend on solid to liquid ratio and there are about 2 orders of magnitude more Ca than Sr. (The measurements carried out in this work and presented in Appendix A, are entirely consistent with the data given previously in POINSSOT et al. (1999).) The inventory of Ca in the conditioned Na-illite is ~50 to ~60 mmol kg^{-1}, see for example Tables A-3 and A-4 in Appendix A, and POINSSOT et al. (1999). This is far more than the quantity arising from the Ca loading on the cation exchange sites which results from conditioning at 0.1 M $NaClO_4$ and pH ~7. (Estimated to be ~1 mmol kg^{-1}). Therefore, there is a strong suspicion that this "extra" Ca can only come from a calcium-containing solid phase which is only dissolved completely at very low pH values. As can be seen from the Ca measurements made in this study (see Figs. A-1 to A-6 in Appendix A), the Ca concentration generally increases rapidly from pH ~6 and then plateaus at pH < 4.

The form of the titration plots at pH < 4 clearly indicates that the back titrations do not compensate for the proton consumption in the forward direction. The study of BAEYENS & BRADBURY (1995a) indicated that at low pH values clay dissolution coupled with the uptake of dissolved cations by exchange on the clay mineral could be one of the reasons for the large differences between the forward and back titration measurements.

In fact, two main cation exchange processes are able to influence the titration curve. The first, of lesser importance, is proton exchange. Using a reasonable value for the H-Na selectivity coefficient of unity (GILBERT & LAUDELOUT, 1965, FOSCOLOS & BARSHAD, 1969) and an illite CEC of 225 meq kg^{-1}, the calculated fractional proton occupancy (N_H), under the most extreme experimental conditions used (pH 3 and 0.01 M $NaClO_4$), is ~0.09 which is equivalent to ~20 meq kg^{-1}. If an ≡SOH site capacity of 90 mmol kg^{-1} is taken (estimated later in Chapter 5) and it is assumed that all sites are deprotonated at pH 3, then the total proton consumption would be only (20 + 90) mmol kg^{-1} i.e. the maximum contribution from proton exchange to the total proton consumption can only be ~20 % under the most unfavourable conditions. At higher $NaClO_4$ concentrations the proton exchange contribution becomes insignificant.

At low pH values a potentially more significant process is the release of Al into solution via the dissolution of the clay and its removal by cation exchange. In order for Al to effectively cation exchange it must be present as the trivalent cation. The concentration of Al^{3+} becomes negligible at pH > 6 (BAES & MESMER, 1976). Although a new estimate for the Al-Na selectivity coefficient for illite has been obtained (see Chapter 9), and thus allowed more precise corrections to be made, it turned out in practice that the corrections applied to the 0.1 and 0.5 M $NaClO_4$ data made little difference to the form of the curve. At 0.01 M $NaClO_4$ and low pH, the clay is predominantly loaded with Ca^{2+} and Al^{3+} and the competition for exchange sites is essentially between these two cations. The corrections were somewhat erratic because they depend on the cube of the Ca concentration and the inverse square of the Al concentration (see Eq. 6). Such dependencies tend to magnify any uncertainties in these concentrations.

Finally, there is the role played by the unknown Ca containing phase. The ~50 to ~60 mmol kg^{-1} of Ca released at low pH values in the forward titration, still remain in solution after back titrating to neutral conditions. Thus, any proton consumption occurring during the dissolution of this phase is not compensated for in the back titration.

The most likely main problem with such measurements at pH <4 and >10 is simply that the major proton consumption process during the forward titration is the dissolution of the illite

(and Ca containing phase) and this is not compensated for in the back titration because the phases can not be reconstituted. Thus, there are two different processes occurring in the forward and back titrations, and therefore results from the latter cannot be used correct the measurements in the former.

We are left with a somewhat unsatisfactory situation. Batch titration measurements on clay minerals are difficult to perform and difficult to interpret. In the pH range from 5.5 to 8.5, where the proton activities are low and slight changes may have a strong influence on the net proton balance, good reproducibility is difficult to achieve. (In sorption edge measurements a buffer is required in this pH range in order to achieve acceptable reproducibility, see for example BAEYENS & BRADBURY, 1995b.) At low pH values complex dissolution processes are occurring which are not well understood. Further, dissolved cations may interact with the clay via cation exchange reactions. Also, kinetic factors are involved and the water chemistry is solid to liquid ratio dependent. Because of these factors it is not at all clear that the back titration data are of any real relevance in clay mineral systems. Even less is understood in the high pH region.

Nevertheless, and despite these difficulties and uncertainties, batch titration data on clay minerals can be interpreted to yield estimates of ≡SOH site capacities and protolysis constants. However, because of the general problems with the measurements, “best fits” for the parameters in a particular surface complexation model can only be approximately determined from the titration data alone. An iterative procedure is necessary using other data sets such as sorption edges and isotherms measured at different pH values and ionic strengths, to refine the parameter values and produce an internally consistent set of site capacities and protolysis constants.

5 Modelling Na-illite titration data

5.1 Background

Montmorillonite and illite have essentially the same structures consisting of a two dimensional array of aluminium–oxygen-hydroxyl octahedra sandwiched between a two dimensional array of silica-oxygen tetrahedra; TOT class of clay minerals (GRIM, 1953). In the case of montmorillonite, isomorphous substitution occurs in both the tetrahedral (e.g. Al for Si) and octahedral (e.g. Fe or Mg for Al) layers and the excess negative lattice charge is compensated by the adsorption of exchangeable cations on the layer surfaces. Whereas in illite, lattice substitutions occur predominantly in the tetrahedral layer and the compensating interlayer cation is predominantly potassium, which is not generally exchangeable. Only the cations on the external surfaces are exchangeable which is why the cation exchange capacity of illite (~200 meq kg^{-1}) is considerably less than montmorillonite (~1000 meq kg^{-1}) even though there is a higher degree of isomorphous substitution in illite (VAN OLPHEN, 1963). One of the main differences between illite and montmorillonite is the absence of interlayer swelling with water or organic molecules in the former.

Despite some differences, illite and montmorillonite are considered to be sufficiently structurally similar to justify the premise that essentially the same protolysis and sorption models may be valid for both systems.

5.2 The 2 site protolysis non electrostatic (2SPNE) model

In some previous work BRADBURY & BAEYENS (1997a, 1999, 2002) published a series of papers on the titration behaviour of purified Na-montmorillonite and the uptake of Ni, Zn and Eu on Na- and Ca-montmorillonite as a function of pH, element concentration and ionic strength for 1:1 and 2:1 background electrolytes.

A two site protolysis model with no electrostatic term (2SPNE model) was developed to describe the protonation and deprotonation of the amphoteric surface hydroxyl groups (sites) situated at clay platelet edges on montmorillonite. Using a two site approach with equal site capacities (4×10^{-2} mol kg^{-1}) and individual protolysis constants enabled a satisfactory description of the titration data to be obtained, particularly the ionic strength independent behaviour. The same model is used here to describe the illite titration data.

The titration curves are modelled in terms of protonation

$$\equiv SOH + H^+ \Leftrightarrow \equiv S\,OH_2^+ \qquad (1)$$

and deprotonation

$$\equiv SOH \Leftrightarrow \equiv SO^- + H^+ \qquad (2)$$

reactions on two types of weak sites ($\equiv S^{W1}OH$ and $\equiv S^{W2}OH$) described in terms of stability constants and mass action relationships without an electrostatic term

e.g. for Eq. 1

$$K^+_{protolysis} = \frac{(\equiv SOH_2^+)}{(\equiv SOH) \cdot \{H^+\}} \qquad (3)$$

where ( ) represents concentration and { } activities.

A more detailed description of the 2SPNE plus surface complexation and cation exchange sorption model, and the modelling procedures, is given later in Chapter 7.

5.3 Modelling illite titration data

As stated in section 5.1, the starting point for the modelling of the titration and sorption data in the illite system was the premise that a similar model and similar model parameters as used in the case of montmorillonite might also be appropriate to illite.

The dotted curve in Fig. 5.1 was obtained by taking the site capacities and protolysis constants for montmorillonite (BRADBURY & BAEYENS, 1997a) and applying them directly, without any changes, to model the illite titration data. As can be seen, the basic form of the calculated curve approximates that of the measured ones.

A series of iterations then followed in which the first step was to find a "best set" of parameter values for the $\equiv S^{W1}OH$ sites which fitted the acid region of the plot. This was followed by a similar procedure for the $\equiv S^{W2}OH$ sites and the basic region of the curve. Subsequently individual parameters were changed in order to fine tune the parameter set to give the best fit-by-eye to the measured data. These parameters were then preliminary fixed for the modelling exercise for the sorption edges and isotherms and then subsequently modified. This was an integral part of the iterative procedure for finally being able to fix weak site capacities and protolysis constants. (See also Chapter 8.) For example, site capacity values determine where saturation effects begin to influence sorption values and the deprotonation constant influences the position and magnitude of the peak sorption values of the different species making a contribution to the sorption edge, see sections 6.1 and 6.2. Of course, the same site capacities and protolysis constants have to be applicable to all of the sorption measurements for every metal for which reliable data exists. Each time a protolysis parameter is changed, the modelling of the titration measurements has to be repeated. Once other data, in addition to the titration data, are included in the iterative procedure used to fix the protolysis parameters, the scope for parameter variation becomes very narrow.

The outcome of this procedure is shown in Fig. 5.1, where the solid line has been modelled using the site types, site capacities and protolysis constants estimated for Na-illite and summarised in Table 5.1. These values are now fixed in all future calculations for the sorption edges and isotherms.

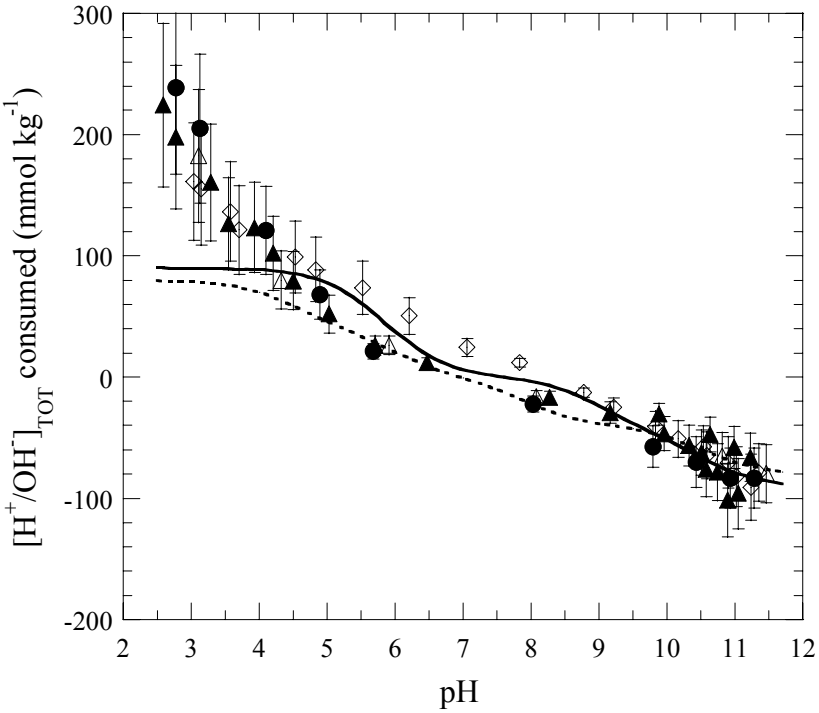

Fig. 5.1: Titration data plus modelling using the 2SPNE model. The dotted line is calculated using the montmorillonite site capacities and protolysis constants (BRADBURY & BAEYENS, 1997a). The full line is calculated with the parameters given in Table 5.1.

Table 5.1: Summary of site types, site capacities and protolysis constants determined for Na-illite.

Site types:	Site capacities:
$\equiv S^{S}OH$	2.0×10^{-3} mol kg^{-1}
$\equiv S^{W1}OH$	4.5×10^{-2} mol kg^{-1}
$\equiv S^{W2}OH$	4.5×10^{-2} mol kg^{-1}
Surface complexation reactions	**log $K_{protolysis}$**
$\equiv S^{S}OH + H^{+} \Leftrightarrow \equiv S^{S}OH_2^{+}$	5.5
$\equiv S^{S}OH \Leftrightarrow \equiv S^{S}O^{-} + H^{+}$	-6.2
$\equiv S^{W1}OH + H^{+} \Leftrightarrow \equiv S^{W1}OH_2^{+}$	5.5
$\equiv S^{W1}OH \Leftrightarrow \equiv S^{W1}O^{-} + H^{+}$	-6.2
$\equiv S^{W2}OH + H^{+} \Leftrightarrow \equiv S^{W2}OH_2^{+}$	9.0
$\equiv S^{W2}OH \Leftrightarrow \equiv S^{W2}O^{-} + H^{+}$	-10.5

6 Sorption measurements

6.1 Procedures and techniques

Batch sorption experiments were designed to produce two main types of data sets: sorption measured at trace radionuclide concentrations as a function of pH at a fixed ionic strength (sorption edges), and sorption measured as a function of sorbate concentration at constant pH and ionic strength (sorption isotherms).

The preparatory experiments carried out prior to the sorption tests, and the methodology used for the sorption measurements themselves, were essentially the same as those reported in BAEYENS & BRADBURY (1995b), POINSSOT et al. (1999), and are briefly outlined below. Further details can be found in the above references.

Radiotracers: Source radiotracer solutions of ^{85}Sr and ^{63}Ni were purchased from Amersham International Plc, U.K., and ^{152}Eu from Isotope Products Europe, Germany. A ~4.2×10^{-4} M $^{233}U(VI)$ source solution was used for the uranium sorption experiments. Each source tracer solution was diluted in ~50 ml of de-ionised water to produce a stock solution having a pH of ~1. The stock solutions were then used to label standard solutions at the required $NaClO_4$ concentrations. The standard solutions were always allowed to stand at least overnight in the glove box in order to ensure equilibrium with the container walls before pipetting aliquots for use in the experiments.

Radio-assay: Aqueous activities were measured using either a Canberra Packard Tri-Carb 2250 CA liquid scintillation analyser (^{63}Ni and ^{233}U), or a Canberra Packard Cobra Quantum gamma counter (^{85}Sr and ^{152}Eu). Labelled solutions having comparable activities and background electrolyte concentrations to those used in the experiments were also prepared as counting standards. These were always counted simultaneously with the solutions from the batch sorption tests.

Glove Boxes: All experiments were carried out in controlled N_2 atmosphere glove boxes. ($CO_2 \leq 2$ ppm, $O_2 \leq 2$ ppm.)

pH: For the sorption experiments at 0.01 and 0.1 M $NaClO_4$ the pH measurements were carried out using a WTW Microprocessor 535 or a Metrohm 691 pH meter and Inlab (Mettler) and Metrohm combination pH electrodes. Electrode calibrations were carried out using Titrisol™ buffer solutions from Merck. For the experiments at 0.5 M $NaClO_4$ Metrohm double junction pH electrodes were used which contained 3 M KCl in the inner electrode and 3 M NaCl in the outer electrode. This avoided $KClO_4$ precipitation which tended to occur with standard combination electrodes containing 3 M KCl. The double junction electrodes were calibrated in 0.5 M $NaClO_4$ solutions containing known concentrations of HNO_3 and NaOH. The pH was obtained from the known proton concentration and the solution activity coefficient at 0.5 M $NaClO_4$ calculated using the Davies equation with $C_D = 0.3$ (DAVIES, 1962).

Buffers: The buffers listed in Table 6.1 were used at concentrations of ~10^{-3} M in the sorption edge and isotherm experiments to maintain constant pH conditions. A series of separate experiments showed that there was no significant influence of these buffers on sorption for the range of conditions used.

Table 6.1: Buffers used in the sorption measurements. (Data taken from PERRIN & DEMPSEY, 1974.)

Buffer	pK_a	pH range
AA (Acetic Acid)	4.76	4.2 - 5.2
MES (2-(N-morpholino)ethane-sulphonic acid)	6.15	5.7 - 6.7
MOPS (3-(N-morpholino)propanesulphonic acid)	7.20	6.8 - 7.7
TRIS (Tris(hydroxymethyl)aminomethane	8.06	7.5 - 8.5
CHES (3-(cyclohexyl amino)ethanesulphonic acid)	9.55	9.0 - 10.0

Solution stability: Sr is highly soluble under the experimental conditions used to measure the isotherm at pH 7 and the maximum concentration used was 10^{-3} M.

The maximum Ni concentrations used in the sorption isotherm measurements made at pH 7 and at pH 6 were 10^{-3} and 10^{-2} M respectively. These values lie approximately two orders of magnitude below the predicted solubility limits for $NiO/Ni(OH)_2$.

For the Eu isotherm at pH 5.5 the maximum concentration used in the experiments was 10^{-3} M. This is orders of magnitude less than the solubility limit predicted for either crystalline or amorphous $Eu(OH)_3$. At pH 7, a Eu solution concentration of 4 x 10^{-4} M was shown to be stable. However, this concentration is above the solubility limit predicted for crystalline $Eu(OH)_3$, but below that predicted for amorphous $Eu(OH)_3$ (HUMMEL et al., 2002). Only data measured at concentrations less than 10^{-4} M Eu were used in the isotherm plot given in Fig. 10.11.

The highest initial concentrations used in the U isotherm measurements carried out at pH 4.8 and 5.8 were 10^{-3} and 10^{-5} M respectively. Both stability tests (radioactivity assays made before and after centrifugation at 96000 *g* (max.)) and speciation calculations indicated that these solutions were stable and there were no indications in the sorption experiments that precipitation was occurring over the time scale of the tests.

Phase separation: Sorption experiments were generally performed in 40 ml polypropylene tubes (S:L ratio ~1 g L^{-1}) and phase separations were carried out by centrifugation in a Beckman L7 for one hour at 96000 *g* (max.).

Sorption kinetics: Kinetic tests were performed at trace concentrations in buffered 0.1 M $NaClO_4$ suspensions of conditioned Na-illite (S:L ~0.3 g L^{-1}) as a function of pH for times between 1 and 18 days as described in detail in POINSSOT et al. (1999).

The sorption kinetics for Sr and U (this work) were rapid, reaching equilibrium in less than 1 day. For Ni and Eu the kinetics were similar to one another but slower than for Sr. Nevertheless, only ~3 days were required to reach a steady state. Subsequent sorption experiments were shaken for at least 7 days.

Wall Sorption: For the conditions used in the majority of experiments described in this report, the effect of wall sorption in the batch sorption tests was to introduce an uncertainty in the log R_d values of ~0.05 log units.

Errors: A formal estimate of the maximum absolute error yielded an uncertainty in log R_d of ~0.15 log units. Sets of repeat measurements indicated that ± 0.2 log units covered the spread in the log R_d values, BAEYENS & BRADBURY (1995b).

However, for very low sorption values (only a few % of the radiotracer sorbed) or where sorption was very high (~99% of the radiotracer sorbed), the variability in comparable data indicated that the uncertainties in the log R_d values could be ± 0.5 log units, or even higher.

6.2 Sorption edges and isotherms

Sorption edge measurements were always carried out at trace radionuclide concentrations. (Initial tracer concentrations are listed in the tables summarising the experimental conditions for each radionuclide in Tables 9.1, 10.1, 10.3 and 10.5). The procedure used was similar for all radionuclides. The standard labelled $NaClO_4$ solution (0.01 M, 0.1 M, 0.5 M) were pipetted into a 40 ml polypropylene centrifuge tube. In the pH range 4 to 9 it was necessary to use buffers (~10^{-3} M) in order to ensure pH stability during the experiments. The particular buffers were chosen (Table 6.1) because of their very weak tendencies to complex with metals. For strongly acidic (pH < 4) or alkaline conditions (pH > 9), buffers were not used and just HNO_3 or NaOH Titrisol™ solutions were added. As the last step in the preparation procedure aliquots of conditioned Na-illite suspensions (corresponding to ~50 mg Na-illite) were pipetted from the vigorously stirred stock suspension into the centrifuge tubes. The tubes were then closed with screw caps and shaken end-over-end for at least 7 days. Subsequently they were removed from the glove box and centrifuged at 96000 *g* (max.) for one hour before returning them to the glove box for pH measurement and sampling of the supernatant solution for radio-assay.

For the isotherm determinations a series of salt solutions covering the nuclide concentration range required was made up at the desired pH in a constant $NaClO_4$ background electrolyte containing buffer and labelled as appropriate. Aliquots of conditioned Na-illite suspensions were pipetted into 40 ml centrifuge tubes followed by additions of the labelled salt solutions. An identical procedure to that described above was then followed.

6.3 Presentation of the sorption results

Sorption measurements are often presented in terms of percentage or fraction of the nuclide inventory sorbed as a function of some parameter (pH, time, equilibrium concentration, ionic strength). However, it has been pointed out by several authors that representing data in this way can often be less sensitive than when sorption results are expressed as distribution coefficients, R_d values (see for example JANNASCH et al., 1988; BRADBURY & BAEYENS, 1997b). In the following, batch sorption edge measurements are presented in terms of the logarithm of the distribution ratio, R_d, defined in the usual manner as:

$$R_d = \frac{C_{init.} - C_{eq.}}{C_{eq.}} \cdot \frac{V}{m} \qquad (4)$$

where,

$C_{init.}$: Total (active + inactive) initial aqueous nuclide concentration (mol L^{-1})

$C_{eq.}$: Total (active + inactive) equilibrium aqueous nuclide concentration (mol L^{-1})

V: volume of liquid phase (L)

m: mass of solid phase (kg)

Sorption isotherms data are plotted as the quantity of element sorbed per unit mass of solid (mol kg^{-1}) versus the equilibrium aqueous concentration (mol L^{-1}). In such plots, a gradient of unity is indicative of linear sorption, i.e. R_d is constant as a function of concentration, and a gradient less than unity indicates non-linear sorption behaviour, i.e. R_d decreases with increasing concentration.

7 Sorption model description

The multi-site sorption model combining surface complexation and cation exchange used to describe the uptake of aqueous metal species on montmorillonite is summarised below together with the associated assumptions and simplifications (BRADBURY & BAEYENS, 1997a). The same model was also applied to quantitatively describe the sorption of Sr(II), Ni(II), Eu(III) and U(VI) on illite.

7.1 Cation exchange

The permanent negative charge on clay mineral surfaces, arising from isomorphous substitution, is compensated by an excess of aqueous cations held by electrostatic attraction closely around the outside of the Si-Al units. Electrostatically bound cations can exchange with other cations in solution in reactions which are fast, stoichiometric and reversible (GRIM, 1953; VAN OLPHEN, 1963; BOLT et al., 1976). In principle, the sorption due to cation exchange is independent of pH except, for example, where dissolution of the clay mineral leads to the release of competing cations (see Chapter 9).

The well-established and widely used approach of representing cation exchange reactions in terms of a selectivity coefficient (VANSELOW, 1932; GAINES & THOMAS, 1953; BOLT, 1967) obtained by the application of the mass action law has been used. Consider a metal B of valency z_B exchanging with metal A valency z_A on a clay mineral in the A-form:

$$z_B A^{z_A}\text{-clay} + z_A B^{z_B} \;<=>\; z_A B^{z_B}\text{-clay} + z_B A^{z_A} \tag{5}$$

Following the GAINES & THOMAS (1953) convention, the thermodynamic constant, K, for the reaction can be defined as:

$${}^{B}_{A}K = \frac{(N_B)^{z_A}}{(N_A)^{z_B}} \cdot \frac{(f_B)^{z_A}}{(f_A)^{z_B}} \cdot \frac{[A]^{z_B}}{[B]^{z_A}} \cdot \frac{(\gamma_A)^{z_B}}{(\gamma_B)^{z_A}} = {}^{B}_{A}K_c \cdot \frac{(f_B)^{z_A}}{(f_A)^{z_B}} \tag{6}$$

where:

${}^{B}_{A}K$ = thermodynamic exchange constant

${}^{B}_{A}K_c$ = selectivity coefficient

N_A and N_B = equivalent fractional occupancies, defined as the equivalents of A (or B) sorbed per unit mass divided by the CEC in eq. kg^{-1}

f_A and f_B = surface activity coefficients

[A] and [B] = aqueous concentrations (mol L^{-1})

γ_A and γ_B = aqueous phase activity coefficients.

A selectivity coefficient can be derived from experimental data in the following way. Defining the distribution ratio, R_d, as:

$$R_d = \frac{\text{Quantity of sorbate on the solid per unit mass}}{\text{Equilibrium sorbate aqueous concentration}} \tag{7}$$

and noting that ($N_B \cdot$ CEC) equals the quantity of metal B sorbed in eq. kg^{-1}, Eq. 7 then becomes:

$$ {}^{B}R_d = \frac{N_B}{[B]} \cdot \frac{CEC}{z_B} \tag{8} $$

At trace sorbate concentrations, $N_A \sim 1$, Eq. 6 can be re-arranged to give:

$$ {}^{B}_{A}K_c = \left({}^{B}R_d\right)^{z_A} \cdot \frac{(z_B)^{z_A}}{(CEC)^{z_A}} \cdot [A]^{z_B} \cdot \frac{(\gamma_A)^{z_B}}{(\gamma_B)^{z_A}} \tag{9} $$

The selectivity coefficient, ${}^{B}_{A}K_c$, calculated from the experimental sorption edge measurements (see section 4.1) equals the thermodynamic constant ${}^{B}_{A}K$ multiplied by the ratio of the surface activity coefficients, $(f_A)^{z_B}/(f_B)^{z_A}$, see Eq. 6. Surface activity coefficients are not well known quantities and could vary as a function of the relative occupancies (GAINES & THOMAS, 1953; BOLT, 1982). ${}^{B}_{A}K_c$ can only be regarded as being a constant at trace concentrations ($N_A \rightarrow 1$, $f_A \rightarrow 1$), or under the condition that $(f_A)^{z_B}/(f_B)^{z_A}$ remains constant as the occupancy of B changes. In the latter case the sorption due to cation exchange as a function of sorbate concentration would then remain constant.

7.2 Surface complexation

The pH dependent component of sorption on montmorillonite is described by sorbate uptake on the amphoteric surface hydroxyl groups (≡SOH sites) situated at clay platelet edges (see for example SPOSITO, 1984; DAVIS & KENT, 1990). Similar to the proposals presented for oxides by DZOMBAK & MOREL (1990), strong (≡S^SOH) and weak (≡S^WOH) sorption site types are considered, with the difference that two weak site types (≡S^{W1}OH and ≡S^{W2}OH) were required to describe the titration behaviour of montmorillonite. (The modelling of titration measurements carried out at different ionic strengths indicated that the ≡S^{W1}OH and ≡S^{W2}OH sites have the same capacities but different protolysis constants.) The ≡S^SOH and ≡S^{W1}OH type sites are assumed to have the same protolysis constants (see Table 5.1) and, as discussed in BRADBURY & BAEYENS (1997a), surface complexation reactions occur predominantly on these sites. The ≡S^SOH sites have a much smaller capacity but form considerably stronger complexes with metals and dominate the sorption at trace concentrations.

A surface complexation reaction representing for example the sorption of a metal Me of valency z_M on the strong sites may be written as:

$$ \equiv S^SOH + Me^{z_M} \;<=>\; \equiv S^SOMe^{(z_M-1)} + H^+ \tag{10} $$

In a non-electrostatic model, the corresponding surface complexation constant, $K_{Me^{z_M}}$, can be expressed as:

$$ K_{Me^{z_M}} = \frac{[\equiv S^SOMe^{(z_M-1)}]}{[\equiv S^SOH]} \cdot \frac{f_{\equiv SOM^{(z_M-1)}}}{f_{\equiv SOH}} \cdot \frac{\{H^+\}}{\{Me^{z_M}\}} \tag{11} $$

where { } terms are aqueous activities and [ ] terms are concentrations. Following the discussions given in DZOMBAK & MOREL (1990), the same assumption concerning surface activity coefficients is made here i.e. the ratio of the surface activity coefficients in the mass action equations describing the surface complexation reactions is taken to be unity.

A major feature of the modelling exercises performed by BRADBURY & BAEYENS (1997a, 1999, 2002) was that an electrostatic term was not required in the mass action equations describing protolysis and surface complexation reactions used to reproduce the experimental data. This does not imply that the surface species are not charged nor that electrostatic effects may not be involved in protolysis and aqueous metal species uptake on the ≡SOH sites, but rather, unlike the case of oxides, electrostatic terms are apparently of secondary importance in the model description of sorption on montmorillonite, see BRADBURY & BAEYENS (1995, 1997b).

Outer sphere complexes of Me on the edge sites are not considered in the model. As mentioned above, the relative capacities of the permanent charge sites and the maximum outer sphere complex capacity of the edge sites are well over an order of magnitude different. Modelling the cation exchange contribution to the overall sorption was achieved using a single selectivity coefficient for each data set. Generally, good agreement with the data was found over a wide range of conditions: pH, background electrolyte concentrations and sorbate concentration. Thus, on the basis of the currently available experimental evidence, it was not considered a necessity to introduce an additional parameter describing the formation of outer sphere complexes.

7.3 MINSORB

In all of the fitting/modelling work described in the following chapters, the computer code MINSORB was used (BRADBURY & BAEYENS, 1997a). MINSORB is basically the geochemical speciation code MINEQL (WESTALL et al., 1976) containing a sub-routine for calculating surface complexation via a non-electrostatic model. Cation exchange was incorporated into the code and is included in all of the calculations given later using the selectivity coefficients derived from sorption edge measurements.

MINSORB is a relatively flexible code allowing speciation and sorption by cation exchange and surface complexation to be calculated simultaneously for mixtures of elements in any given water chemistry on different solid phases. Aqueous activity coefficients are calculated using the Davies relation with a value of 0.3 for the C_D constant (DAVIES, 1962). The hydrolysis constants used in the modelling are given in Table 7.1. For U(VI) polynuclear species (HUMMEL et al., 2002) were included in the calculations and were assumed to be non-sorbing.

Table 7.1: Hydrolysis constants for Sr(II), Ni(II), Eu(III) and U(VI) used in the sorption modelling.

	*Sr(II)	*Ni(II)	**Eu(III)	*U(VI)
$Me(OH)^{(z_M-1)}$	-13.29	-9.5	-7.2	-5.2
$Me(OH)_2^{(z_M-2)}$	-	-18	-15.1	-12.0
$Me(OH)_3^{(z_M-3)}$	-	-29.7	-26.2	-19.2
$Me(OH)_4^{(z_M-4)}$	-	-45	-	-33.0

* HUMMEL et al. (2002)

** NEA (2003). The stability constants for Eu were assumed to be the same as those for Cm and Am.

8 Modelling approach

The approach adopted to model the sorption data on Na-illite was the same throughout. The procedures outlined below are a somewhat simplified version of the iterative process actually used. (Further details can be found in BRADBURY & BAEYENS, 1997a.)

Site types, their individual capacities and the protolysis constants associated with them, were considered to be non-adjustable parameters and were fixed in all of the calculations at the values given in Table 5.1. A value of 225 meq kg^{-1} was used throughout for the CEC of illite.

In the modelling of the pH dependency in the sorption edges, a stepwise approach was adopted by considering, in sequence, simple chemically reasonable surface complexation reactions based on the aqueous speciation.

As an illustrative example consider again a metal Me of valency z_M. The initial step was to calculate the aqueous speciation of Me in the pH range and for the background electrolyte used in the sorption measurements. In the pH range where the dominant aqueous species was the free Me^{z_M} cation, the first and simplest surface complexation reaction to be considered was:

$$\equiv S^SOH + Me^{z_M} \quad \Leftrightarrow \quad \equiv S^SOMe^{(z_M-1)} + H^+ \tag{12}$$

The situation often arose that the rising edge of the sorption curve and the sorption plateau at higher pH could not be fitted simultaneously with a single reaction: any approximate fit to the first resulted in a substantial underestimate in the second. In this case the procedure was to find the best fit for the free metal cation to part of the edge, Eq. 12, and then fix this surface complexation constant in the subsequent modelling steps. Next, a surface reaction with the first hydrolysis species was considered, Eq. 13, and the process repeated and so on for the second, Eq. 14, third, Eq. 15, etc hydolysis species until a satisfactory fit to the whole sorption edge was obtained.

$$\equiv S^SOH + Me^{z_M} + H_2O \quad \Leftrightarrow \quad \equiv S^SOMeOH^{(z_M-2)} + 2\ H^+ \tag{13}$$

$$\equiv S^sOH + Me^{z_M} + 2\ H_2O \quad \Leftrightarrow \quad \equiv S^sOMe(OH)_2^{(z_M-3)} + 3\ H^+ \tag{14}$$

$$\equiv S^SOH + Me^{z_M} + 3\ H_2O \quad \Leftrightarrow \quad \equiv S^SOMe(OH)_3^{(z_M-4)} + 4\ H^+ \tag{15}$$

An iterative procedure then followed to find the best fit to the data and "fine tune" the surface complexation constants. It was found that with sorption edges presented in the log R_d versus pH form, the fits to the data are rather sensitive to the surface complexation constants chosen and that fitting by eye worked quickly and well for the stepwise procedures used. Where isotherms or sorption edges at higher sorbate concentrations were modelled, a similar modelling procedure to that given above was applied to the weak sites, $\equiv S^{W1}OH$.

All of the parameter values required in surface complexation models cannot be measured independently, and hence calibration by fitting parameters to experimental data is an integral part of the modelling process. Generally it is relatively easy to find a model and fit parameters which provide a good quantitative description to individual data sets e.g. a titration curve or a sorption edge. Finding such a fit to one set of data alone does not allow any statement concerning the general validity of a model and the associated fit parameters to be made. However, if other sets of measurements are available, and the fit parameters derived from one data set become a fixed sub-set of parameters for a description of all of the subsequent data sets, then the overall constraints on the model and parameters becomes large. It is clear from the

above that a significant quantity of measured data has to be in place in order to be able to adequately test the model.

In the acid region of the sorption edges, R_d values are normally observed to be constant and independent of pH. The uptake of the particular sorbate is then interpreted as being due to cation exchange on the permanently charged planar sites. Appropriate equations, similar to those given in section 7.1, are then used to fit a single selectivity coefficient to the experimental data. The selectivity coefficient is then fixed and cation exchange is included in all of the calculations. However, in the experiments with illite, the trivalent Al^{3+} cation (pH < 5) and Ca + Mg are known to be present in the aqueous phase at sufficient concentrations to compete strongly with the radionuclide for the available exchange sites. The corresponding Al-Na and (Ca+Mg)-Na selectivity coefficients had to be determined in order to model the measurements carried out at low ionic strength (0.01 M $NaClO_4$) and pH. This is described in Chapter 9. The competitive effects are complex because the Al and Ca + Mg concentrations change as a function of pH necessitating a separate calculation at each pH.

Experience with the modelling indicated that it was easier and more efficient in the initial iteration to fit the surface complexation component of sorption first. Once the preliminary surface complexation parameters had been determined, these, together with the fixed Al-Na and (Ca + Mg)-Na selectivity coefficients and corresponding Al and Ca + Mg concentrations at a particular pH, were used, together with an estimate of the radionuclide selectivity coefficient, to calculate a sorption value. Once the experimental sorption value had been reproduced reasonably well, similar calculations were then carried out at other pH values using this radionuclide selectivity coefficient. Iterations over the different pH values were continued until a satisfactory fit with one set of parameters was achieved. An attempt was then made to model the next set of data, and the iterations were then carried out between the different sorption edge data sets. Finally, the radionuclide selectivity coefficient was defined.

In some cases sorption edge measurements have been extended to above pH 10 and even though the values appear to be consistent with the rest of the measurements there exists some doubt regarding the validity of such data because of clay dissolution effects. It is well known that clay minerals become unstable at high pH values (see for example SAVAGE et al., 1990, 1991) and the potential effects this may have on the surface condition of the clay, and hence the sorption site characteristics, is unknown. Further, the dissolution of clay mineral forming elements such as Al and Si may form secondary mineral phases in the alkaline media which could also influence the sorption measurements. Consequently, the sorption edge measurements and modelled curves above pH 10 should be treated with caution.

9 Sorption of Sr(II) on Na-illite

Sorption edges for Sr on Na-illite were determined at trace concentrations in 0.01 and 0.1 M $NaClO_4$. An isotherm in 0.1 M $NaClO_4$ was also measured at neutral pH. The measurements are presented in Figs. 9.1 and 9.2 respectively and the corresponding experimental conditions are summarised in Table 9.1.

Table 9.1: Experimental conditions for the Sr sorption measurements on conditioned Na-illite.

Type of experiment	edge	edge	isotherm
$NaClO_4$ (M)	0.01	0.1	0.1
pH	2.7 – 11.1	2.7 – 10.9	7.0 ±0.1
S:L ratio (g L^{-1})	1.5 – 1.9	1.8	1.8
Initial Sr concentration (M)	10^{-9}	10^{-9}	10^{-3} - 10^{-5}
Buffers	Yes	Yes	MOPS
Equilibration time (days)	7	7	7

In a bivalent-monovalent cation exchange system the competition to the sorption of the bivalent cation increases as the square of the monovalent cation concentration, see Eq. 9. Consequently measurements at 0.5 M $NaClO_4$ were not performed because the Sr sorption would be a factor of 25 times less than at 0.1 $NaClO_4$ and thus hardly measurable.

The uptake of Sr on Na-illite is expected to be dominated by a cation exchange processes. Although this is in general what the plots in Fig. 9.1 indicate, their forms cannot be described by a simple Sr-Na exchange reaction.

From the discussion in section 4.5, and the data presented in Appendix B, there is clear and quantitative evidence that the solution in equilibrium with a conditioned Na-illite/$NaClO_4$ background electrolyte varies significantly as a function of pH. Furthermore, the composition is also a function of time and S:L ratio (POINSSOT et al., 1999).

Figs. B-1 to B-3 in Appendix B show the concentrations of Mg, Ca and Al in 0.01 and 0.1 M solutions of $NaClO_4$ respectively, which were contacted with Na-illite at S:L ratios and times comparable to those used in the sorption tests. The concentrations of Mg, Ca and Al at selected pH values were taken from these figures and are given in Tables 9.2 and 9.3 for 0.01 and 0.1 M $NaClO_4$ illite systems respectively. Mg and Ca appear as ubiquitous impurities in the aqueous phase of illite suspensions despite the fact that a careful conditioning process was carried out. (Note that other cations were also present (see Tables B-1 to B-3) but are not considered further here because their concentrations were too low to influence the exchange reactions of Sr.)

At neutral pH, the principal impurity cations in solution arising from the interaction between the Na-illite and the background electrolyte are Mg and Ca, Tables 9.2 and 9.3. (The Al is no longer present as a trivalent cation at this pH.) The chemistries of these two elements are so similar to Sr that to a good, first approximation, the three cations can be treated the same. That is, the selectivity coefficients and sorption behaviour of Sr, Ca and Mg in the two systems under consideration are considered to be essentially the same. Thus the distribution ratio measured for Sr at trace concentrations is the same as the distribution ratios for Ca and Mg in the same system (Ca ≡ Mg ≡ Sr ≡ Me).

Table 9.2: Average Mg, Ca and Al concentrations in 0.01 M $NaClO_4$ conditioned Na-illite. (Taken from Figs. B-1 and B-2, Appendix B.)

pH	Mg (M)	Ca (M)	Al (M)
3	3.0×10^{-5}	1.2×10^{-4}	9.0×10^{-5}
4	1.4×10^{-5}	9.0×10^{-5}	1.2×10^{-5}
5	5.0×10^{-6}	3.5×10^{-5}	3.0×10^{-6}
6	2.0×10^{-6}	1.2×10^{-5}	2.0×10^{-6}
7	2.0×10^{-6}	7.0×10^{-6}	3.0×10^{-6}

Table 9.3: Average Mg, Ca and Al concentrations in 0.1 M $NaClO_4$ conditioned Na-illite. (Taken from Fig. B-3, Appendix B.)

pH	Mg (M)	Ca (M)	Al (M)
3	3.0×10^{-5}	1.1×10^{-4}	1.2×10^{-4}
4	1.7×10^{-5}	1.1×10^{-4}	4.0×10^{-5}
5	1.0×10^{-5}	8.0×10^{-5}	1.2×10^{-5}
6	5.0×10^{-6}	4.5×10^{-5}	4.0×10^{-6}
7	3.0×10^{-6}	2.0×10^{-5}	1.2×10^{-6}

At 0.01 M $NaClO_4$ the occupancy of Ca + Mg can be calculated at pH 7 from the sum of the Ca and Mg concentrations and the Sr distribution ratio, Table 9.4. If the calculated occupancy of ~72 meq kg^{-1} is used with a CEC of 225 meq kg^{-1} for illite, a selectivity coefficient for (Ca+Mg)-Na exchange of 9.3 can be obtained from

$$ {}^{(Ca+Mg)}_{Na}K_c = \frac{N_{(Ca+Mg)}}{(N_{Na})^2} \cdot \frac{[(Na) \cdot \gamma_{Na}]^2}{(Ca + Mg) \cdot \gamma_{(Ca+Mg)}} \qquad (16) $$

where

$$ N_{(Ca+Mg)} = \frac{\text{quantity (Ca + Mg) sorbed (meq kg}^{-1})}{\text{CEC (meq kg}^{-1})} , $$

$$ N_{Na} = \frac{\text{quantity Na sorbed (meq kg}^{-1})}{\text{CEC (meq kg}^{-1})} , $$

( ) represent molar concentrations, γ are solution activity coefficients.

At 0.1 M $NaClO_4$ and pH 7, the loadings of bivalent ions are so low that they cannot be calculated with any accuracy from the solution concentrations and the sorption data. A good approximation in this case is to take the fractional occupancy of Na (N_{Na}) to be unity. Under these circumstances Eq. 9, can be used to calculate the selectivity coefficient directly (see for example BRADBURY & BAEYENS, 1994).

$$ {}^{Sr}_{Na}K_c = 2 \cdot R_d(Sr) \cdot \frac{1}{CEC} \cdot \frac{(\gamma_{Na})^2}{\gamma_{Sr}} \cdot (Na)^2 \qquad (17) $$

Table 9.4: Sr distribution ratios (R_d(Sr)) together with Ca and Mg concentrations measured in the liquid phase at pH 7 in 0.01 and 0.1 M $NaClO_4$.

	0.01 M $NaClO_4$	0.1 M $NaClO_4$
log R_d (Sr) (L kg^{-1})	3.6	2.0
Ca concentration (M)	7.0×10^{-6}	2.0×10^{-5}
Mg concentration (M)	2.0×10^{-6}	3.0×10^{-6}
Occupancy of (Ca+Mg) (meq kg^{-1})	72	-
Occupancy of Na (meq kg^{-1})	153	-
${}^{Sr}_{Na}K_c$	9.3	14.3

For an R_d (Sr) value of 100 L kg^{-1}, Fig. 9.1, a CEC of 0.225 eq. kg^{-1}, the calculated ${}^{Sr}_{Na}K_c$ is 14.3.

From the two sets of Sr sorption edge data an average value for ${}^{Sr}_{Na}K_c$ of 11 was taken and held constant in all further calculations. (As stated previously, this selectivity coefficient is also valid for Ca and Mg)

In the pH range below ~7, the concentrations of Ca, Mg and Al, and the aqueous speciation of Al, are pH dependent, Tables 9.2 and 9.3. Hence the modelling had to be done on a pH-by-pH basis. In this pH region the Al^{3+} component of the total dissolved aluminium concentration will compete with the bivalent cations for the available exchange sites. It was found that with a fixed value of ${}^{Sr}_{Na}K_c$ equal to 11 the two Sr sorption edges at 0.01 and 0.1 M $NaClO_4$ could be modelled as a function of pH and solution concentration using a single value for the Al-Na selectivity coefficient of 10. The modelled curves are given as continuous lines in Fig. 9.1, pH < 7.

What remained was to model the Sr sorpton edge behaviour at pH values greater than 7. Some previous work on the uptake of Ca on montmorillonite (BRADBURY & BAEYENS, 1995) showed that this bivalent alkali earth metal is taken up on the clay mineral by surface complexation on the $\equiv S^{W2}OH$ sites. The modelling of the Sr sorption edges on Na-illite revealed the same behaviour i.e. there was no contribution required from the $\equiv S^{S}OH$ and $\equiv S^{W1}OH$ sites to model the data. (Note that for the reasons given above, Sr will behave the same as Ca + Mg.) Both data sets in Fig. 9.1 could be modelled over the whole pH range by simultaneously considering cation exchange (as above) and the surface complexation reaction:

$$\equiv S^{W2}OH + Sr^{2+} \Leftrightarrow \equiv S^{W2}OSr^{+} + H^{+} \quad (18)$$

The Sr isotherm at pH 7 in Fig. 9.2 was modelled with the single selectivity coefficient of 11 for Me-Na exchange, as given above. The background concentration of Ca + Mg in this experiment was 9×10^{-6} M which, because "Ca ≡ Mg ≡ Sr", sets a limit to the lowest equilibrium concentration at which the sorption of Sr can be measured in the system. The surface reactions, selectivity coefficients and surface complexation constants used to model the Sr sorption edges and isotherm data in Figs. 9.1 and 9.2 are summarised in Table 9.5.

Table 9.5: Site types, site capacities and mass action equations and associated constants used in the modelling of Sr on Na-illite.

Site types:	Site capacities:
CEC	2.25×10^{-1} meq kg^{-1}
$\equiv S^{W2}OH$	4.5×10^{-2} mol kg^{-1}
Cation exchange reactions	K_C
2 Na-illite + $Me^{2+} \Leftrightarrow$ Me-illite + 2 Na^+	11
3 Na-illite + $Al^{3+} \Leftrightarrow$ Al-illite + 3 Na^+	10
Surface complexation reaction	log K_{SC}
$\equiv S^{W2}OH + Me^{2+} \Leftrightarrow \equiv S^{W2}OMe^+ + H^+$	-5.0

Me = Mg, Ca, Sr

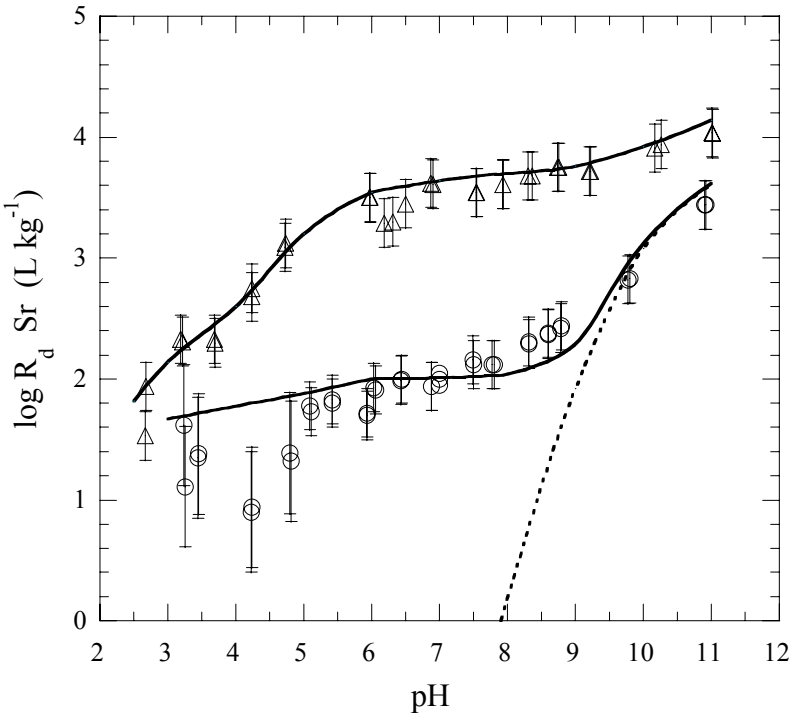

Fig. 9.1: Sr sorption edge measurements (Poinssot et al., 1999) on conditioned Na-illite (IdP-1) in (○) 0.1 M NaClO4 and (△) 0.01 M $NaClO_4$. The full lines are the modelled curves using the data given in Tables 5.1 and 9.5. The dotted line represents the contribution from Sr uptake on the $\equiv S^{W2}OH$ type sites.

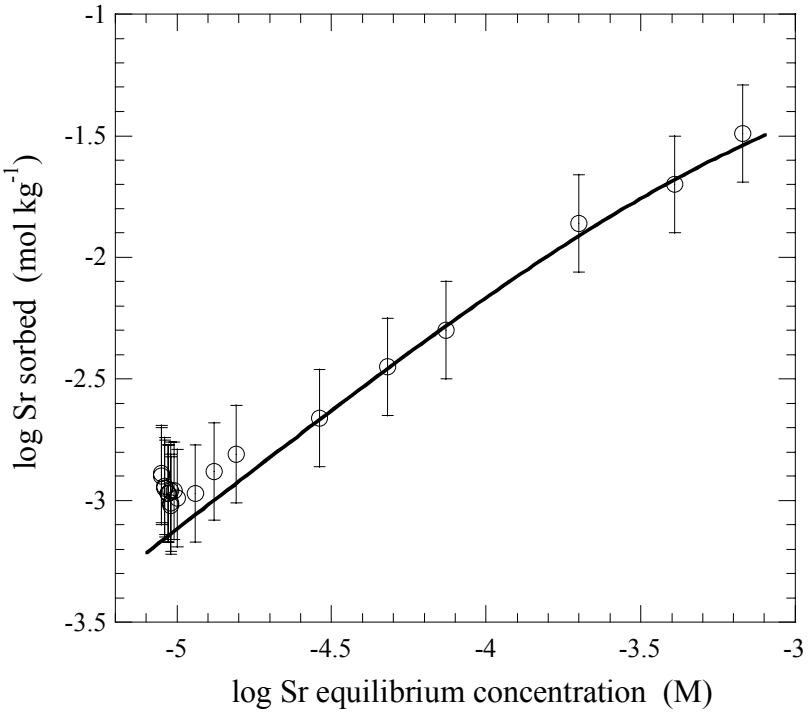

Fig. 9.2: Sr sorption data (POINSSOT et al., 1999) as a function of equilibrium concentration on conditioned Na-illite (IdP-1) in 0.1 M $NaClO_4$ at pH 7.0. The full line is the modelled curve using the data given in Tables 5.1 and 9.5.

10 Sorption of Ni(II), Eu(III) and U(VI) on Na-Illite

10.1 General

The modelling of the sorption edges for Ni, Eu and U was somewhat more difficult than for Sr. Particularly in the case of the measurements in 0.01 M $NaClO_4$, uptake by both surface complexation and cation exchange, including competition, appeared to be determining the form of the curves at pH < 7. In order to avoid modelling with two or more parameters simultaneously (associated with two different mechanisms), the following approach was adopted.

For a sorption edge, the contribution of cation exchange to the overall sorption generally becomes less the higher the background electrolyte concentration and the higher the pH. Consequently, the data at the highest $NaClO_4$ concentrations were considered first (0.5 M $NaClO_4$ in the case of Ni and Eu, and 0.1 M $NaClO_4$ in the case of U(VI)) and modelled in terms of surface complexation reactions only, following the procedure described in Chapter 8. After this initial modelling step the edge data at 0.1 M $NaClO_4$ were included (for Ni and Eu) and the calculations were iterated between the two data sets until the best fits-by-eye were found. (For U, only the one data set at 0.1 M $NaClO_4$ was available.) The surface complexation constants arising from this first modelling attempt were then (preliminarily) fixed. At these relatively high ionic strengths the modelling indicated that cation exchange processes only began to contribute significantly to sorption at pH values less than 5.

An interesting result from this part of the modelling exercise arose when the surface complex model, with the parameter values derived from the above procedures, was applied to the sorption edges measured for Ni, Eu and U(VI) at 0.01 M $NaClO_4$. The surface complexation modelling underestimated the sorption at pH values less than neutral, and did not follow the form of the curves at all. Although the shape of the curves in these plots look very similar to classic sorption edges, the pH dependency had essentially nothing to do with uptake on the amphoteric ≡SOH edge sites. Rather, the subsequent modelling indicated that the dominant sorption mechanism was cation exchange, but strongly influenced by competition effects from Ca and Al whose concentrations and speciation (Al) were varying as a function of pH.

In a next step, cation exchange reactions were introduced. At pH values < 6, the sorption modelling (surface complexation plus cation exchange) had to be carried out on a pH by pH basis because the competitive effects arising from the changing water chemistry and speciation as a function of pH had to be taken into account for the cation exchange. (This was particularly so for the measurements at 0.01 M $NaClO_4$.) The CEC, Me-Na and Al-Na selectivity coefficients and the background concentrations of Ca, Mg and Al in 0.01 and 0.1 M $NaClO_4$ as a function of pH (Tables 9.2 and 9.3) were all fixed at the same values used to model the Sr data. (Note that at 0.5 M $NaClO_4$ the competitive effects of Ca, Mg and Al cations are insignificant.) The sorption edges for the three metals were then modelled in an iterative manner using in each case the corresponding selectivity coefficient with respect to Na as the only free parameter. Once the initial modelling was completed, further iterations and fine tuning steps followed until finally a complete set of parameter for each radionuclide describing the sorption edge measurements was obtained.

These parameter sets were then fixed, and surface complexation on the $\equiv S^{W1}OH$ sites considered in order to model the sorption isotherm data. Again, guidance for the surface complexes was provided by aqueous speciation calculations in the manner described in Chapter 8.

10.2 Ni sorption on Na-illite

Sorption edges for Ni on Na-illite were determined at trace concentrations in 0.01, 0.1 and 0.5 M $NaClO_4$. Three isotherms in 0.1 M $NaClO_4$ were measured at pH 6, 7 and 7.8. The edges and isotherms are presented in Figs. 10.1 to 10.6, and the corresponding experimental conditions are summarised in Table 10.1. In Fig. 10.3 sorption kinetic data measured between 3 and 84 days are given. For times longer than 3 days, all of the data lie within the measurement uncertainty band of ±0.2 log units.

Table 10.1: Experimental conditions for the Ni sorption measurements on conditioned Na-illite.

Type of experiment	edge	edge	edge	isotherm	isotherm	isotherm
$NaClO_4$ (M)	0.01	0.1	0.5	0.1	0.1	0.1
pH	2.7 – 11.1	2.7 – 10.9	3.3 – 10.8	6.0 ± 0.1	7.0 ± 0.1	7.8 ± 0.1
S:L ratio ($g\ L^{-1}$)	1.5/1.9	1.8/2.3	1.6	2.4	1.8/1.5	2.5/3.9
Initial Ni conc. (M)	7×10^{-9}	2×10^{-9}	7×10^{-9}	10^{-2} - 10^{-8}	10^{-3} - 10^{-8}	10^{-4} - 10^{-8}
Buffers	yes	yes	yes	MES	MOPS	TRIS
Time (days)	7	7	3 to 84	7	7 to 56	7

The modelling was carried out as described in section 10.1 and the continuous lines in Figs. 10.1 to 10.6 were calculated using the surface reactions and parameter values given in Table 5.1 and 10.2 together with the ancillary data in Table 9.5. (The selectivity coefficient for Ni with respect to Na was taken to have the same value as Sr and Ca, see for example BRUGGENWERT & KAMPHORST, 1982.)

As mentioned in section 10.1, the pH dependency of the sorption of Ni, Eu, and U(VI) at pH < 7 in 0.01 M $NaClO_4$ background electrolyte is not due to uptake on ≡SOH edge sites but to cation exchange and the competitive effects of Ca and Al.

The Ni sorption edge at 0.01 M $NaClO_4$, Fig. 10.1, is taken as an example to illustrate the contributions and influences of the different processes. The dashed-dotted line represents the contribution to the Ni sorption by surface complexation, and, as can be immediately seen, the curve lies well below the measured values at pH < 6. The inclusion of an additional component to Ni sorption from cation exchange (without competition) yields the dashed line, and, in this case the curve lies well above the measured values. If competition with Ca^{2+} is included, the contribution of Ni uptake by cation exchange to the overall sorption is reduced, dotted line, but the calculated curve still does not correspond to the measured data. Only when competition from Al^{3+} is included do the modelled and experimental data coincide, as shown by the continuous line.

Table 10.2: Mass action equations and associated constants used in the modelling of Ni on Na-illite.

Cation exchange reaction	K_C
2 Na-illite + $Ni^{2+} \Leftrightarrow$ Ni-illite + 2 Na^+	11
Surface complexation reactions on strong sites	**log K_{SC}**
$\equiv S^SOH + Ni^{2+} \Leftrightarrow \equiv S^SONi^+ + H^+$	0.7
$\equiv S^SOH + Ni^{2+} + H_2O \Leftrightarrow \equiv S^SONiOH^o + 2\ H^+$	-8.5
$\equiv S^SOH + Ni^{2+} + 2\ H_2O \Leftrightarrow \equiv S^SONi(OH)_2^- + 3\ H^+$	-17.1
Surface complexation reaction on weak sites	**log K_{SC}**
$\equiv S^{W1}OH + Ni^{2+} \Leftrightarrow \equiv S^{W1}ONi^+ + H^+$	-1.8

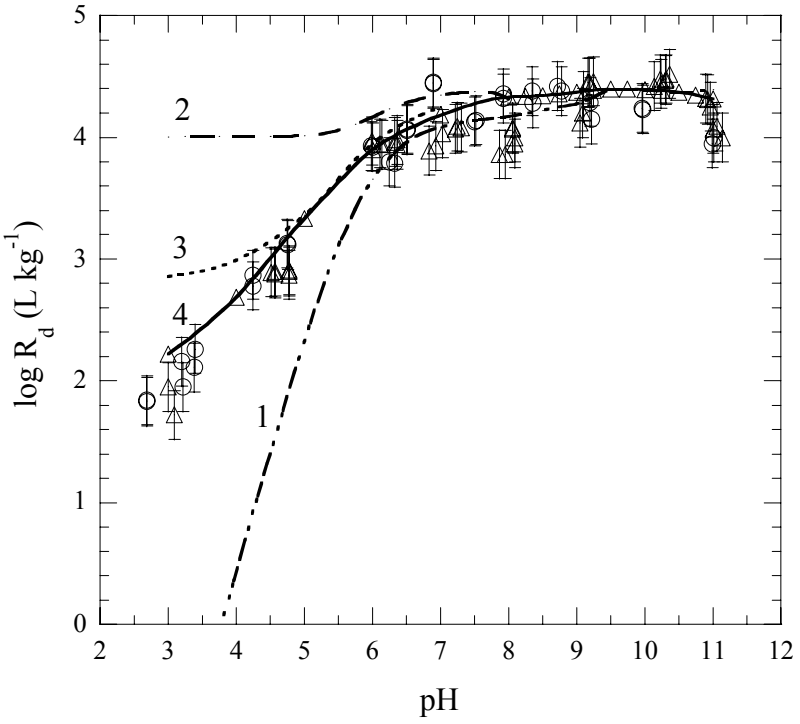

Fig. 10.1: Ni sorption edge measurements (O, POINSSOT et al. (1999), △, this study) and modelling on conditioned Na-illite (IdP-1) in 0.01 M $NaClO_4$. Line 1: only SC; line 2: SC + CE without competition; line 3: SC + CE with Ca competition; line 4: SC + CE with Ca and Al competition.

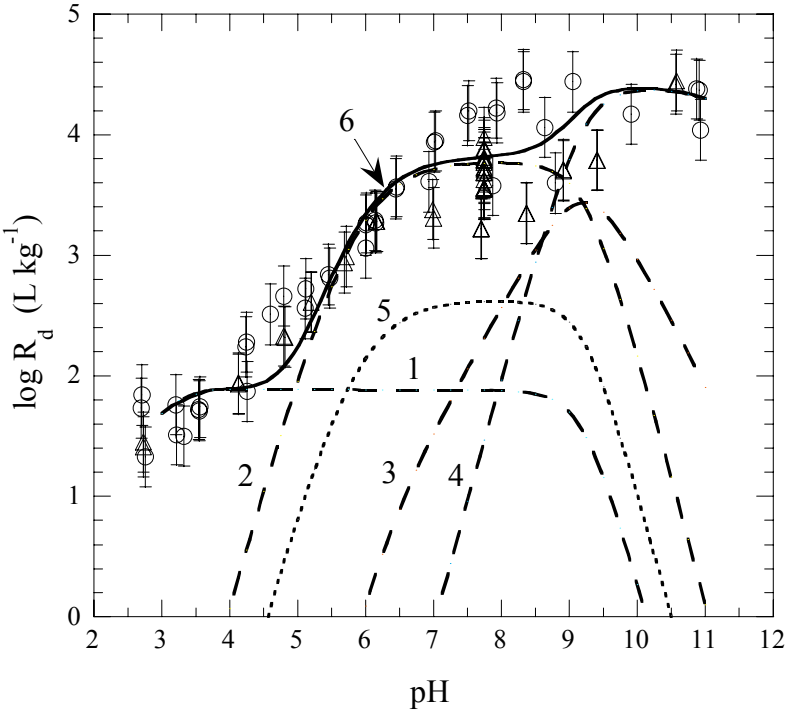

Fig. 10.2: Ni sorption edge measurements (O, POINSSOT et al. (1999), △, this study) and modelling on conditioned Na-illite (O, IdP-1: △, IdP-2) in 0.1 M $NaClO_4$. The modelling calculations are given by the curves: 1: CE-Ni^{2+}; 2: $\equiv S^SO\text{-}Ni^+$; 3: $\equiv S^SO\text{-}NiOH^o$; 4: $\equiv S^SO\text{-}NiOH^{-1}$; 5: $\equiv S^{W1}O\text{-}Ni^+$; 6: overall sorption.

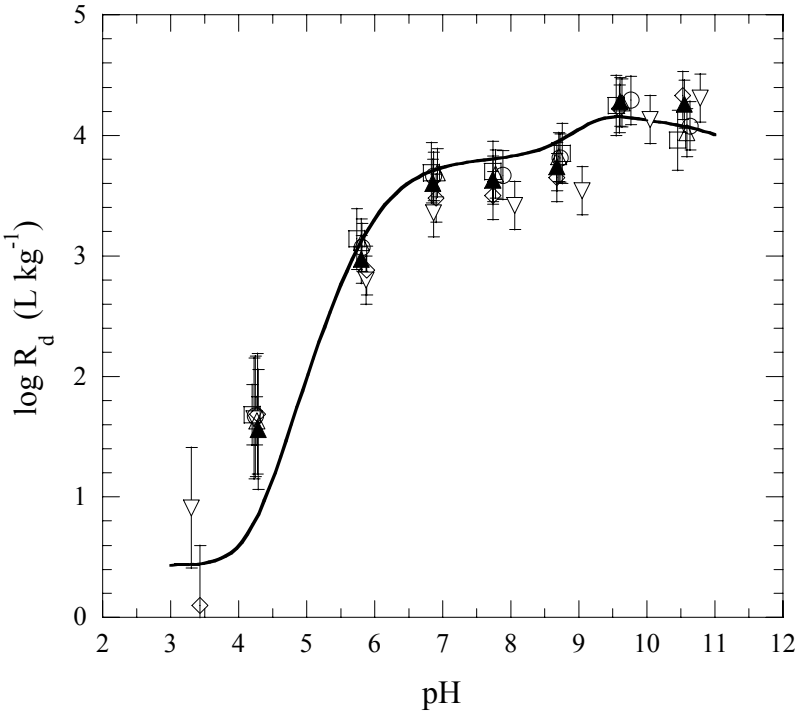

Fig. 10.3: Ni sorption edge measurements and modelling (full line) on conditioned Na-illite (IdP-1) in 0.5 M $NaClO_4$. (▽ 3 days, ◇ 8 days, ▲ 21 days, ○ 42 days, △ 63 days, □ 84 days).

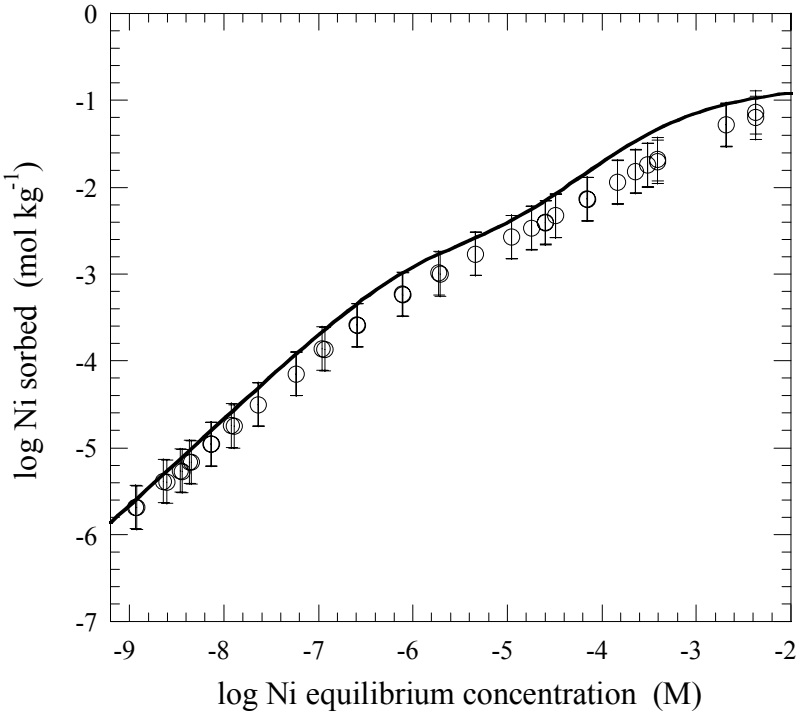

Fig. 10.4: Ni sorption isotherm measurements and modelling (full line) on conditioned Na-illite (IdP-2) in 0.1 M $NaClO_4$ at pH 6.0.

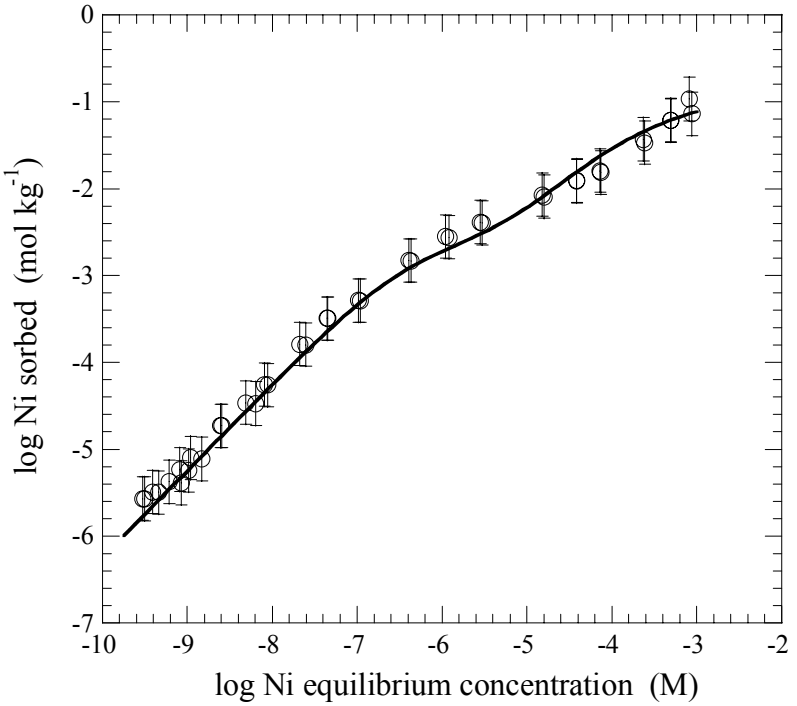

Fig. 10.5: Ni sorption isotherm measurements (POINSSOT et al., 1999) and modelling (full line) on conditioned Na-illite (IdP-1) in 0.1 M $NaClO_4$ at pH 7.0.

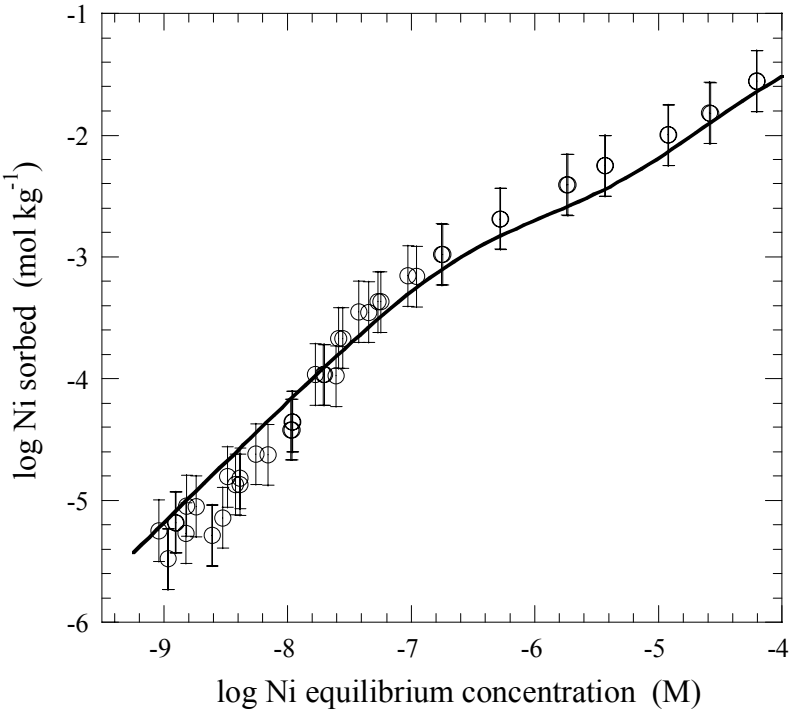

Fig. 10.6: Ni sorption isotherm measurements and modelling (full line) on conditioned Na-illite (IdP-2) in 0.1 M $NaClO_4$ at pH 7.8.

10.3 Eu sorption on Na-illite

Sorption edges for Eu on Na-illite were determined at trace concentrations in 0.01, 0.1 and 0.5 M $NaClO_4$. Two isotherms in 0.1 M $NaClO_4$ were measured at pH 5.5 and 7. The edges and isotherms are presented in Figs. 10.7 to 10.11, and the corresponding experimental conditions are summarised in Table 10.3.

Table 10.3: Experimental conditions for the Eu sorption measurements on conditioned Na-illite.

Type of experiment	edge	edge	edge	isotherm	isotherm
$NaClO_4$ (M)	0.01	0.1	0.5	0.1	0.1
pH	2.7 – 11.1	2.7 – 10.8	3.3 – 10.8	5.5 ±0.1	7.0 ±0.1
S:L ratio (g L^{-1})	1.9	1.8	1.4	1.4	1.2/1.8
Initial Eu conc. (M)	3×10^{-9}	3×10^{-9}	5×10^{-10}	$10^{-3} – 10^{-9}$	$4 \times 10^{-4} – 10^{-9}$
Buffers	yes	yes	yes	MES	MOPS
Time (days)	7	7	1 to 60	7	7

The continuous lines in Figs. 10.7 to 10.11 were calculated using the surface reactions and parameter values given in Tables 5.1 and 10.4 together with the ancillary data in Table 9.5. Although stability constant values for the negatively charged tetrahydroxy Eu complex exists in many thermodynamic data bases, there is increasing doubt as to whether this species actually exists (NECK pers. comm.) and it was not included in the modelling results for Eu presented here.

Table 10.4: Mass action equations and associated constants used in the modelling of Eu on Na-illite.

Cation exchange reaction	K_c
3 Na-illite + $Eu^{3+} \Leftrightarrow$ Eu-illite + 3 Na^+	76
Surface complexation reactions on strong sites	**log K_{SC}**
$\equiv S^SOH + Eu^{3+} \Leftrightarrow \equiv S^SOEu^{2+} + H^+$	3.1
$\equiv S^SOH + Eu^{3+} + H_2O \Leftrightarrow \equiv S^SOEuOH^+ + 2\ H^+$	-4.4
$\equiv S^SOH + Eu^{3+} + 2\ H_2O \Leftrightarrow \equiv S^SOEu(OH)_2^o + 3\ H^+$	-12.7
Surface complexation reaction on weak sites	**log K_{SC}**
$\equiv S^{W1}OH + Eu^{3+} \Leftrightarrow \equiv S^{W1}OEu^{2+} + H^+$	0.3
$\equiv S^{W1}OH + Eu^{3+} + H_2O \Leftrightarrow \equiv S^{W1}OEuOH^+ + 2\ H^+$	-6.2

The Eu sorption edge measured in 0.01 M $NaClO_4$ (Fig. 10.7, open symbols) has a somewhat unusual shape. The sorption rises continuously and sharply from pH ~2 to reach a broad maximum at pH ~7 and thereafter decreases shallowly to pH ~12. Although there is some scatter in the measurements, the data are reproducible.

The modelled curve reproduces the data reasonably well up to pH 7-8 and thereafter overestimates the measured data increasingly as the pH increases. (A similar, though less well pronounced effect is seen for uranium, Fig. 10.13, but is not apparent at all for nickel, Fig. 9.1, where there is very good correspondence between modelled and experimental data.) The reason for the decrease in the measured Eu sorption values at pH > 8 is not definitely known. However, a plausible explanation is that colloids are responsible. At high pH the illite particles become negatively charged, and this, combined with the low ionic strength, strongly favours peptisation. The standard phase separation method of centrifugation at 96000 *g* (max.) for one hour is probably no longer sufficiently efficient for such low ionic strength solutions. The above is of course true not only for Eu but also for Ni and U. The reason that corresponding reductions in sorption are not seen for Ni and only slight reductions for U lies in the differences in sorption values. In the pH range under consideration the sorption of Eu is probably in excess of 10^6 L kg^{-1}; U is an order of magnitude less and Ni two orders of magnitude lower. In the case of Eu, and the data presented in Fig. 10.7, only ~0.1 wt.% of illite needs to be in the form of colloids in the supernatant solutions to explain the decrease in sorption.

In order to test this hypothesis a series of Eu sorption experiments were repeated at pH ~11.5 in 0.01 M $NaClO_4$ and phase separation carried out in the standard manner. The measured sorption values were the same as in previous experiments. Then, a 1.0 M solution of $NaClO_4$ was added to the supernatant solution to give a total concentration of 0.5 M $NaClO_4$. The solution was shaken for 3 days and then centrifuged and sampled again. The measured sorption values were considerably higher (solid triangles, Fig. 10.7) and similar to those measured in the pH range 6 - 9. This result is fully in accord with colloidal material being responsible for the reduction in sorption of Eu at high pH values in low $NaClO_4$ concentration solutions.

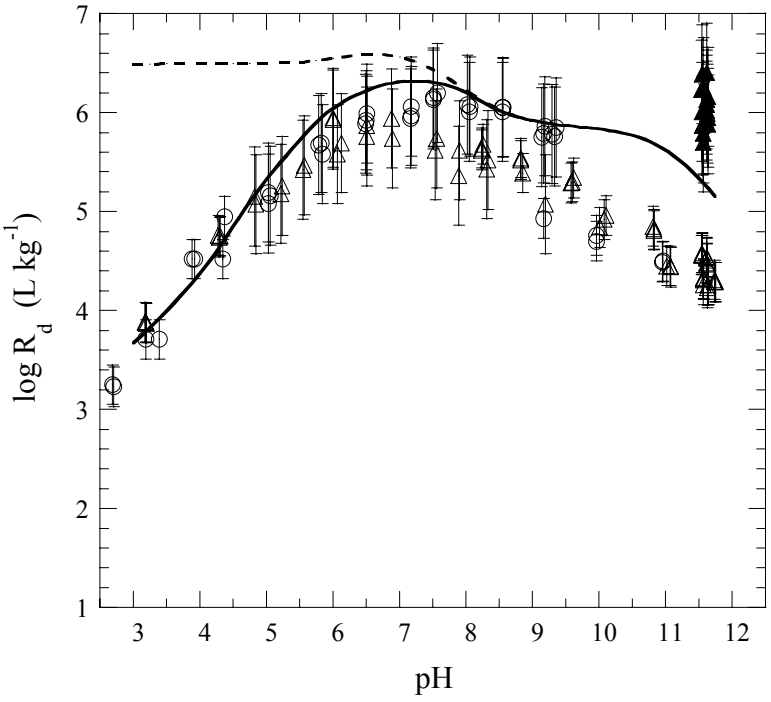

Fig. 10.7: Eu sorption edge measurements (O, POINSSOT et al. (1999), △, this study) and modelling on conditioned Na-illite (O, IdP-1: △, IdP-2) in 0.01 M $NaClO_4$. Continuous line, SC + CE with competition; dotted line: SC + CE with no competition. (▲, IdP-2 in 0.5 M $NaClO_4$, see text for details).

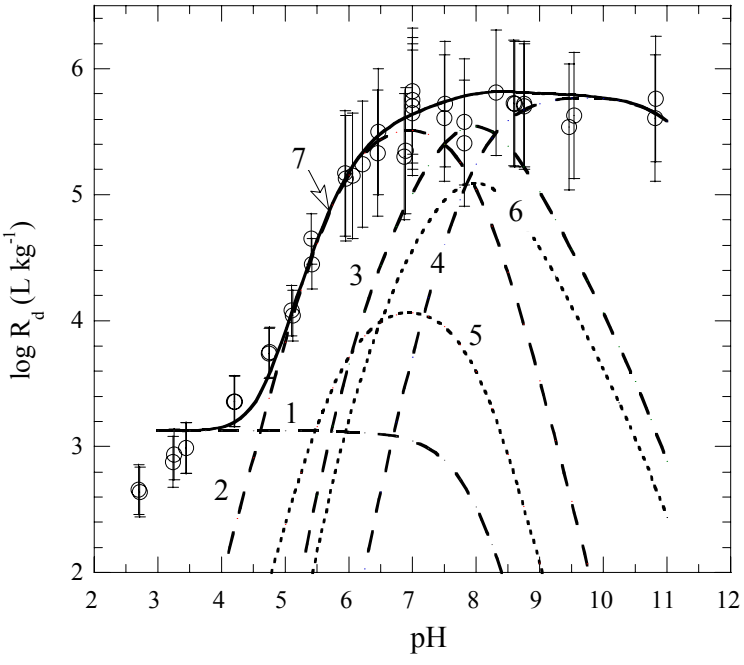

Fig. 10.8: Eu sorption edge measurements on conditioned Na-illite (IdP-1) and modelling in 0.1 M $NaClO_4$. The contribution to the overall sorption (curve 7) of the individual sorbed Eu species are shown by the different curves. 1: CE-Eu^{3+}; 2: $\equiv S^{S}O\text{-}Eu^{2+}$; 3: $\equiv S^{S}O\text{-}EuOH^{+}$; 4: $\equiv S^{S}O\text{-}Eu(OH)_2^{o}$; 5: $\equiv S^{W1}O\text{-}Eu^{2+}$; 6: $\equiv S^{W1}O\text{-}EuOH^{+}$.

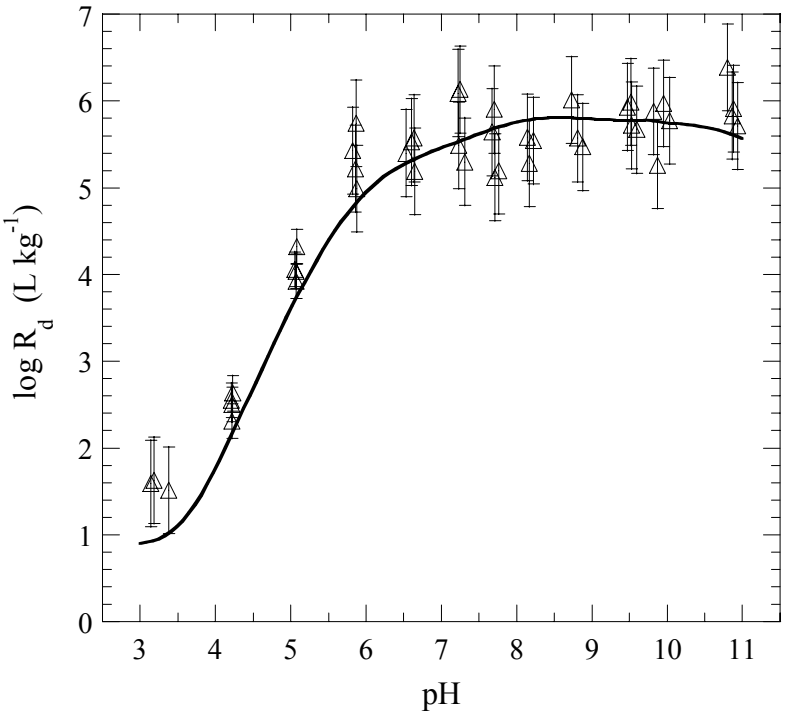

Fig. 10.9: Eu sorption edge measurements on conditioned Na-illite (IdP-2) and modelling (full line) in 0.5 M $NaClO_4$.

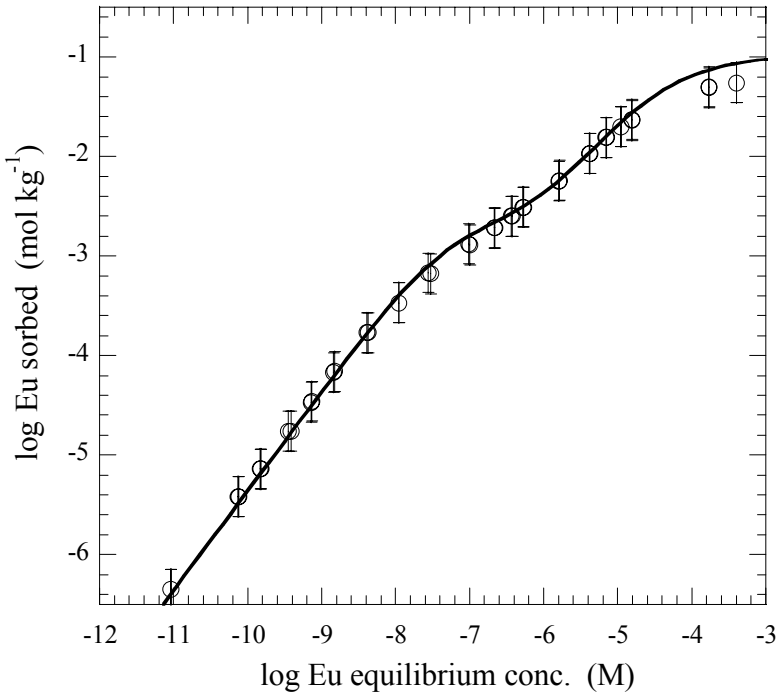

Fig. 10.10: Eu sorption isotherm measurements and modelling (full line) on conditioned Na-illite (IdP-1) in 0.1 M $NaClO_4$ at pH 5.5.

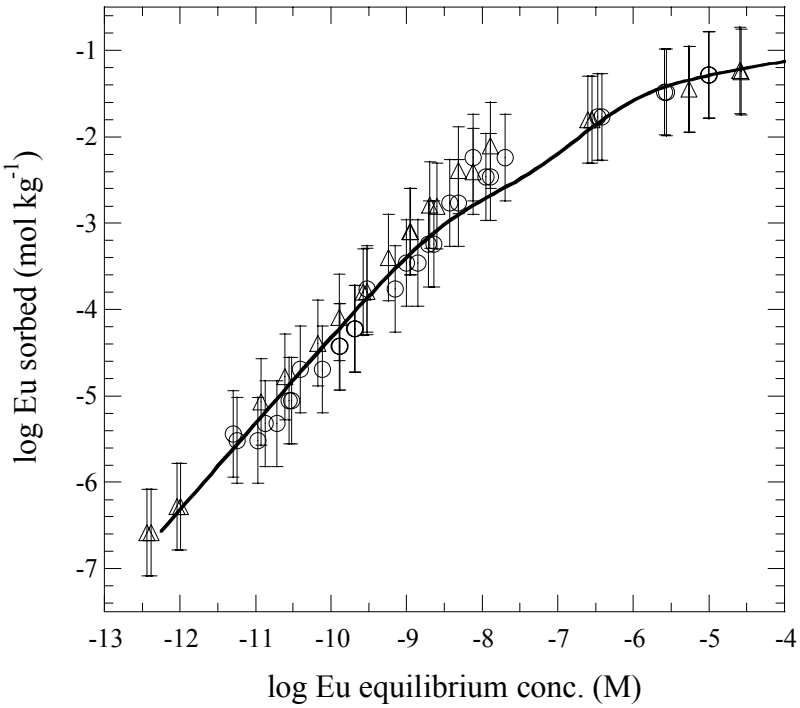

Fig. 10.11: Eu sorption isotherm measurements and modelling (full line) on conditioned Na-illite in 0.1 M $NaClO_4$ at pH 7.0; (O) IdP-1; (Δ) IdP-2.

In the cases of Sr, Ni and U no further surface species other than those given in the appropriate sections would be necessary to model the measured sorption values at higher pH values than 10. However this is not the case for Eu which would require an additional surface species. The inclusion of this species does not induce changes in other surface species constants and the surface species distribution. As an exercise it was assumed that the sorption measurements above pH 10 were valid and these data were included in the overall modelling. The major difference was that in order to maintain the high sorption up to pH 12 as indicated by the measurements given for example in Figs. 10.7 (solid triangles), 10.8 and 10.9, the following surface complexation reaction had to be included

$$\equiv S^SOH + Eu^{3+} + 3\ H_2O \Leftrightarrow \equiv S^SOEu(OH)_3^- + 4\ H^+ \qquad \log K_{SC} = -23.8$$

The influence on the surface speciation is illustrated by re-modelling the sorption edge at 0.1 M $NaClO_4$ including the above surface reaction, Fig. 10.12. Modelling the sorption edge measurements to pH 12 did not formally present any difficulties and if Fig. 10.8 is compared with Fig. 10.12 no significant differences are apparent except of course the additional surface species $\equiv S^SOEu(OH)_3^-$ in Fig. 10.12.

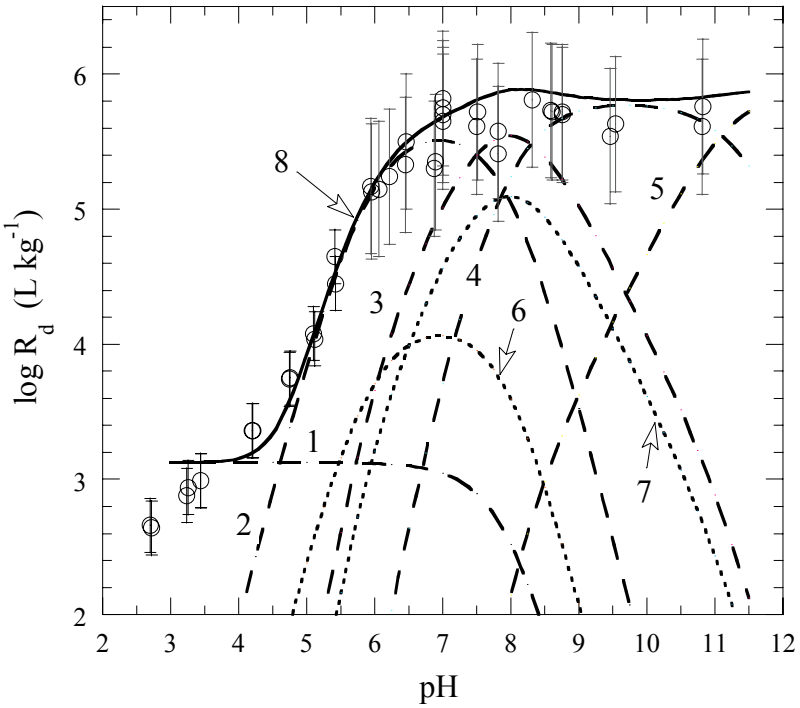

Fig. 10.12: Eu sorption edge measurements on conditioned Na-illite (IdP-2) and modelling in 0.1 M $NaClO_4$. The contribution to the overall sorption (curve 8) of the individual sorbed Eu species are shown by the different curves.
1: CE-Eu^{3+}; 2: $\equiv S^SO\text{-}Eu^{2+}$; 3: $\equiv S^SO\text{-}EuOH^+$; 4: $\equiv S^SO\text{-}Eu(OH)_2^o$;
5: $\equiv S^SO\text{-}Eu(OH)_3^-$; 6: $\equiv S^{W1}O\text{-}Eu^{2+}$; 7: $\equiv S^{W1}O\text{-}EuOH^+$.

10.4 U(VI) sorption on Na-illite

Sorption edges for U on Na-illite were determined at trace concentrations in 0.01 and 0.1 M $NaClO_4$. Two isotherms in 0.1 M $NaClO_4$ were measured at pH 4.8 and 5.8. The edges and isotherms are presented in Figs. 10.13 to 10.16, and the corresponding experimental conditions are summarised in Table 10.5.

Table 10.5: Experimental conditions for the U(VI) sorption measurements on conditioned Na-illite.

Type of experiment	edge	edge	isotherm	isotherm
$NaClO_4$ (M)	0.01	0.1	0.1	0.1
pH	2.7 – 11.1	2.7 – 10.8	4.8 ±0.1	5.8 ±0.1
S:L ratio (g L^{-1})	1.9	2.6	1.8	0.5 - 1.6
Initial U conc. (M)	10^{-7}	10^{-7}	10^{-3} - 10^{-7}	10^{-5} - 10^{-7}
Buffers	yes	yes	AA	MES
Time (days)	7	7	7	7

The continuous lines in Figs. 10.13 to 10.16 were calculated using the surface reactions and parameter values given in Tables 5.1 and 10.6 together with the ancillary data in Table 9.5.

Modelling sorption isotherm data measured for U on illite conditioned in the standard manner (section 2.1) could not be realised because of step changes in the sorption at certain combinations of concentration and pH. This behaviour was very reproducible and thought to be related to an unidentified Ca-phase in the Na-illite releasing Ca into solution (section 4.5). In order to avoid such effects it was decided to apply an additional treatment to remove as much of the Ca as possible from the system. To do this, illite suspensions contained in dialysis bags were placed in approximately 1 litre of 0.1 M $NaClO_4$ and acidified to pH ~3.5, S:L ~5 g L^{-1}. After shaking end-over-end for ~1 hour, the pH was re-adjusted back to pH ~3.5 and shaking was continued for a further ~3 hours. The solution was then discarded to remove the dissolved elements from the system and replaced by a fresh 0.1 M $NaClO_4$ solution at pH ~3.5. The whole procedure was repeated twice more. In a final cycle the illite was left in contact with the acidified $NaClO_4$ for 24 hours before discarding the solution and adjusting the pH to neutral in a fresh 0.1 M $NaClO_4$ solution. (The background Ca concentration at pH ~7 was reduced to ~3 x 10^{-7} M.) Illite conditioned in this manner was used to produce the isotherms shown in Figs. 10.15 and 10.16 which were free from any artefacts and could be modelled in the normal manner.

Table 10.6: Mass action equations and associated constants used in the modelling of U(VI) on Na-illite.

Cation exchange reaction	K_c
2 Na-illite + $UO_2^{2+} \Leftrightarrow UO_2$-illite + 2 Na^+	4.5
Surface complexation reactions on strong sites	**log K_{SC}**
$\equiv S^SOH + UO_2^{2+} \Leftrightarrow \equiv S^SOUO_2^+ + H^+$	2.6
$\equiv S^SOH + UO_2^{2+} + H_2O \Leftrightarrow \equiv S^SOUO_2OH^0 + 2\ H^+$	-3.6
$\equiv S^SOH + UO_2^{2+} + 2\ H_2O \Leftrightarrow \equiv S^SOUO_2(OH)_2^- + 3\ H^+$	-10.3
$\equiv S^SOH + UO_2^{2+} + 3\ H_2O \Leftrightarrow \equiv S^SOUO_2(OH)_3^{2-} + 4\ H^+$	-17.5
Surface complexation reaction on weak sites	**log K_{SC}**
$\equiv S^{W1}OH + UO_2^{2+} \Leftrightarrow \equiv S^{W1}OUO_2^+ + H^+$	0.1
$\equiv S^{W1}OH + UO_2^{2+} + H_2O \Leftrightarrow \equiv S^{W1}OUO_2OH^0 + 2\ H^+$	-5.3

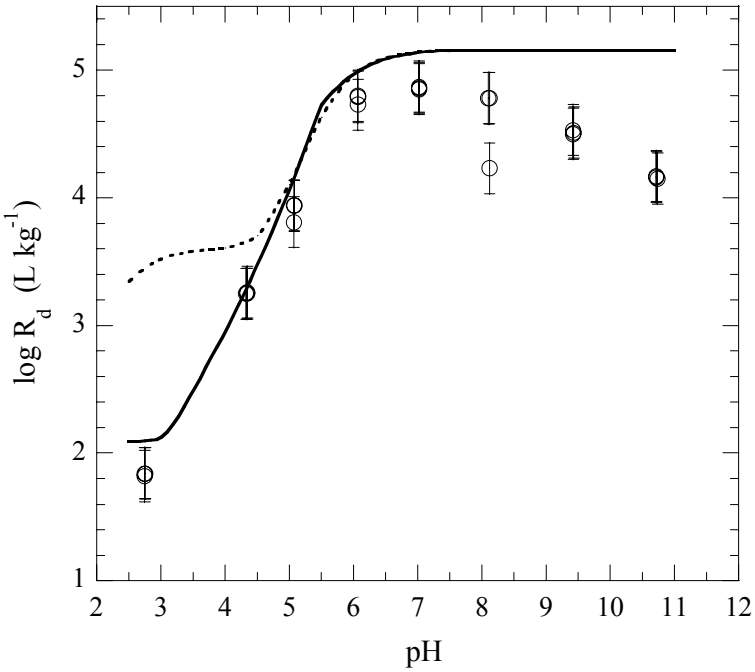

Fig. 10.13: U(VI) sorption edge measurements and modelling (full line) on conditioned Na-illite (IdP-2) in 0.01 M $NaClO_4$. The dotted line is a model calculation without competition. The discrepancy between modelled and measured values at pH > 7 is explained by sorption onto colloids, see text for details.

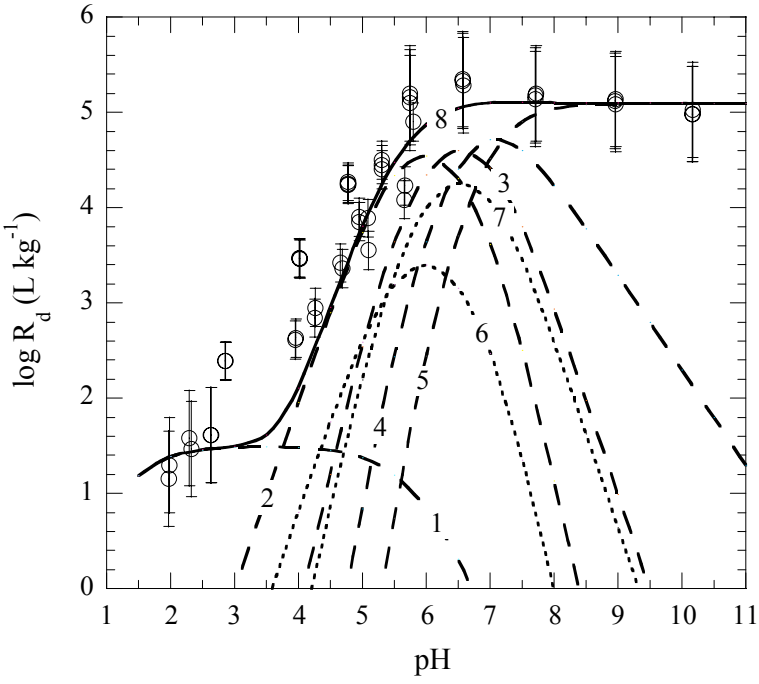

Fig. 10.14: U(VI) sorption edge measurements on conditioned Na-illite (IdP-2) and modelling in 0.1 M $NaClO_4$. The contribution to the overall sorption (curve 8) of the individual sorbed U(VI) species are shown by the different curves.
1: CE-UO_2^{2+}; 2: ≡S^SO-UO_2^+; 3: ≡S^SO-UO_2OH^o; 4: ≡S^SO-$UO_2(OH)_2^-$;
5: ≡S^SO-$UO_2(OH)_3^{2-}$; 6: ≡S^{W1}O-UO_2^+; 7: ≡S^{W1}O-UO_2OH^o.

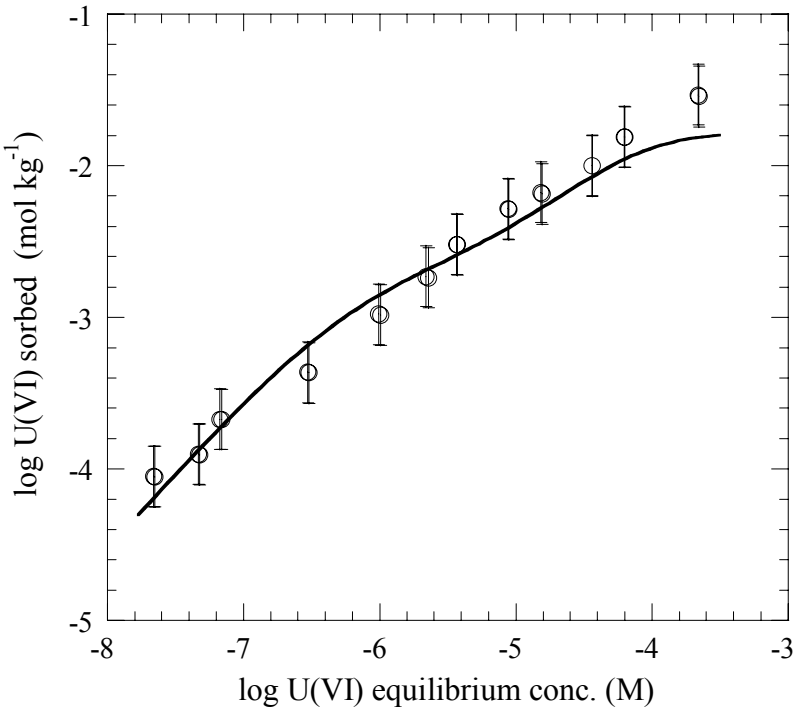

Fig. 10.15: U(VI) sorption isotherm measurements and modelling (full line) on specially conditioned Na-illite (IdP-2) in 0.1 M $NaClO_4$ at pH 4.8. (See text for details.)

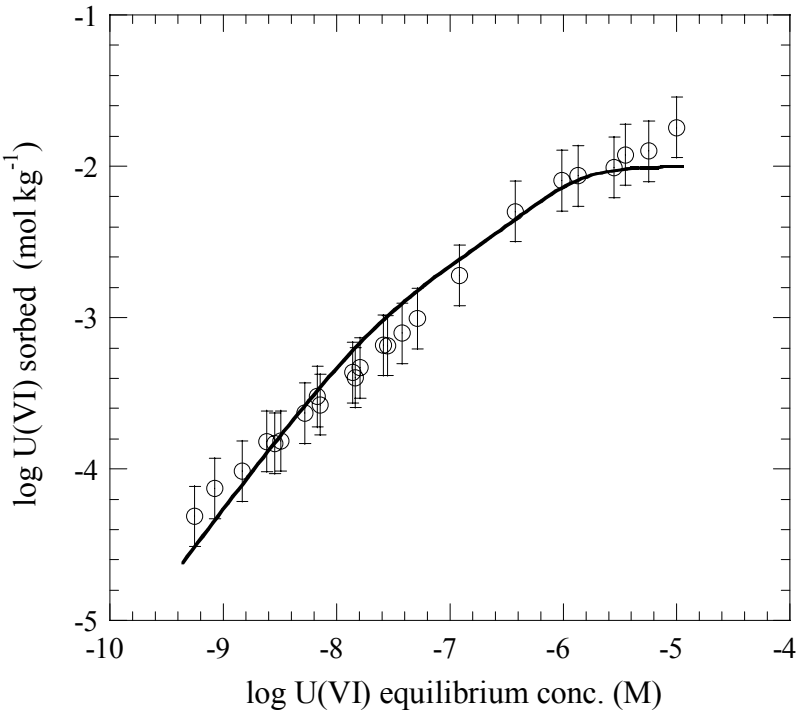

Fig. 10.16: U(VI) sorption isotherm measurements and modelling (full line) on specially conditioned Na-illite (IdP-2) in 0.1 M $NaClO_4$ at pH 5.8. (See text for details.)

11 Summary

Illite is an important clay mineral component in many argillaceous rocks under consideration as host formations for the deep disposal of radioactive waste. A good understanding of the sorption characteristics of such rock types over a wide range of conditions is particularly important in this context. This study continues the "bottom up" approach to sorption begun with the investigations on montmorillonite and bentonite. The idea is that by understanding the sorption processes on single mineral phases and developing models to describe them, this knowledge can be applied to understand and quantitatively predict the uptake of elements in complex mineral/groundwater systems. The aim of this work was to provide a basis for this approach in systems where illite is a major mineral component.

Suspensions of illite du Puy (< 63 μm) were carefully conditioned to the Na-form and physico-chemically characterised in terms of their mineralogy, structural formula, surface area and cation exchange capacity. Particular attention was paid to water chemistry in these experiments and in the subsequent titration and sorption tests.

Previous experience had shown that a relatively large data base is required to develop a model and determine the associated parameters in a credible manner. Consequently, potentiometric titrations on suspensions of the Na-illite were carried out using a batch back titration technique in 0.01, 0.1 and 0.5 M $NaClO_4$ background electrolytes from pH ~2 to pH ~12. Sorption edges were determined for Sr(II), Ni(II), Eu(III) and U(VI) for trace concentrations at different $NaClO_4$ concentrations, and sorption isotherms for the same set of radionuclides in Na-illite suspensions in 0.1 M $NaClO_4$ at various pH values. All experiments were carried out in inert atmosphere glove boxes ($CO_2 \leq 2$ ppm, $O_2 \leq 2$ ppm.).

It was found that the same model developed for montmorillonite i.e. a 2 site protolysis non electrostatic surface complexation plus cation exchange (2SPNE SC/CE) model, could be used to describe the titration and sorption data obtained for illite very satisfactorily over the whole range of experimental conditions used.

The modelling exercise yielded an internally consistent set of site types and capacities for protolysis ($\equiv S^{W1}OH$ and $\equiv S^{W2}OH$), and for surface complexation (strong $\equiv S^{S}OH$ and weak $\equiv S^{W1}OH$), protolysis constants, surface complexation constants for strong and weak sites, cation exchange capacity and selectivity coefficients for Sr(II), Ni(II), Eu(III) and U(VI). Together with some previous work on Cs(I), BRADBURY & BAEYENS (2000), sorption models representing alkali, alkali earth, transition, trivalent and hexavalent metals are now available for the illite system.

An interesting observation was made for all sorption edge experiments for Sr, Ni, Eu and U carried out in 0.01 M $NaClO_4$ illite suspensions at pH <7. At first sight the sorption measurements appeared to have a pH dependency very reminiscent of what would be expected from a surface complexation mechanism. However, detailed modelling revealed that the dominant sorption mechanism was in fact cation exchange. The form of the sorption edge was determined by competition for the exchange sites arising from the presence of Ca and Al. The concentration of these two elements varied with pH and hence also their competitive effects. Modelling under these conditions up to pH~7 had to be done individually at each pH. It was found that with a fixed value of ${}^{Me}_{Na}K_c$ equal to 11, (Me = Ca, Mg, Sr), an Al-Na selectivity coefficient of 10 and the corresponding sorbate selectivity coefficient, all the sorption edge data measured at 0.01 and 0.1 M $NaClO_4$ and pH < 7 could be successfully modelled. A further point worthy of note here is that Al is present in all clay systems but because no suitable tracer exists, its sorption characteristics are virtually unknown. The sorption modelling allowed an estimate to be made for the Al-Na selectivity coefficient.

12 Acknowledgements

The contributions of M. Mantovani and A. Schaible to the experimental work are gratefully acknowledged. Cation analyses were carried out by R. Keil. Prof. P. Toulhoat (University Cl. Bernard Lyon 1) is thanked for his critical and constructive review comments on the manuscript. Partial financial support was provided by NAGRA.

13 References

ANDRA (2001) Référentiel géologique du site de Meuse/Haute Marne. Rapp. A RP ADS 99-005 de l'Agence nationale pour la gestion des déchets radioactifs, Châtenay-Malabry, France.

AOKI, K. (2002) Recent activities at underground research laboratories in Japan. Proc. Internat. Symp. NUCEF 2001, Japan Atomic Energy Research Institute, JAERI-Conf. 2002-04, pp. 361-362.

BAES, C.F. & MESMER, R.E. (1976) The Hydrolysis of Cations. John Wiley & Sons, New York, NY.

BAEYENS, B. & BRADBURY, M.H. (1995a) A quantitative mechanistic description of Ni, Zn and Ca sorption on Na-montmorillonite. Part I: Physico-chemical characterisation and titration measurements. PSI Bericht Nr. 95-10. Paul Scherrer Institut, Villigen and Nagra Technical Report NTB 95-04, Nagra, Wettingen, Switzerland.

BAEYENS, B. & BRADBURY, M.H. (1995b) A quantitative mechanistic description of Ni, Zn and Ca sorption on Na-montmorillonite. Part II: Sorption measurements. PSI Bericht Nr. 95-11. Paul Scherrer Institut, Villigen and Nagra Technical Report NTB 95-05, Nagra, Wettingen, Switzerland.

BAEYENS, B & BRADBURY, M.H. (1997) A mechanistic description of Ni and Zn sorption on Na-montmorillonite. Part I: Titration and sorption measurements. J. Contam. Hydrol. 27, 199-222.

BAEYENS, B. & BRADBURY, M.H. (2004) Cation exchange capacity measurements of illite using the Na and Cs isotope dilution technique: Effects of the index-cation, electrolyte concentration and competition: Modelling. Clays Clay Minerals 52, 421-431.

BEENE, G.M., BRYANT, R. & WILLIAMS, D.J.A. (1991) Electrochemical properties of illites. J. Colloid Interface Sci. 147, 358-369.

BOLT, G.H. (1967) Cation-exchange equations used in soil science; a review. Neth. J. Agric. Sci. 15, 81-103.

BOLT, G.H., BRUGGENWERT, M.G.M. & KAMPHORST, A. (1976) Adsorption of cations by soils. In Soil Chemistry. A. Basic Element (Eds. G.H. Bolt & M.G.M. Bruggenwert) Elsevier, Amsterdam, pp. 54-90.

BOLT, G.H., 1982. Thermodynamics of cation exchange. In Soil Chemistry B. Physico-Chemical Models (Ed. G.H. Bolt) Elsevier, Amsterdam, pp. 27-46.

BONIN, B. (1998) Deep geological disposal in argillaceous formations: studies at the Tournemire site. J. Contam. Hydrol. 35, 315-330.

BRADBURY, M.H. & BAEYENS, B. (1994) Sorption by cation exchange. Incorporation of a cation exchange model into geochemical computer codes. PSI Bericht Nr. 94-07. Paul Scherrer Institut, Villigen and Nagra Technical Report NTB 94-11, Nagra, Wettingen, Switzerland.

BRADBURY, M.H. & BAEYENS, B. (1995) A quantitative mechanistic description of Ni, Zn and Ca sorption on Na-montmorillonite. Part III: Modelling. PSI Bericht Nr. 95-12. Paul Scherrer Institut, Villigen and Nagra Technical Report NTB 95-06, Nagra, Wettingen, Switzerland.

BRADBURY, M.H. & BAEYENS, B. (1997a) A mechanistic description of Ni and Zn sorption on Na-montmorillonite. Part II: Modelling. J. Contam. Hydrol. 27, 223-248.

BRADBURY, M.H. & BAEYENS, B. (1997b) Reply to some comments. J. Contam. Hydrol., 28, 11-16.

BRADBURY, M.H. & BAEYENS, B. (1999) Modelling the sorption of Zn and Ni on Ca-montmorillonite. Geochim. Cosmochim. Acta 63, 325-336.

BRADBURY, M.H. & BAEYENS, B. (2000) A generalised sorption model for the concentration dependent uptake of caesium by argillaceous rocks. J. Contam. Hydrol. 42, 141-163.

BRADBURY, M.H. & BAEYENS, B. (2001) A mechanistic description of Ni sorption on Na-montmorillonite. In: Using Thermdynamic Sorption Models for Guiding Radioelement Distribution Coefficient (Kd) Investigations. International Meeting on Chemical Modelling of Sorption in the Field of Radioactive Waste Management, 6-8 May 1997, Oxford, UK. NEA OECD Publications, Paris, France, pp. 105-106.

BRADBURY, M.H. & BAEYENS, B. (2002) Sorption of Eu on Na- and Ca-montmorillonites: Experimental investigations and modelling with cation exchange and surface complexation. Geochim. Cosmochim. Acta 66, 2325-2334.

BRUGGENWERT, M.G.M. & KAMPHORST, A. (1982) Survey of experimental information on cation exchange in soil systemsIn Soil Chemistry B. Physico-Chemical Models (Ed. G.H. Bolt) Elsevier, Amsterdam, pp. 141-203.

DAVIS, J.A., JAMES, R.O. & LECKIE, J.O. (1978) Surface ionisation and complexation at the oxide/water interface. I. Computation of electrical double layer properties in simple electrolytes. J. Colloid Interface Sci. 63, 480-499.

DAVIS, J.A. & KENT, D.B. (1990) Surface complexation modelling in aqueous geo-chemistry. In Mineral-Water Interface Geochemistry (M.F. Hochella & White, A.F., Eds.) Reviews in Mineralogy 23, pp. 177-260.

DAVIES, C.W. (1962) Ion Association. Butterworths, London.

DZOMBAK, D.A. & MOREL, F.M.M. (1990) Surface Complexation Modelling: Hydrous Ferric Oxides. John Wiley & Sons, New York, NY.

FOSCOLOS, A.E. & BARSHAD, I. (1969) Equilibrium constants between both freshly prepared and aged H-montmorillonites and chloride salt solutions. Soil Sci. Soc. Am. Proc. 33, 242-247.

GABIS, V. (1958) Etude préliminaire des argiles oligocènes du Puy-en-Velay (Haute-Loire). Bull. Soc. Franç. Minéral. Cristallog. 81, 183-185.

GAINES, G.I. & THOMAS, H.C. (1953). Adsorption studies on clay minerals. II. A formulation of the thermodynamics of exchange adsorption. J. Chem. Phys. 21, 714-718.

GILBERT, M. & LAUDELOUT, H. (1965). Exchange properties of hydrogen ions in clays. Soil Sci. 100, 157-162.

GORGEON, L. (1994) Contribution à la modélisation physico-chimique de la retention de radioéléments à vie longue par des matériaux argileux. PhD Thesis. Université Paris 6.

GRIM, R.E. (1953) Clay mineralogy. Mc Graw-Hill, New York.

HAYES, K.F., REDDEN, G., ELA, W. & LECKIE, J.O. (1991) Surface complexation models: An evaluation of model parameter estimation using FITEQL and oxide mineral titration data. J. Colloid Interface Sci. 142, 448-469.

HIEMSTRA, T., VAN RIEMSDIJK, W.H. & BRUGGENWERT, M.G.M. (1987) Proton adsorption mechanism at the gibbsite and aluminium oxide solid/solution interface. Neth. J. Agr. Sci. 35, 281-293.

HUMMEL, W., BERNER, U., CURTI, E., PEARSON, F.J. & THOENEN, T. (2002) Nagra/PSI Chemical Thermodynamic Data Base 01/01. Nagra Technical Report NTB 02-16, Nagra, Wettingen, Switzerland, and Universal Publishers/uPublish.com, Parkland, Florida, USA.

JAMES, R.O. & PARKS, G.A. (1982) Characterization of aqueous colloids by their electrical double-layer and intrinsic surface chemical properties. In Surface and Colloid Science, Vol. 12 (Ed. E. Matijevic), Plenum Press, pp. 119-216.

JANNASCH H. W., HONEYMAN B. D. & BALISTRIERI L. S. (1988) Kinetics of trace element uptake by marine particles. Geochim. Cosmochim. Acta 52, 567-577.

KRAEPIEL, A.M.L., KELLER, K. & MOREL, F.M.M. (1998) On the acid-base chemistry of permanently charged minerals. Envir. Sci. Techn. 32, 2829-2838.

KULIK, D.A., AJA, S.U., SINITSYN, V.A. & WOOD, S.A. (2000) Acid-base surface chemistry and sorption of some lanthanides on K^+-saturated Marblehead illite: II. A multisite-surface complexation modeling. Geochim. Cosmochim. Acta 64, 195-213.

LÖVGREN, L., SJOBERG, S. & SCHINDLER, P.W. (1990) Acid/base reactions and Al(III) complexation at the surface of goethite. Geochim. Cosmochim. Acta 54, 1201-1306.

NAGRA (2002) Project Opalinus Clay: Safety Report. Demonstration of disposal feasibility (Entsorgungsnachweis) for spent fuel, vitrified high-level waste and long-lived intermediate-level waste. Nagra Technical Report NTB 02-05, Nagra, Wettingen, Switzerland.

NAGY, K.L. (1995) Dissolution and precipitation kinetics of sheet silicates. In Chemical Weathering Rates of Silicate Minerals, Vol. 31 (Eds. A.F. White & S.L. Brantley) Mineralogical Society of America, pp. 176-233.

NEA (2003) Update on the chemical thermodynamics of uranium, neptunium, plutonium, americium and technecium. OECD Nuclear Energy Agency, Ed. Elsevier, Amsterdam.

ONDRAF (2001) SAFIR 2: Safety assessment and feasibility interim report 2. NIROND-2001-06 E. Ondraf, Brussels.

PERRIN, D. D. & DEMPSEY, B. (1974) Buffers for pH and metal ion control. Chapman and Hall, London.

POINSSOT, C., BAEYENS, B. & BRADBURY, M.H. (1999) Experimental studies of Cs, Sr, Ni and Eu sorption on Na-illite and the modelling of Cs sorption. PSI Bericht Nr. 99-06. Paul Scherrer Institut, Villigen and Nagra Technical Report NTB 99-04, Nagra, Wettingen, Switzerland.

SAVAGE, D., HUGHES, C.R., MILODOWSKI, A.E., BATEMAN, K., PEARCE, J.M., RAE, E. & ROCHELLE, C.R. (1990): The evaluation of chemical mass transfer in the disturbed zone of a deep geological disposal facility for radioactive wastes. I. Reactions of silicates with calcium hydroxide fluids. Nirex Safety Assessment Series Report, NSS/R244.

SAVAGE, D., HUGHES, C.R., MILODOWSKI, A.E., BATEMAN, K., PEARCE, J.M., RAE, E. & ROCHELLE, C.R. (1991): The evaluation of chemical mass transfer in the disturbed zone of a deep geological disposal facility for radioactive wastes. II. Reactions of silicates with Na-K-Ca hydroxide fluids. Nirex Safety Assessment Series Report, NSS/R283.

SCHINDLER, P.W. & STUMM, W. (1987) The surface chemistry of oxides, hydroxides, and oxide minerals. In Aquatic Surface Chemistry (Ed. W. Stumm), John Wiley, pp. 83-110.

SCHULTHESS, C.P. & SPARKS, D.L. (1986) Back titration technique for proton isotherm modelling of oxide surfaces. Soil Sci. Soc. Am. J. 50, 1406-1411.

SCHULTHESS, C.P. & SPARKS, D.L. (1987) Two-site model for aluminium oxide with mass balanced competitive pH+salt/salt dependent reactions. Soil Sci. Soc. Am. J. 51, 1136-1144.

SCHULTHESS, C.P. & SPARKS, D.L. (1988) A critical assessment of surface adsorption models. Soil Sci. Soc. Am. J. 52, 92-97.

SINITSYN, V.A., AJA, S.U., KULIK, D.A. & WOOD, S.A. (2000) Acid-base surface chemistry and sorption of some lanthanides on K^+-saturated Marblehead illite: I. Results of an experimental investigation. Geochim. Cosmochim. Acta 64, 185-194.

SPOSITO, G. (1984) The Surface Chemistry of Soils. Oxford University Press, New York, NY.

VANSELOW A.P. (1932) Equilibria of the base-exchange reactions of bentonites, permutites, soil colloids and zeolites. Soil Sci. 33, 95-113.

VAN OLPHEN, H. (1963) An Introduction to Clay Colloid Chemistry. Interscience Publishers, New York, NY.

WANNER, H., ALBINSSON, Y., KARNLAND, O, WIELAND, E., WERSIN, P. & CHARLET, L. (1994) The acid/base chemistry of montmorillonite. Radiochim. Acta 66/67, 157-162.

WESTALL, J., ZACHARY, J.L. & MOREL, F. (1976) MINEQL: A computer program for the calculation of chemical equilibrium composition of aqueous systems. Technical Note 18, Dept. of Civil Eng., Massachusetts Institute of Technology, Cambridge, Massachusetts.

Appendix A

Summary tables of titration data measured in 0.5 M $NaClO_4$

Table A-1: Experimental conditions for the titration tests on conditioned Na-illite (IdP-1) in 0.5 M $NaClO_4$.

Experimental Conditions	
pH range	3.0 - 11.4
S:L ratio (g L^{-1})	8.3
reaction time (hours)	24
Nr. of data points (titration with HNO_3/NaOH)	10/10

Table A-2: Results of titration measurements on conditioned Na-illite (IdP-1) in 0.5 M $NaClO_4$ (S:L ratio = 8.3 g L^{-1}, 1 day equilibration time).

Data point	Added acid (µmol)[1)]	Base used in back titration (µmol)[2)]	Total H^+ consumed (µmol)	Total H^+ consumed (mmol kg^{-1})[3)]	pH
1	196.74	143.23	53.50	161.25	3.04
2	139.97	88.38	51.58	155.47	3.15
3	96.19	50.82	45.38	136.76	3.58
4	71.55	31.23	40.32	121.52	3.71
5	47.89	15.06	32.83	98.95	4.53
6	38.26	8.80	29.46	88.78	4.84
7	29.04	4.62	24.42	73.59	5.52
8	18.61	1.92	16.69	50.30	6.21
9	9.28	1.10	8.18	24.64	7.06
10	4.48	0.53	3.95	11.91	7.83
Data point	Added base (µmol)[1)]	Acid used in back titration (µmol)[2)]	Total OH^- consumed (µmol)	Total OH^- consumed (mmol kg^{-1})[3)]	pH
11	4.53	0.32	4.21	12.68	8.77
12	10.18	1.97	8.21	24.74	9.22
13	19.68	6.24	13.44	40.51	9.83
14	29.38	12.46	16.91	50.97	10.17
15	38.74	19.66	19.07	57.48	10.54
16	48.56	27.15	21.41	64.52	10.59
17	74.08	50.75	23.33	70.31	10.90
18	99.49	72.22	27.26	82.17	11.02
19	145.73	119.62	26.11	78.70	11.35
20	195.74	165.66	30.08	90.66	11.24

[1)] Acid or base added to 40 ml of suspension
[2)] Acid or base added to supernatant solutions (normalised to 40 ml)
[3)] The total amount of Na-illite was 3.32 x 10^{-4} kg

Table A-3: Chemical analyses results (mol L^{-1}) of the supernatant solutions from titration experiments with conditioned Na-illite (IdP-1) in 0.5 M $NaClO_4$ corresponding to Table A-2. (S:L ratio = 8.3 g L^{-1}; 1 day equilibration time).

Data point	pH	K	Mg	Ca	Sr	Si	Al	Fe	Mn
1	3.04	1.1 E-4	8.0 E-5	5.5 E-4	1.8 E-6	4.6 E-4	3.9 E-4	1.6 E-5	7.6 E-6
2	3.15	1.0 E-4	6.5 E-5	5.6 E-4	1.8 E-6	4.0 E-4	3.2 E-4	1.3 E-5	7.1 E-6
3	3.58	8.1 E-5	4.8 E-5	5.5 E-4	1.8 E-6	3.2 E-4	2.2 E-4	2.7 E-6	5.8 E-6
4	3.71	7.5 E-5	4.0 E-5	4.6 E-4	1.7 E-6	3.0 E-4	1.4 E-4	2.3 E-6	4.6 E-6
5	4.53	5.0 E-5	3.4 E-5	3.1 E-4	1.5 E-6	2.5 E-4	5.7 E-5	< rdl	3.4 E-6
6	4.84	6.7 E-5	3.0 E-5	2.5 E-4	1.3 E-6	2.4 E-4	2.8 E-5	< rdl	2.7 E-6
7	5.52	5.8 E-5	2.5 E-5	1.9 E-4	1.2 E-6	1.9 E-4	8.2 E-6	< rdl	2.0 E-6
8	6.21	3.6 E-5	2.1 E-5	1.2 E-4	8.9 E-7	1.5 E-4	1.9 E-6	< rdl	3.1 E-6
9	7.06	4.1 E-5	1.3 E-5	6.0 E-5	5.1 E-7	1.1 E-4	1.5 E-6	< rdl	4.2 E-7
10	7.83	8.3 E-5	1.1 E-5	5.2 E-5	4.3 E-7	8.6 E-5	9.6 E-6	< rdl	2.3 E-7
11	8.77	3.3 E-5	4.4 E-6	2.7 E-5	3.5 E-7	3.7 E-5	6.3 E-6	< rdl	< rdl
12	9.22	2.6 E-5	2.0 E-6	2.1 E-5	3.1 E-7	3.7 E-5	8.5 E-6	< rdl	< rdl
13	9.83	3.7 E-5	1.3 E-6	2.0 E-5	2.4 E-7	-	1.0 E-5	< rdl	< rdl
14	10.17	4.0 E-5	1.4 E-6	1.8 E-5	2.2 E-7	-	9.6 E-6	< rdl	< rdl
15	10.54	2.8 E-5	1.1 E-6	1.5 E-5	2.0 E-7	-	2.0 E-5	< rdl	< rdl
16	10.59	2.2 E-5	1.3 E-6	1.5 E-5	1.9 E-7	-	2.2 E-5	< rdl	< rdl
17	10.90	3.1 E-5	2.8 E-6	1.4 E-5	1.8 E-7	-	3.3 E-5	9.0 E-7	< rdl
18	11.02	-	8.4 E-7	8.1 E-6	1.3 E-7	-	4.1 E-5	< rdl	< rdl
19	11.35	2.8 E-5	7.4 E-7	4.2 E-6	9.1 E-8	-	5.9 E-5	< rdl	< rdl
20	11.24	3.3 E-5	1.2 E-6	6.7 E-6	9.1 E-8	-	6.8 E-5	< rdl	< rdl

- : no reliable measurement
< rdl: below reliable detection limit

Table A-4: Chemical analyses results (mol L^{-1}) of the supernatant solutions from additional batch tests with conditioned Na-illite (IdP-2) in 0.5 M $NaClO_4$. (S:L ratio = 8.3 g L^{-1}, 1 day equilibration time).

pH	K	Mg	Ca	Sr	Si	Al	Fe	Mn
2.58	4.2 E-5	4.5 E-5	4.3 E-4	1.8 E-6	1.7 E-4	-	7.6 E-6	7.6 E-7
2.70	4.1 E-5	4.1 E-5	4.3 E-4	1.8 E-6	1.6 E-4	2.4E-4	6.8 E-6	7.3 E-7
2.88	3.7 E-5	3.5 E-5	4.3 E-4	1.8 E-6	1.3 E-4	2.1E-4	4.9 E-6	6.7 E-7
3.04	3.6 E-5	3.2 E-5	4.3 E-4	1.8 E-6	1.3 E-4	1.9E-4	4.9 E-6	6.5 E-7
3.26	3.2 E-5	2.8 E-5	4.3 E-4	1.8 E-6	1.1 E-4	1.6E-4	3.1 E-6	5.9 E-7
3.81	2.6 E-5	1.8 E-5	3.0 E-4	1.4 E-6	7.7 E-5	7.2E-5	1.1 E-6	3.9 E-7
4.32	3.4 E-5	1.3 E-5	1.5 E-4	8.9 E-7	6.1 E-5	2.1E-5	5.4 E-7	2.1 E-7
5.04	1.9 E-5	9.0 E-6	7.1 E-5	5.8 E-7	4.7 E-5	3.7E-6	3.8 E-7	1.0 E-7
5.66	1.8 E-5	6.3 E-6	3.9 E-5	3.5 E-7	3.3 E-5	2.2E-6	5.3 E-7	5.6 E-8
5.81	1.8 E-5	5.2 E-6	3.4 E-5	2.9 E-7	2.2 E-5	3.5E-6	7.6 E-7	3.1 E-8
6.62	1.7 E-5	4.3 E-6	2.9 E-5	2.5 E-7	1.5 E-5	3.9E-6	8.1 E-7	1.6 E-8
7.32	1.7 E-5	-	-	-	-	3.3E-6	7.3 E-7	2.0 E-8
7.36	2.1 E-5	2.6 E-6	2.2 E-5	2.0 E-7	1.1 E-5	3.3E-6	7.1 E-7	1.0 E-8
9.08	1.5 E-5	8.0 E-7	1.4 E-5	1.5 E-7	1.1 E-5	2.2E-6	1.3 E-7	9.1 E-9
10.26	1.6 E-5	3.7 E-7	7.2 E-6	1.0 E-7	2.7 E-5	1.0E-5	1.5 E-7	-
10.81	1.6 E-5	3.9 E-7	6.8 E-6	7.0 E-8	5.8 E-5	2.7E-5	1.7 E-7	-
10.96	1.6 E-5	5.0 E-7	7.8 E-6	7.0 E-8	7.3 E-5	3.5E-5	1.8 E-7	-
11.06	1.6 E-5	4.1 E-7	4.9 E-6	6.2 E-8	8.4 E-5	4.2E-5	2.5 E-7	1.1 E-8
11.22	1.7 E-5	8.0 E-7	6.6 E-6	6.1 E-8	1.1 E-4	5.7E-5	7.5 E-7	1.7 E-8
11.32	1.7 E-5	4.5 E-7	5.1 E-6	5.1 E-8	1.3 E-4	6.9E-5	3.0 E-7	1.4 E-8

- : no reliable measurement

Summary tables of titration data measured in 0.1 M $NaClO_4$

Table A-5: Experimental conditions for the titration tests on conditioned Na-illite in 0.1 M $NaClO_4$. (S:L ratio = 7.1, 10.7, 12.6 g L^{-1}).

Experimental conditions	IdP-1	IdP-2
pH range	2.6 - 11.1	3.1 – 11.5
S:L ratio (g L^{-1})	7.1, 10.7, 12.6 *	12.9
reaction time (hours)	24	24
Nr. of data points (titration with HNO_3/NaOH)	9/10	3/3

*)The experiments were carried with 3 different conditioned Na-illite suspension batches.

Table A-6: Results of titration measurements on conditioned Na-IdP-1 in 0.1 M $NaClO_4$. (S:L ratio = 7.1, 10.7, 12.6 g L^{-1}, 1 day equilibration time).

Data point	Added acid (µmol) 1)	Base used in back titration (µmol) 2)	Total H^+ consumed (µmol)	Total H^+ consumed (mmol kg^{-1})3)	pH
1	197.17	101.25	95.92	224.32	2.59
2	147.07	62.45	84.61	197.88	2.78
3	98.37	29.71	68.67	160.59	3.28
4	72.91	18.91	54.00	126.29	3.55
5	46.26	11.28	34.98	123.52	3.93
6	36.88	7.95	28.93	102.16	4.21
7	27.60	5.10	22.50	79.45	4.50
8	17.52	2.77	14.75	52.10	5.03
9	8.93	1.49	7.44	26.27	5.71
10	4.45	0.94	3.50	12.37	6.47
Data point	Added base (µmol)1)	Acid used in back titration (µmol)2)	Total OH^- consumed (µmol)	Total OH^- consumed (mmol kg^{-1})3)	pH
11	4.99	0.38	4.61	16.27	8.28
12	9.81	1.50	8.30	29.33	9.17
13	19.94	6.72	13.22	46.67	9.96
14	29.49	13.50	15.98	56.45	10.32
15	39.41	21.71	17.70	62.49	10.51
16	74.69	42.21	32.48	75.96	10.58
17	99.71	66.19	33.52	78.39	10.75
18	149.52	106.13	43.39	101.47	10.89
19	194.53	146.13	48.40	96.03	11.05

1)Acid or base added to 40 ml of suspension.
2)Acid or base added to supernatant solutions (normalised to 40 ml).
3)The total amount of Na-illite in samples 1 to 4 and 16 to 18 was 4.28×10^{-4} kg. The total amount of Na-illite in samples 5 to 10 and 11 to 15 was 2.83×10^{-4} kg. The total amount of Na-illite in sample 19 was 5.04×10^{-4} kg.

Table A-7: Results of titration measurements on conditioned Na-illite (IdP-2) in 0.1 M $NaClO_4$. (S:L ratio = 12.9 g L^{-1}, 1 day equilibration time.)

Data point	Added acid (µmol)[1)]	Base used in back titration (µmol)[2)]	Total H^+ consumed (µmol)	Total H^+ consumed (mmol kg^{-1})[3)]	pH
1	150	54.25	95.75	182.6	3.11
2	50	8.07	41.93	80.0	4.33
3	15	1.23	13.77	26.3	5.91
Data point	Added base (µmol)[1)]	Acid used in back titration (µmol)[2)]	Total OH^- consumed (µmol)	Total OH^- consumed (mmol kg^{-1})[3)]	pH
4	10	1.57	8.43	16.1	8.08
5	75	40.92	34.08	65.0	10.81
6	200	158.27	41.73	79.6	11.46

[1)] Acid or base added to 40 ml of suspension.
[2)] Acid or base added to supernatant solutions (normalised to 40 ml).
[3)] The total amount of Na-illite in samples was 5.16×10^{-4} kg.

Table A-8: Chemical analyses results (mol L^{-1}) of the supernatant solutions from titration experiments with conditioned Na-illite (IdP-1) in 0.1 M $NaClO_4$ corresponding to Table A-6. (S:L ratio = 7.1, 10.7, 12.6 g L^{-1}, 1 day equilibration time).

Data point	pH	K	Mg	Ca	Sr	Si	Al	Fe	Mn
1	2.59	2.1 E-4	9.2 E-5	4.2 E-4	7.1 E-7	7.2 E-4	2.4 E-4	2.1 E-5	6.6 E-6
2	2.78	2.1 E-4	7.7 E-5	4.0 E-4	6.7 E-7	6.1 E-4	1.8 E-4	1.3 E-5	5.7 E-6
3	3.28	1.6 E-4	5.6 E-5	3.8 E-4	6.2 E-7	4.8 E-4	1.0 E-4	6.3 E-6	4.4 E-6
4	3.55	2.7 E-4	3.8 E-5	3.3 E-4	5.5 E-7	4.2 E-4	6.9 E-5	1.9 E-6	2.6 E-6
5	3.93	3.5 E-5	2.9 E-5	2.4 E-4	3.3 E-7	2.4 E-4	4.0 E-5	3.5 E-6	2.0 E-6
6	4.21	2.2 E-5	2.3 E-5	2.3 E-4	2.9 E-7	2.1 E-4	2.7 E-5	4.0 E-6	1.6 E-6
7	4.50	< rdl	2.0 E-5	1.6 E-4	2.1 E-7	1.8 E-4	9.8 E-6	9.0 E-7	9.8 E-7
8	5.03	< rdl	1.6 E-5	9.7 E-5	1.6 E-7	1.6 E-4	6.9 E-6	1.1 E-6	6.1 E-7
9	5.71	< rdl	1.2 E-5	4.4 E-5	< rdl	1.2 E-4	9.8 E-6	1.2 E-6	1.5 E-7
10	6.47	< rdl	7.7 E-6	3.5 E-5	< rdl	8.5 E-5	6.1 E-6	1.4 E-6	< rdl
11	8.28	< rdl	5.6 E-6	3.1 E-5	< rdl	5.8 E-5	6.3 E-6	3.0 E-6	< rdl
12	9.17	< rdl	3.7 E-6	2.4 E-5	< rdl	6.7 E-5	7.4 E-6	3.7 E-6	< rdl
13	9.96	3.2 E-5	3.2 E-6	1.5 E-5	< rdl	6.7 E-5	1.2 E-5	2.9 E-6	< rdl
14	10.32	< rdl	1.4 E-6	1.1 E-5	< rdl	7.6 E-5	1.2 E-5	< rdl	< rdl
15	10.51	< rdl	1.5 E-6	1.2 E-5	< rdl	8.5 E-5	1.8 E-5	< rdl	< rdl
16	10.58	1.4 E-4	2.9 E-7	2.8 E-6	< rdl	1.5 E-4	2.4 E-5	1.6 E-7	< rdl
17	10.75	1.3 E-4	1.9 E-7	1.5 E-6	< rdl	1.9 E-4	3.5 E-5	< rdl	4.2 E-8
18	10.89	1.7 E-4	3.8 E-7	1.4 E-6	< rdl	2.3 E-4	5.9 E-5	1.9 E-7	< rdl
19	11.05	1.3 E-4	4.0 E-7	1.5 E-6	< rdl	2.7 E-4	9.2 E-5	3.7 E-7	< rdl

< rdl: below reliable detection limit

Table A-9: Chemical analyses results (mol L^{-1}) of the supernatant solutions from titration experiments with conditioned Na-illite (IdP-2) in 0.1 M $NaClO_4$ corresponding to Table A-7. (S:L ratio = 12.9 g L^{-1}, 1 day equilibration time).

Data point	pH	K	Mg	Ca	Sr	Si	Al	Fe	Mn
1	3.11	3.3 E-4	7.5 E-5	4.6 E-4	1.9 E-6	7.1 E-4	1.5 E-4	6.5 E-6	9.3 E-7
2	4.33	1.4 E-4	2.8 E-5	2.2 E-4	1.2 E-6	4.2 E-4	2.5 E-5	7.0 E-7	1.6 E-7
3	5.91	1.0 E-4	1.4 E-5	5.2 E-5	3.9 E-7	2.9 E-4	1.9 E-6	2.6 E-7	3.1 E-8
ref	6.74	2.7 E-5	7.0 E-6	2.1 E-5	1.6 E-7	1.4 E-4	4.4 E-7	1.4 E-7	1.5 E-8
ref	7.07	5.8 E-5	7.2 E-6	2.5 E-5	1.6 E-7	1.5 E-4	5.6 E-7	1.9 E-7	1.2 E-8
4	8.08	1.1 E-4	3.5 E-6	1.9 E-5	1.2 E-7	9.6 E-5	2.4 E-6	3.2 E-7	1.2 E-8
5	10.8	1.9 E-4	8.1 E-7	5.2 E-6	2.3 E-8	1.8 E-4	1.8 E-5	3.6 E-7	1.2 E-8
6	11.46	2.5 E-4	6.4 E-7	3.9 E-6	1.2 E-8	3.3 E-4	7.2 E-5	1.9 E-7	9.2 E-9

ref: no acid/base added

Table A-10: Chemical analyses results (mol L^{-1}) of the supernatant solutions from additional batch tests with conditioned Na-illite (IdP-2) in 0.1 M $NaClO_4$. (S:L ratio = 13.1 g L^{-1})

pH	K	Mg	Ca	Sr	Si	Al	Fe	Mn
2.6	8.0 E-5	1.2 E-4	4.6 E-4	2.1 E-6	7.62E-4	2.6 E-4	1.3 E-5	1.3 E-6
3.1	5.8 E-5	8.3 E-5	4.4 E-4	2.0 E-6	6.27E-4	1.5 E-4	5.6 E-6	9.5 E-7
3.5	4.4 E-5	5.7 E-5	4.1 E-4	1.8 E-6	5.23E-4	8.5 E-5	1.4 E-6	5.5 E-7
4.2	2.7 E-5	3.2 E-5	2.2 E-4	1.2 E-6	4.02E-4	2.3 E-5	2.9 E-7	1.9 E-7
4.9	2.2 E-5	2.1 E-5	9.3 E-5	6.9 E-7	3.47E-4	5.4 E-6	7.3 E-7	7.7 E-8
5.5	1.8 E-5	1.6 E-5	4.8 E-5	4.1 E-7	2.94E-4	2.5 E-6	5.2 E-7	4.2 E-8
6.7	1.3 E-5	8.5 E-6	2.1 E-5	2.0 E-7	1.66E-4	1.9 E-7	4.7 E-8	1.3 E-9
8.3	1.2 E-5	4.1 E-6	1.5 E-5	1.2 E-7	1.07E-4	2.1 E-6	4.4 E-7	6.4 E-9
9.1	9.7 E-6	4.9 E-6	6.9 E-6	8.0 E-8	7.80E-5	1.0 E-6	3.2 E-8	9.1 E-10
10.1	8.5 E-6	4.3 E-7	3.8 E-6	3.6 E-8	1.14E-4	5.6 E-6	1.2 E-7	1.3 E-9
10.6	7.8 E-6	5.9 E-7	2.5 E-6	3.0 E-8	1.62E-4	1.3 E-5	3.4 E-7	2.6 E-9
11.2	7.8 E-6	2.6 E-7	1.4 E-6	9.9 E-9	2.98E-4	5.4 E-5	1.5 E-7	1.1 E-9
11.5	6.6 E-6	1.9 E-7	1.3 E-6	8.8 E-9	4.02E-4	1.0 E-4	8.8 E-8	9.1 E-10

Summary tables of titration data measured in 0.01 M $NaClO_4$

Table A-11: Experimental conditions for the titration tests on conditioned Na-illite in 0.01 M $NaClO_4$.

Experimental conditions	IdP-1
pH range	2.8 - 11.3
S:L ratio (g L^{-1})	6.7 to 10.5
reaction time (hours)	24
Nr. of data points (titration with HNO_3/NaOH)	5/5

Table A-12: Results of titration measurements on conditioned Na-illite (IdP-1) in 0.01 M $NaClO_4$ (S:L ratio = 6.7 to 10.5 g L^{-1}, 1 day equilibration time.)

Data point	Added acid (mmol)[1)]	Base used in back titration (mmol)[2)]	Total H^+ consumed (mmol)	Total H^+ consumed (mmol kg^{-1})[2)]	pH
1	148.66	84.66	64.00	238.80	2.8
2	99.19	33.22	65.98	205.16	3.1
3	50.41	4.99	45.42	121.05	4.1
4	29.62	2.51	27.11	68.36	4.9
5	10.14	1.21	8.92	21.34	5.7
Data point	Added base (mmol)[1)]	Acid used in back titration (mmol)[2)]	Total OH^- consumed (mmol)	Total OH^- consumed (mmol kg^{-1})	pH
6	9.64	0.47	9.18	21.95	8.0
7	29.62	6.86	22.76	57.39	9.8
8	49.86	23.56	26.30	70.09	10.4
9	100.04	73.26	26.77	83.25	10.9
10	150.01	127.76	22.26	83.05	11.3

[1)] Acid or base added to the total volume of suspension.
[2)] Acid or base added to supernatant solutions (normalised to the total volume).
[3)] The total amount of Na-Illite in samples 1 and 10 was 2.68 x 10^{-4} kg; in samples 2 and 9 was 3.22 x 10^{-4} kg; in samples 3 and 8 was 3.75 x 10^{-4} kg; in samples 4 and 7 was 3.97 x 10^{-4} kg; in samples 5 and 6 was 4.18 x 10^{-4} kg.

Table A-13: Chemical analyses results (mol L^{-1}) of the supernatant solutions from titration experiments with conditioned Na-illite (IdP-1) in 0.5 M $NaClO_4$ corresponding to Table A-12). (S:L ratio = 6.7 to 10.5 g L^{-1}, 1 day equilibration time.)

Data point	pH	K	Mg	Ca	Si	Al	Fe
1	2.8	9.7 E-5	6.5 E-5	1.3 E-4	3.6 E-4	4.6 E-5	1.1 E-5
2	3.1	6.5 E-5	4.9 E-5	1.2 E-4	3.3 E-4	2.0 E-5	7.2 E-6
3	4.1	5.9 E-5	9.2 E-6	3.5 E-5	2.5 E-4	4.1 E-6	8.0 E-7
4	4.9	3.0 E-5	3.8 E-6	1.4 E-5	2.2 E-4	1.7 E-6	2.1 E-7
5	5.7	3.2 E-5	1.5 E-6	5.7 E-6	1.6 E-4	1.1 E-6	2.7 E-7
6	8.0	3.7 E-5	2.6 E-6	5.0 E-6	8.6 E-5	8.1 E-6	1.7 E-6
7	9.8	7.6 E-5	1.8 E-5	4.8 E-6	2.3 E-4	8.2 E-5	1.7 E-5
8	10.4	4.1 E-5	2.2 E-5	3.9 E-6	3.0 E-4	1.1 E-4	1.9 E-5
9	10.9	5.0 E-5	1.3 E-5	2.6 E-6	3.1 E-4	1.1 E-4	1.2 E-5
10	11.3	7.5 E-5	4.2 E-6	7.4 E-6	2.9 E-4	6.3 E-5	2.7 E-6

Mn and Sr were not measured.

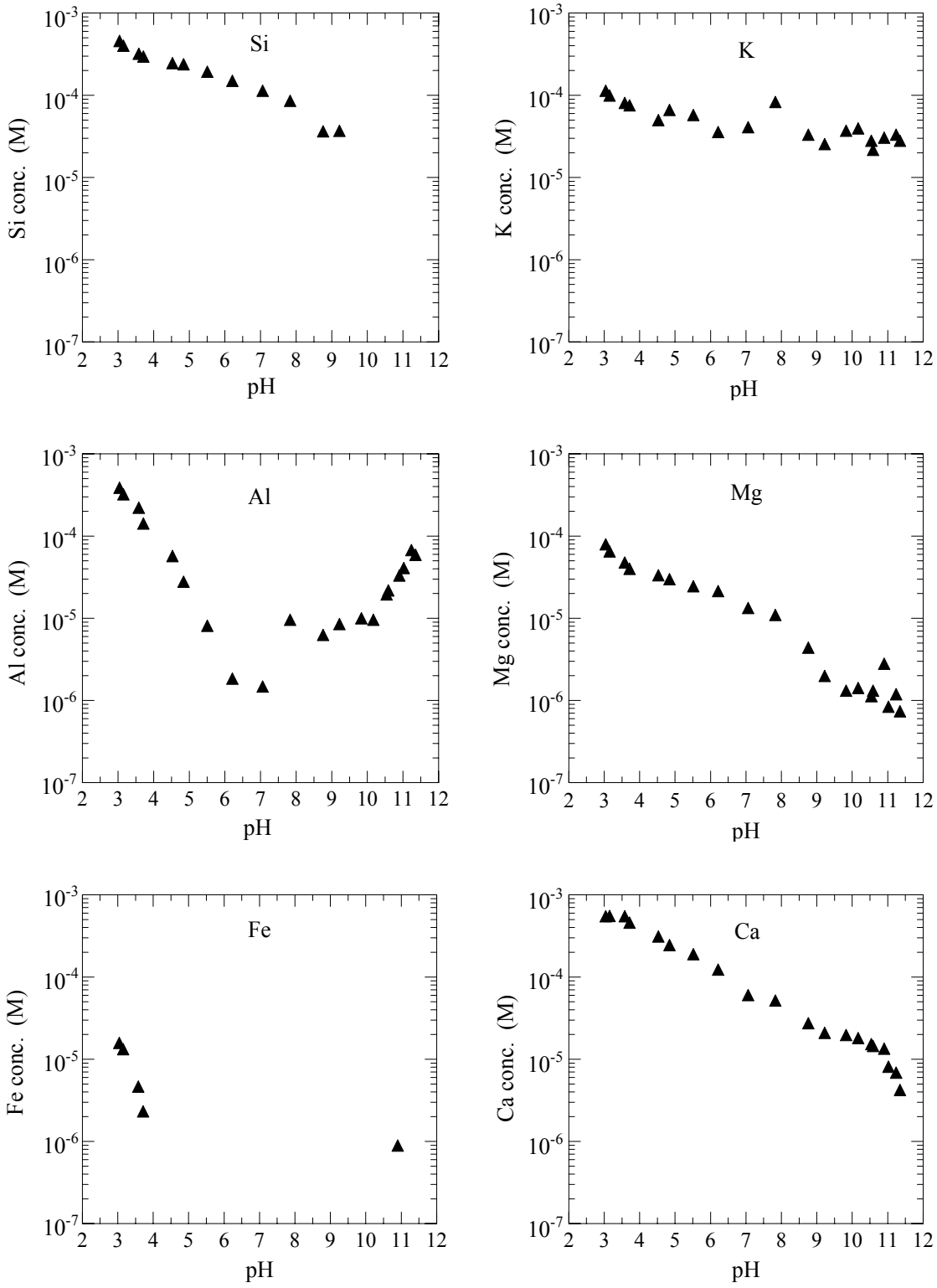

Fig. A-1: Chemical analyses results (mol L^{-1}) for Si, Al, Fe, K, Mg and Ca of the supernatant solutions from titration experiments with conditioned Na-Illite (IdP-1) in 0.5 M $NaClO_4$. S:L ratio = 8.3 g L^{-1} (see Table A-3).

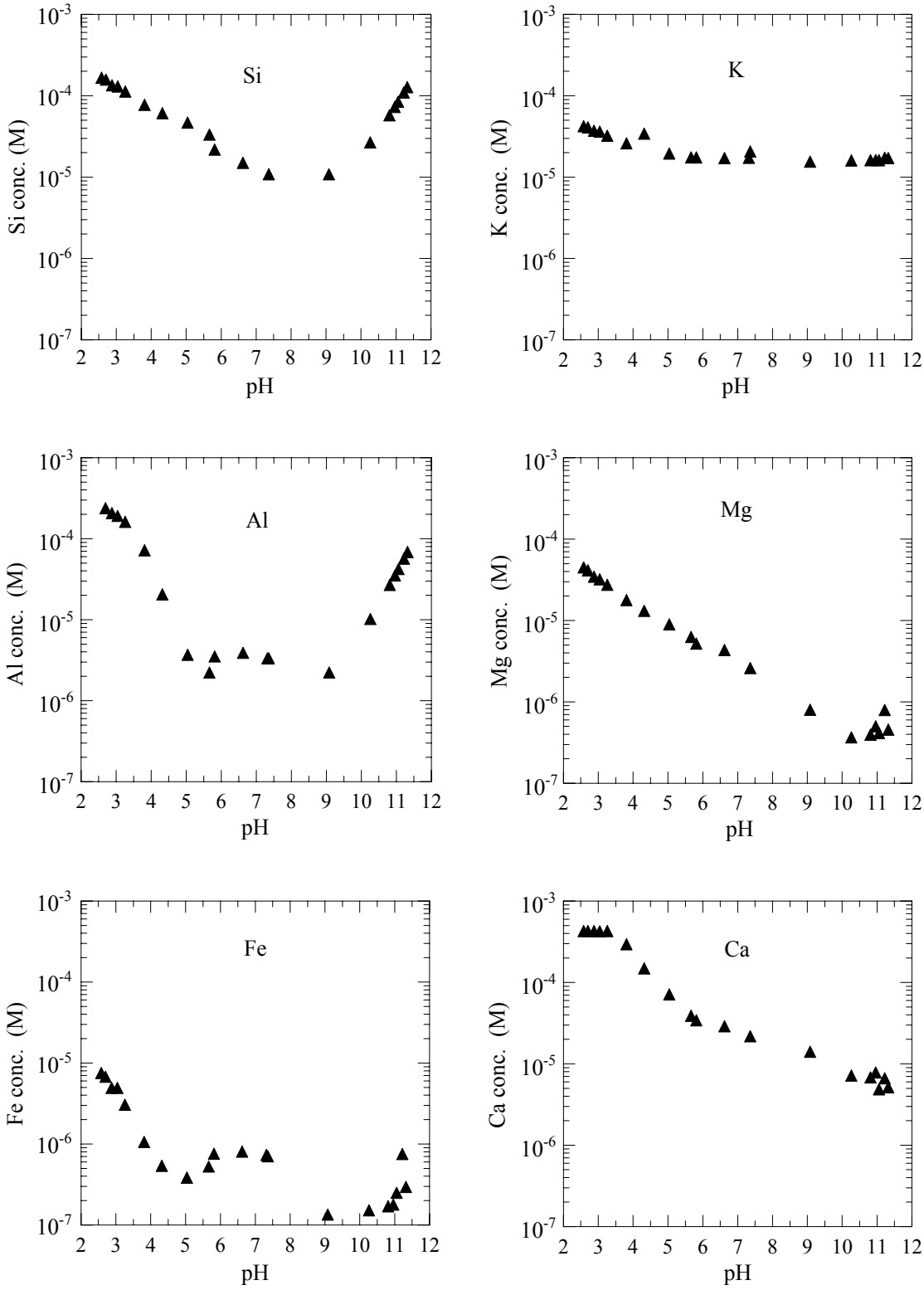

Fig. A-2: Chemical analyses results (mol L^{-1}) for Si, Al, Fe, K, Mg and Ca of the supernatant solutions from additional batch tests with conditioned Na-illite (IdP-2) in 0.5 M $NaClO_4$. S:L ratio = 8.3 g L^{-1} (see Table A-4).

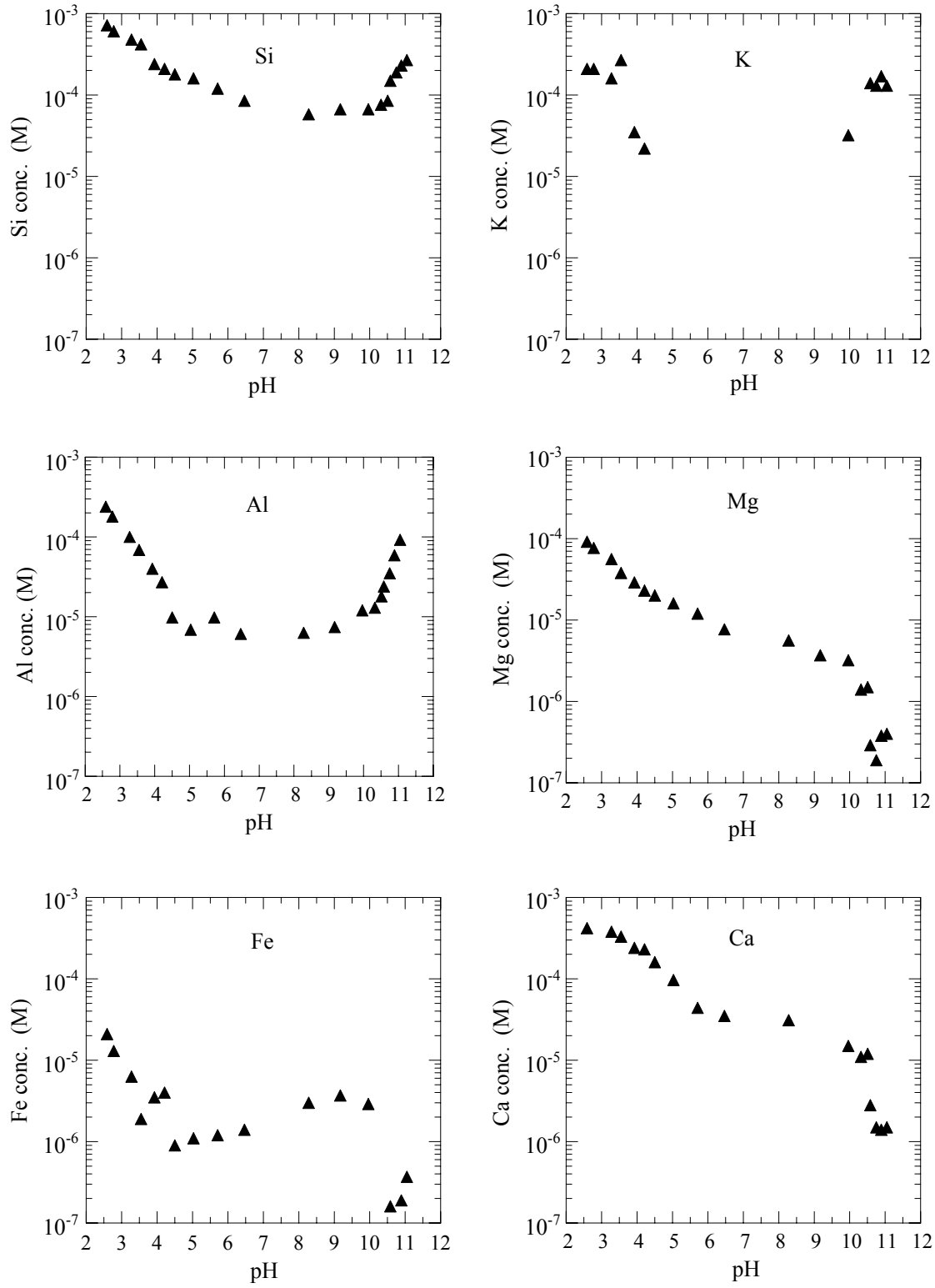

Fig. A-3: Chemical analyses results (mol L^{-1}) for Si, Al, Fe, K, Mg and Ca of the supernatant solutions from titration experiments with conditioned Na-illite (IdP-1) in 0.1 M $NaClO_4$. S:L ratio = 7.1, 10.7 and 12.6 g L^{-1} (see Table A-8).

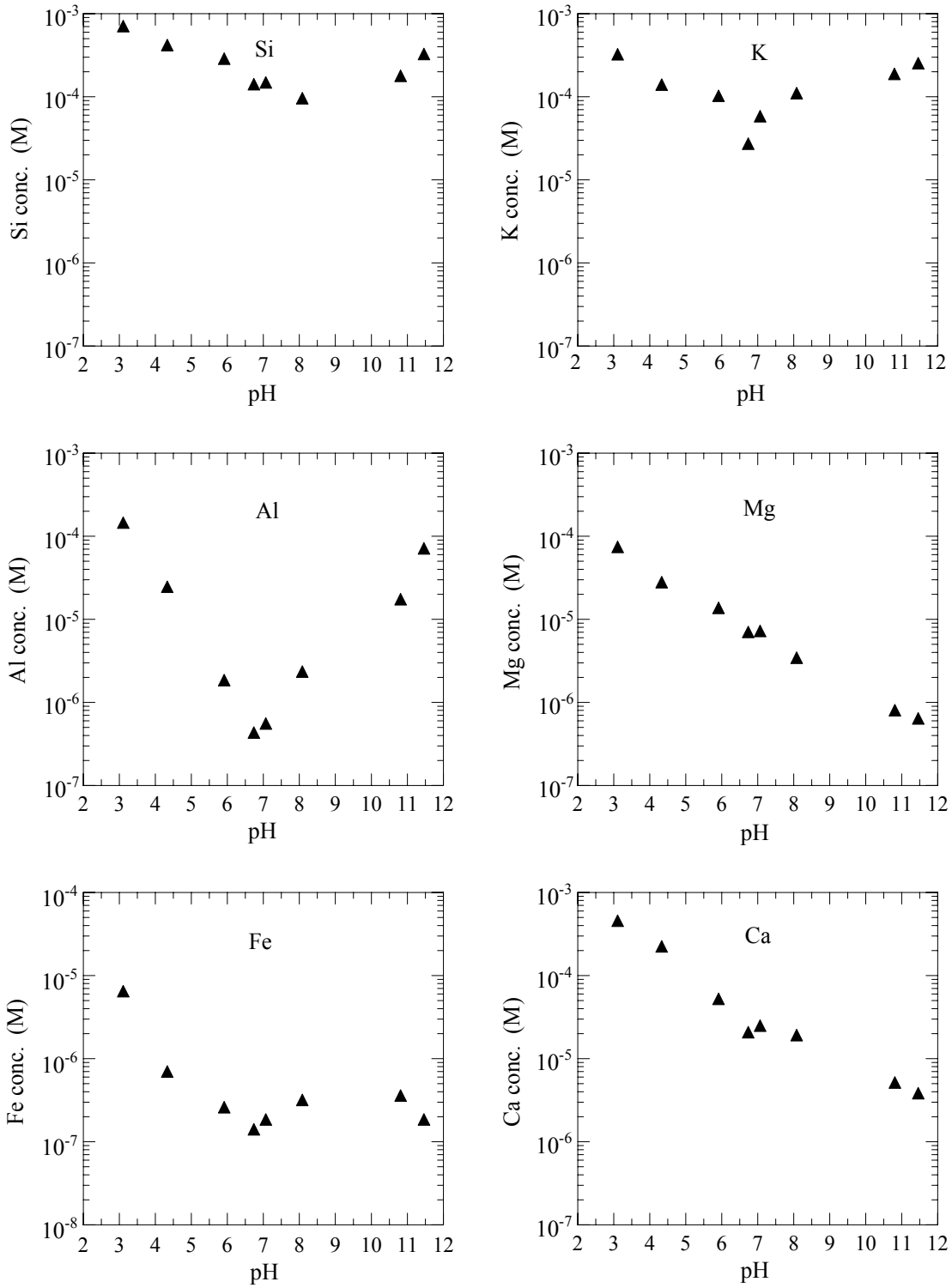

Fig. A-4: Chemical analyses results (mol L^{-1}) for Si, Al, Fe, K, Mg and Ca of the supernatant solutions from titration experiments with conditioned Na-illite (IdP-2) in 0.1 M $NaClO_4$. S:L ratio = 12.9 g L^{-1} (see Table A-9).

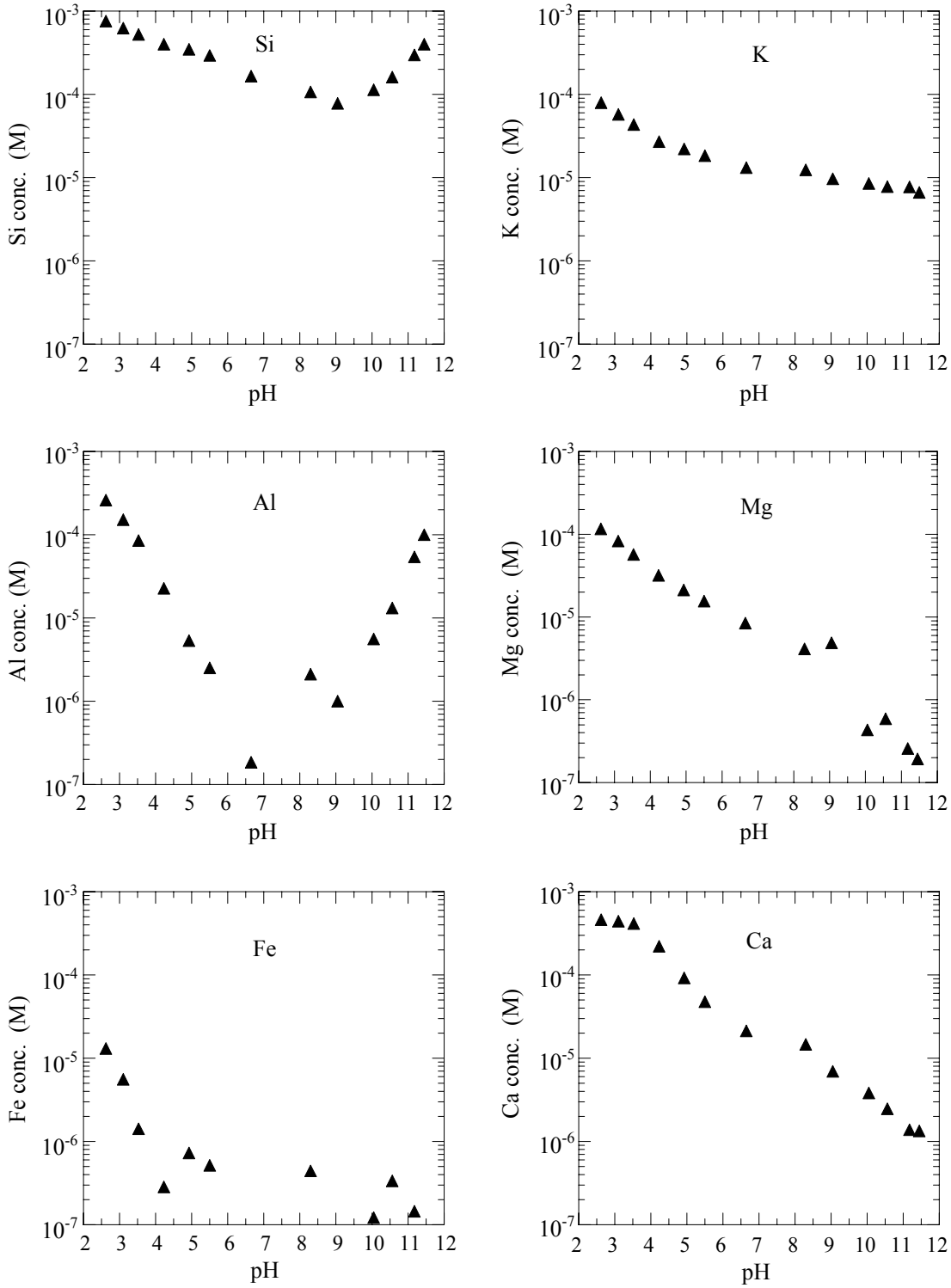

Fig. A-5: Chemical analyses results (mol L^{-1}) for Si, Al, Fe, K, Mg and Ca of the supernatant solutions from additional batch experiments with conditioned Na-illite (IdP-2) in 0.1 M $NaClO_4$. S:L ratio = 13.1 g L^{-1} (see Table A-10).

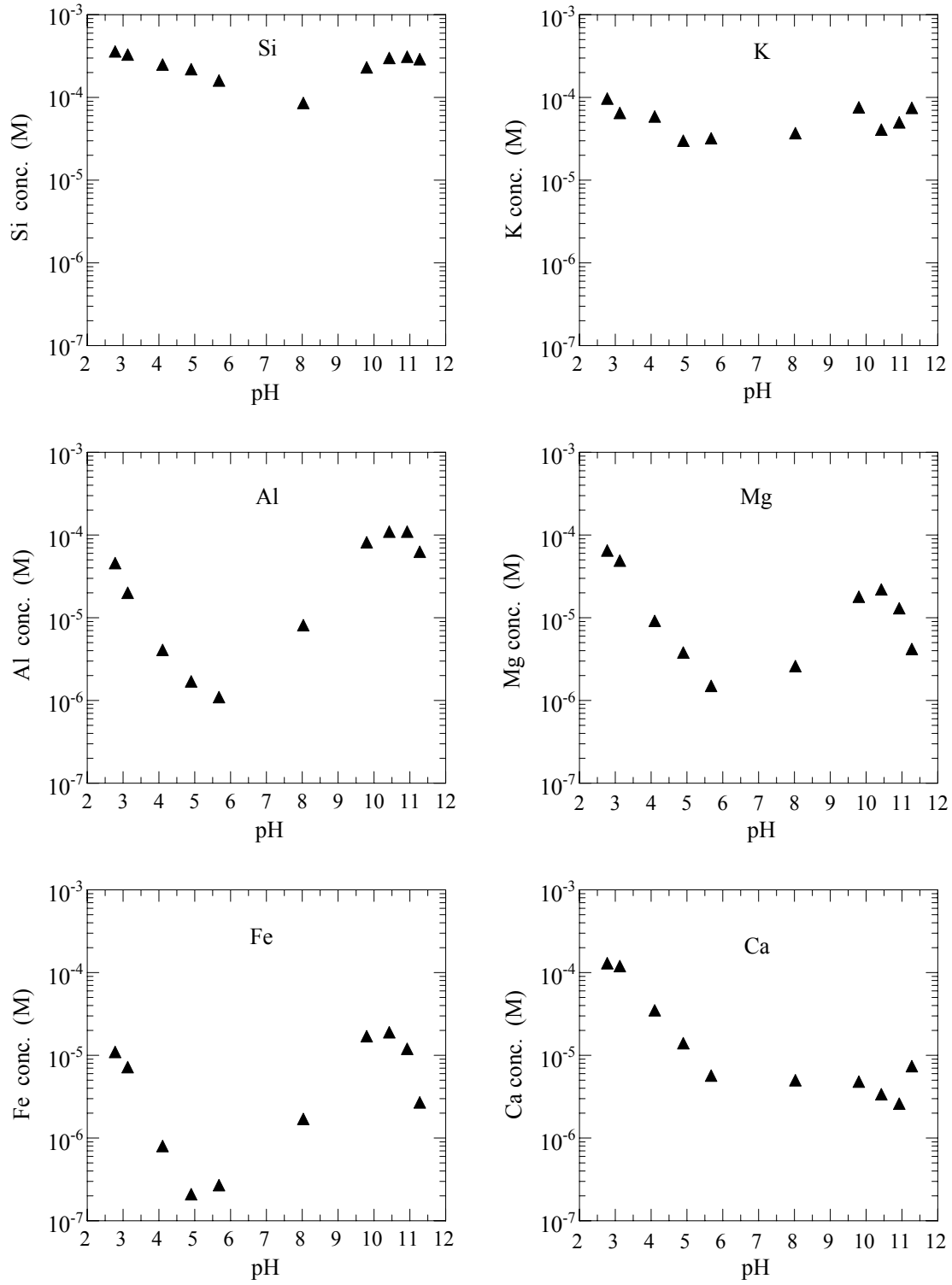

Fig. A-6: Chemical analyses results (mol L^{-1}) for Si, Al, Fe, K, Mg and Ca of the supernatant solutions from titration experiments with conditioned Na-illite (IdP-1) in 0.01 M $NaClO_4$. S:L ratio = 6.7 to 10.5 g L^{-1} (see Table A-13).

Appendix B

Aqueous chemistry data for the evaluation and interpretation of the batch sorption experiments

Table B-1: Chemical analyses of the supernatant solutions (mol L^{-1}) after 7 days interaction time between 0.01 M $NaClO_4$ and conditioned Na-illite (IdP-1). S:L ratio = 2.2 g L^{-1}. (Data taken from POINSSOT et al., 1999).

pH	Si	Al	Fe	Mg	K	Ca	Sr	Mn
3.2	1.7 E-4	3.4 E-5	3.9 E-7	3.1 E-5	2.5 E-5	1.1 E-4	2.2 E-7	1.7 E-6
4.5	9.9 E-5	4.5 E-6	3.8 E-7	1.0 E-5	1.3 E-5	6.4 E-5	1.4 E-7	5.6 E-7
5.8	6.5 E-5	1.8 E-6	1.0 E-6	3.7 E-6	7.7 E-6	2.7 E-5	5.9 E-8	8.0 E-8
6.6	4.6 E-5	4.6 E-6	2.0 E-7	1.6 E-6	4.7 E-6	8.2 E-6	1.9 E-8	6.8 E-9
8.8	4.9 E-5	7.1 E-6	1.4 E-6	2.0 E-6	1.3 E-5	5.1 E-6	-	-
9.7	6.5 E-5	2.9 E-5	3.1 E-6	3.9 E-6	1.6 E-5	4.4 E-6	-	-
11.0	1.6 E-4	7.0 E-5	8.0 E-6	9.0 E-6	2.8 E-5	3.9 E-6	-	9.4 E-8

-: no reliable measurement

Table B-2: Chemical analyses of the supernatant solutions (mol L^{-1}) after 7 days interaction time between 0.01 M $NaClO_4$ and conditioned Na-illite (IdP-2). S:L ratio = 1.9 g L^{-1}. (This study).

pH	Na	K	Mg	Ca	Si	Al	Fe	Mn
3.3	1.0 E-2	2.5 E-5	2.8 E-5	1.4 E-4	1.7 E-4	3.6 E-5	3.2 E-6	2.9 E07
4.4	1.1 E-2	1.7 E-5	9.6 E-6	9.0 E-5	9.2 E-5	1.3 E-5	8.3 E-7	7.7 E-8
5.2	1.1 E-2	9.3 E-6	4.1 E-6	3.2 E-5	6.4 E-5	3.3 E-6	6.1 E-7	2.7 E-8
5.9	9.9 E-3	6.2 E-6	2.0 E-6	1.2 E-5	5.2 E-5	2.5 E-6	7.2 E-7	9.6 E-9
6.7	1.0 E-2	-	1.5 E-6	6.9 E-6	4.3 E-5	2.6 E-6	7.2 E-7	8.2 E-9
7.4	1.0 E-2	6.7 E-6	2.2 E-6	5.7 E-6	4.3 E-5	6.3 E-6	1.5 E-6	1.2 E-8
7.7	9.0 E-3	9.1 E-6	2.8 E-6	6.1 E-6	3.5 E-5	4.9 E-6	1.2 E-6	1.3 E-8
8.1	8.9 E-3	6.1 E-6	2.7 E-6	4.4 E-6	4.1 E-5	9.2 E-6	2.0 E-6	1.5 E-8
8.7	9.6 E-3	7.4 E-6	2.5 E-6	3.9 E-6	3.7 E-5	9.5 E-6	1.6 E-6	1.1 E-8
9.4	1.0 E-2	8.6 E-6	4.1 E-6	2.7 E-6	5.6 E-5	2.2 E-5	3.4 E-6	2.3 E-8
9.9	1.0 E-2	1.3 E-5	7.7 E-6	3.0 E-6	9.7 E-5	4.5 E-5	6.6 E-6	4.8 E-8
10.9	1.1 E-2	4.6 E-5	-	-	3.0 E-4	1.6 E-4	2.3 E-5	2.1 E-7

- : no reliable measurement

Table B-3: Chemical analyses of the supernatant solutions (mol L^{-1}) after 7 days interaction time between 0.1 M $NaClO_4$ and conditioned Na-illite, IdP-1; S:L ratio of 2.4 g L^{-1}. (Data taken from POINSSOT et al., 1999).

pH	Si	Al	Fe	Mg	K	Ca	Sr	Mn
3.2	1.7 E-4	9.1 E-5	5.6 E-6	2.8 E-5	2.7 E-5	1.2 E-4	2.7 E-7	2.1 E-6
4.5	1.0 E-4	2.9 E-5	2.4 E-6	1.4 E-5	1.8 E-5	1.1 E-4	2.6 E-7	1.0 E-6
5.8	6.0 E-5	-	7.6 E-7	7.4 E-6	1.3 E-5	5.2 E-5	1.6 E-7	2.9 E-7
6.6	3.6 E-5	2.2 E-6	9.2 E-7	-	1.5 E-5	-	-	5.7 E-8
7.3	2.9 E-5	9.3 E-7	4.0 E-7	3.0 E-6	-	1.6 E-5	6.4 E-8	-
9.3	2.5 E-5	2.6 E-6	2.6 E-7	6.8 E-7	4.8 E-5	9.3 E-6	3.0 E-8	-
10.9	7.8 E-5	3.3 E-5	2.9 E-7	8.5 E-7	5.4 E-5	3.5 E-6	1.4 E-8	-

-: no reliable measurement

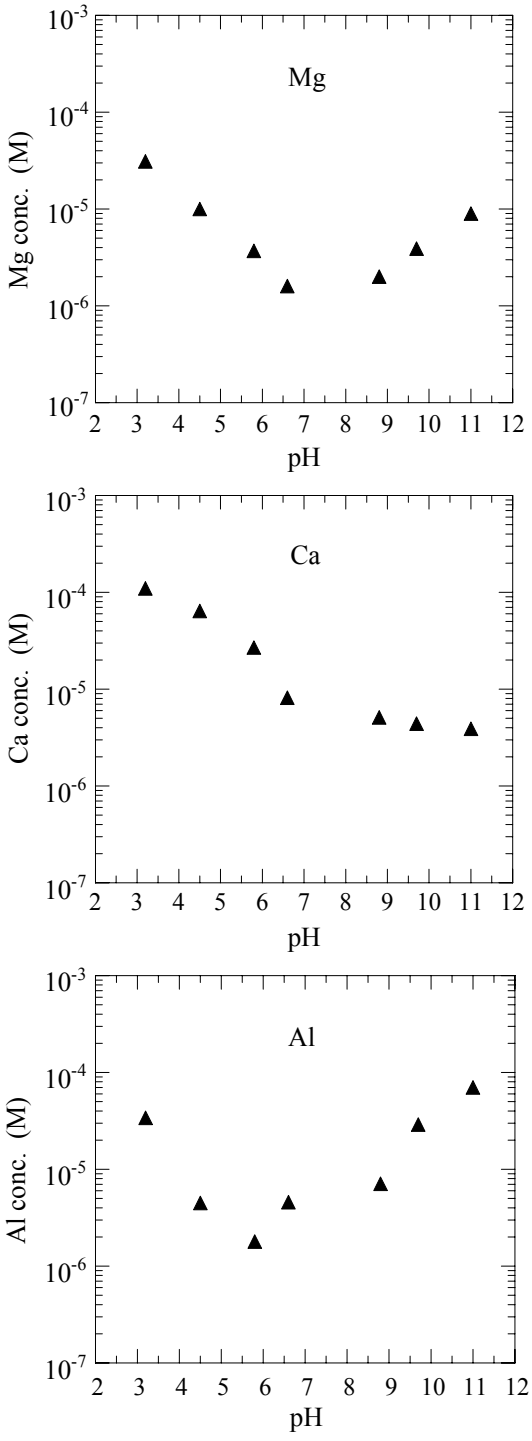

Fig. B-1: Mg, Ca and Al concentrations (mol L^{-1}) in the supernatant solutions after 7 days interaction time between 0.01 M $NaClO_4$ and conditioned Na-illite (IdP-1). S:L ratio = 2.2 g L^{-1} (see Table B-1). (Data taken from POINSSOT et al., 1999).

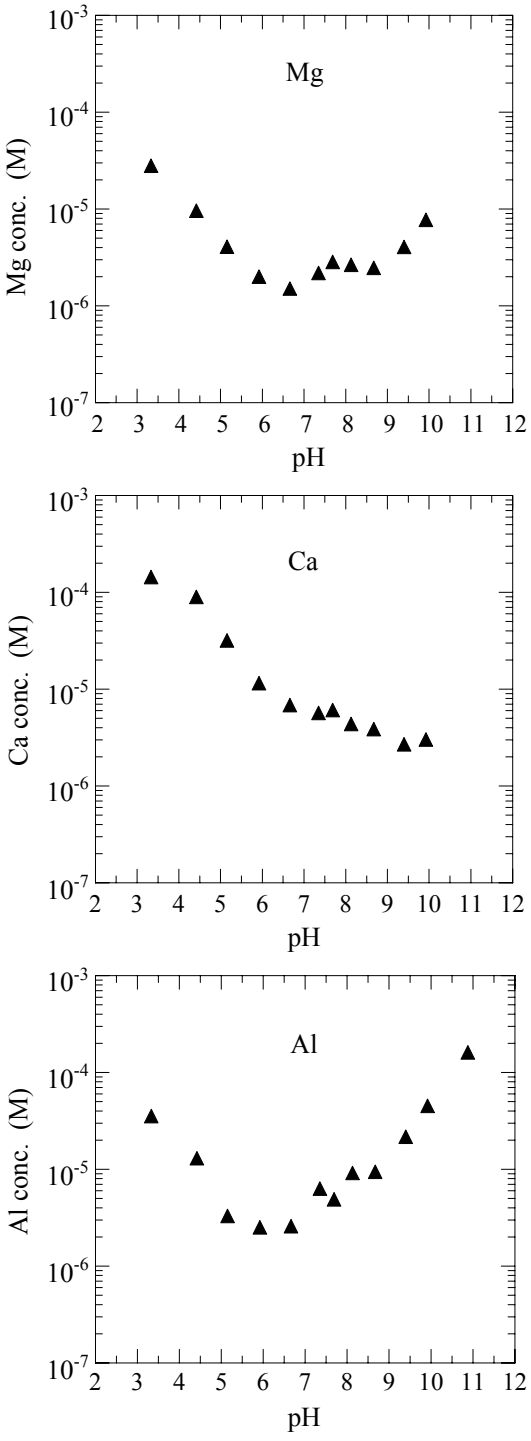

Fig. B-2: Mg, Ca and Al concentrations (mol L^{-1}) in the supernatant solutions after 7 days interaction time between 0.01 M $NaClO_4$ and conditioned Na-illite (IdP-2). S:L ratio = 1.9 g L^{-1} (see Table B-2). (This study.)

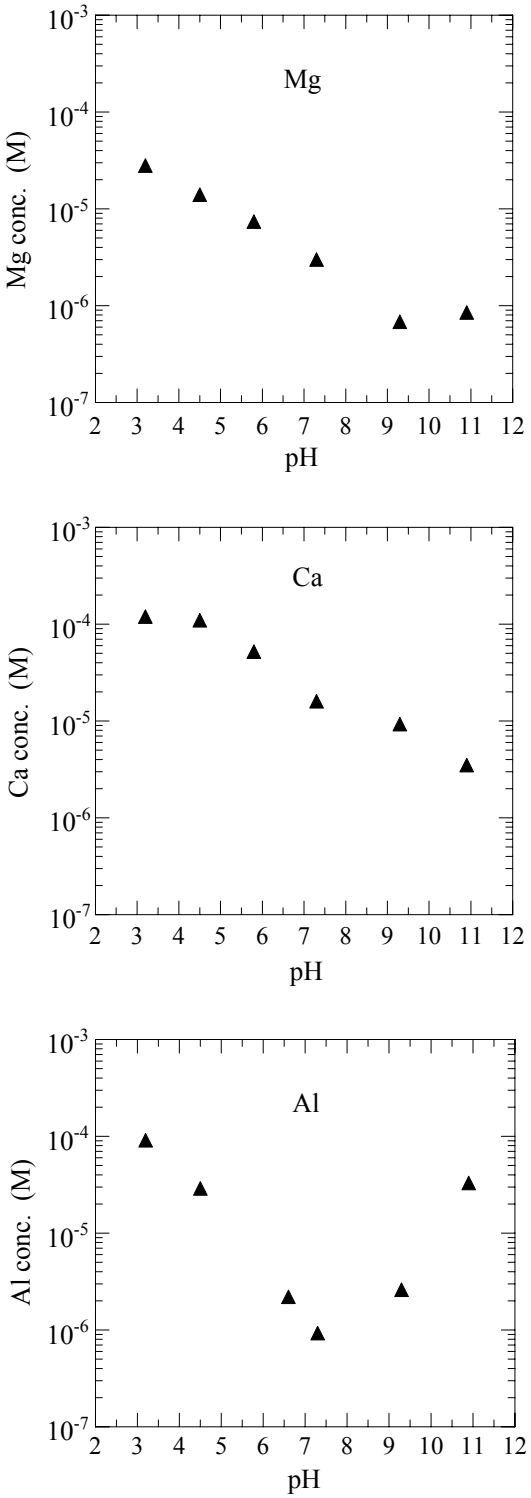

Fig. B-3: Mg, Ca and Al concentrations (mol L^{-1}) in the supernatant solutions after 7 days interaction time between 0.1 M $NaClO_4$ and conditioned Na-illite (IdP-1). S:L ratio = 2.4 g L^{-1} (see Table B-3). (Data taken from POINSSOT et al., 1999).